

**BIOGEOCHEMICAL CYCLING OF PHOSPHORUS IN THE CHESAPEAKE
BAY AND ITS WATERSHED: INSIGHTS FROM PHOSPHATE OXYGEN
ISOTOPE RATIOS**

by

Sunendra R. Joshi

A dissertation submitted to the Faculty of the University of Delaware in partial fulfillment of the requirements for the degree of Doctor of Philosophy in Plant and Soil Sciences

Summer, 2016

© 2016 Sunendra R. Joshi
All Rights Reserved

ProQuest Number: 10191753

All rights reserved

INFORMATION TO ALL USERS

The quality of this reproduction is dependent upon the quality of the copy submitted.

In the unlikely event that the author did not send a complete manuscript and there are missing pages, these will be noted. Also, if material had to be removed, a note will indicate the deletion.



ProQuest 10191753

Published by ProQuest LLC (2016). Copyright of the Dissertation is held by the Author.

All rights reserved.

This work is protected against unauthorized copying under Title 17, United States Code
Microform Edition © ProQuest LLC.

ProQuest LLC.
789 East Eisenhower Parkway
P.O. Box 1346
Ann Arbor, MI 48106 - 1346

**BIOGEOCHEMICAL CYCLING OF PHOSPHORUS IN THE CHESAPEAKE
BAY AND ITS WATERSHED: INSIGHTS FROM PHOSPHATE OXYGEN
ISOTOPE RATIOS**

by

Sunendra R. Joshi

Approved: _____
D. Janine Sherrier, Ph.D.
Chair of the Department of Plant and Soil Sciences

Approved: _____
Mark W. Rieger, Ph.D.
Dean of the College of Agriculture and Natural Resources

Approved: _____
Ann L. Ardis, Ph.D.
Senior Vice Provost for Graduate and Professional Education

I certify that I have read this dissertation and that in my opinion it meets the academic and professional standard required by the University as a dissertation for the degree of Doctor of Philosophy.

Signed:

Deb P. Jaisi, Ph.D.
Professor in charge of dissertation

I certify that I have read this dissertation and that in my opinion it meets the academic and professional standard required by the University as a dissertation for the degree of Doctor of Philosophy.

Signed:

Donald L. Sparks, Ph.D.
Member of dissertation committee

I certify that I have read this dissertation and that in my opinion it meets the academic and professional standard required by the University as a dissertation for the degree of Doctor of Philosophy.

Signed:

William J. Ullman, Ph.D.
Member of dissertation committee

I certify that I have read this dissertation and that in my opinion it meets the academic and professional standard required by the University as a dissertation for the degree of Doctor of Philosophy.

Signed:

Joshua M. McGrath, Ph.D.
Member of dissertation committee

ACKNOWLEDGMENTS

I offer my sincere gratitude to my advisor, Dr. Deb Jaisi, for providing me an opportunity to undertake research under his supervision and for training exquisite details on laboratory methods and isotope systematics, being a source of constant support, suggesting right method and approach to address specific questions. His encouragement and suggestions helped me energize and excel in my research at the University of Delaware. My committee members: Dr. Donald Sparks, Dr. William Ullman, and Dr. Joshua McGrath have been a source of instrumental support, and I would like to express my appreciation for their encouragement and suggestions throughout my research.

I am very grateful to all current and previous members of the Environmental Biogeochemistry Laboratory. They were very instrumental and sources of support at different stages of my research. I appreciate all postdoctoral researches: Jiying Li, Mingjing Sun, Lisa Stout, Dengjun Wang, Wei Li, Xiona Li and Balakrishna Avula, for sharing their knowledge and love of science, and particularly Jiying Li for several fruitful interactions on sediment and water column P cycling in the Chesapeake Bay. My special thank goes to Kristi Bear, a person who crosses boundaries to help others both in science and in personal matters. Also, I would like to thank Hui Li, Yuge Bai, Qiang Li, Prajwal Paudel, and Kiran Upreti for sharing challenges and excitements at different stages of research and mutually learning the tool of the trade in the laboratory. Undergraduates in the EBL lab, Michael Scharf, Ha Vu, and Awet Negusse, are acknowledged for executing series of impossible field tasks and their

helps whenever I needed extra hands for processing samples for isotopes. Financial supports from USDA, NSF-EPSCoR, DSB/MSB, Donald L. and Joy G. Sparks Graduate Fellowship, and UD Dissertation Fellowship are gratefully acknowledged, without which the costly isotope research would not be possible.

I am extremely grateful to my deceased parents. They are the sources of inspiration of my life. I want to thank my wife, Pragya, for encouraging and believing in me. I would like to thank all my friends and family members; without their support, I would not be in this position.

TABLE OF CONTENTS

LIST OF TABLES	xi
LIST OF FIGURES	xii
ABSTRACT	xvii

Chapter

1	INTRODUCTION AND RESEARCH OBJECTIVES	1
1.1	Chesapeake Bay and its water quality issues	1
1.1.1	Sources of phosphorus in the Chesapeake Bay	4
1.1.2	Phosphorus cycling in agricultural soils	5
1.1.3	Phosphorus cycling in sediments	7
1.2	Research objectives	8
	REFERENCES	10
2	TRANSFORMATION OF PHOSPHORUS POOLS IN AN AGRICULTURAL SOIL: AN APPLICATION OF OXYGEN-18 LABELING IN PHOSPHATE	13
2.1	Abstract	13
2.2	Introduction	14
2.3	Materials and methods	17
2.3.1	Site description and soil characterization	17
2.3.2	Application of ¹⁸ O labeled phosphate and soil sampling	18
2.3.3	Extraction of soil phosphate pools	19
2.3.4	Sample purification and measurement of phosphate oxygen isotope ratios	20
2.4	Results and Discussion	23
2.4.1	Soil properties	23
2.4.2	Phosphate pools and isotopic compositions in the control site ...	24

2.4.3	Phosphate pools and isotopic compositions in oxygen-18-labeled inorganic phosphorus applied site.....	27
2.4.4	Dynamics of concentrations and isotopic compositions of phosphorus pools: Interplay of biotic and abiotic reactions	31
2.4.5	Variable sources and pathways of hydrochloric acid extractable inorganic phosphorus	34
2.5	Conclusions and implications.....	36
2.6	Acknowledgement.....	37
	REFERENCES.....	38
3	SOURCES AND MECHANISMS OF FORMATION OF ACID EXTRACTABLE PHOSPHORUS POOLS IN AN AGRICULTURAL SOIL	44
3.1	Abstract.....	44
3.2	Introduction	45
3.3	Materials and methods.....	48
3.3.1	Site description and soil sampling.....	48
3.3.2	Soil characterization	49
3.3.3	³¹ P Solid-State NMR Spectroscopy.....	51
3.3.4	Extraction of soil phosphate pools	51
3.3.5	Purification of extracted solution for isotope analysis	52
3.3.6	Measurement of phosphate oxygen isotope ratios.....	54
3.4	Results	56
3.4.1	Soil pH and elemental compositions	56
3.4.2	Mineralogical composition of soils	57
3.4.3	³¹ P NMR results on the composition of phosphorus minerals	58
3.4.4	Concentrations and isotopic compositions of P pools.....	59
3.4.5	Concentrations of P, Fe, Al, and Ca in acid extraction	61
3.5	Discussion.....	65
3.5.1	Sources of acid extractable P pools.....	65
3.5.2	Mechanisms of P transformation and formation of acid extractable P	69
3.5.3	Leaching of phosphorus to deeper soil horizons	70
3.6	Conclusions and implications.....	72

	REFERENCES	74
4	DISTINCT PATHWAYS OF PHOSPHORUS CYCLING IN THE UPSTREAM AND DOWNSTREAM SECTIONS OF A CREEK IN AN AGRICULTURAL RUNOFF DOMINATED WATERSHED	82
4.1	Abstract.....	82
4.2	Introduction	83
4.3	Materials and methods.....	86
4.3.1	Sampling sites.....	86
4.3.2	Collection and characterization of sediment and water samples .	87
4.3.3	Extraction of phosphorus pools in suspended particulate matter and sediments	88
4.3.4	Sample purification and silver phosphate precipitation	89
4.3.5	Measurement of phosphate and water oxygen isotope ratios	90
4.4	Results	90
4.4.1	Dissolved phosphorus in the surface water	90
4.4.2	Concentration and isotopic composition of P pools in suspended particulate matter	92
4.4.3	Isotopic composition of oxygen in the pore water	94
4.4.4	Concentration and isotopic composition of dissolved phosphate in the pore water	95
4.4.5	Phosphorus pools in the sediments.....	98
4.5	Discussion.....	99
4.5.1	Phosphorus loss from land and transport and cycling in the water column	99
4.5.2	Contrasting pathways of phosphorus cycling in sediments in agriculture-dominated headwater sites and wetland sites near the bay	102
4.6	Conclusions and implications.....	105
4.7	Acknowledgements	106
	REFERENCES	107
5	ORGANIC MATTER REMINERALIZATION PREDOMINATES PHOSPHORUS CYCLING IN THE MID-BAY SEDIMENTS IN THE CHESAPEAKE BAY.....	113

5.1	Abstract.....	113
5.2	Introduction	114
5.2.1	Chesapeake Bay and coastal hypoxia.....	114
5.2.2	Organic matter remineralization vs. Fe-P coupled (remobilization) pathway of P cycling	115
5.3	Experimental section	118
5.3.1	Sampling sites and sediment characterization.....	118
5.3.2	Extraction of sediment P pools.....	119
5.3.3	Sample purification and measurement of phosphate $\delta^{18}\text{O}_p$ values.....	120
5.3.4	X-Ray diffraction and ^{57}Fe Mössbauer spectroscopy.....	121
5.4	Results and discussion.....	122
5.4.1	Sediment composition: XRD and Mössbauer results	122
5.4.2	Sediment P composition and P pools	128
5.4.3	Isotopic composition of sediment P pools.....	131
5.4.4	Concentration and isotopic composition of pore water P.....	134
5.4.5	Insignificant coupled Fe:P cycling (remobilization) pathway...	136
5.4.6	Predominance of organic matter remineralization pathway of P cycling	138
5.5	Conclusions and implications.....	140
5.6	Acknowledgements	141
	REFERENCES	142
6	PHOSPHORUS SOURCES AND CYCLING IN SEDIMENTS IMPACTED BY BOTTOM WATER HYPOXIA IN THE CHESAPEAKE BAY.....	151
6.1	Abstract.....	151
6.2	Introduction	152
6.3	Materials and methods.....	154
6.3.1	Sampling sites and sediment characterization.....	154
6.3.2	X-Ray Diffraction.....	156
6.3.3	Total dissolution of sediments.....	156
6.3.4	Extraction of sediment phosphorus pools.....	157
6.3.5	Purification of extracted solutions.....	157
6.3.6	Measurement of phosphate oxygen isotope ratios.....	158

6.4	Results	159
6.4.1	Mineralogical composition of sediments.....	159
6.4.2	Elemental compositions of sediments	160
6.4.3	Concentration of sediment phosphorus pools.....	161
6.4.4	Isotopic compositions of sediment phosphorus pools	163
6.5	Discussion.....	164
6.5.1	Anomalous Fe-P pool and variation of major sediment P sinks along the salinity gradient	164
6.5.2	Dominance of coupled Fe-P and C-P pathways: Insights from phosphate oxygen isotope ratios.....	168
6.5.2.1	Ferric Fe-bound P and coupled Fe-P pathway:	168
6.5.2.2	Authigenic Ca-P and coupled C-P pathways:	169
6.6	Conclusions and implications.....	172
	REFERENCES	174
7	CONCLUSIONS AND IMPLICATIONS	182
8	LIMITATIONS AND FUTURE DIRECTIONS	185
	REFERENCES	187
Appendix		
A	PERMISSION FOR JOSHI ET AL. 2015	188
B	PERMISSION FOR JOSHI ET AL. 2016	189

LIST OF TABLES

Table 2.1 Physical and Chemical properties of soils collected from four depths.	19
Table 2.2 Elemental concentration of P, Fe, Al, and Ca in soils at different depths measured by inductively coupled plasma optical emission spectrometry before and after sequential extraction.....	20
Table 2.3 Organic P concentration in NaHCO ₃ and NaOH extracted pools before and after the DAX 8 Superlite resin treatment.	22
Table 3.1 Selected soil properties at six different depth intervals in the study site.	56
Table 3.2 Mineralogical compositions of soil residues i) after NaOH extraction, ii) HCl extraction, and iii) after HNO ₃ extraction at six different depth intervals.	57
Table 5.1 Concentration of dissolved ions in 0.5 N HCl extracted solution from pristine sediments for 24 hrs (expressed as wt %) from three different depths in the Chesapeake Bay	127
Table 5.2 Elemental concentration of Fe, Ca, Fe, Mn, P and S in sediment from different depths. Inorganic P% is calculated from solution ³¹ P ⁴³ extracted from the sediment.	131

LIST OF FIGURES

Figure 1.1 Map of the Chesapeake Bay watershed (Andrews, 2008).	2
Figure 1.2 Change in DIN:DIP ratio during early spring and late spring eutrophication in the Chesapeake Bay (Prasad et al., 2010).	3
Figure 1.3 P budget in the Chesapeake Bay (after Boynton et al., 1995).	5
Figure 1.4 P cycling in soil-plant system (Frossard et al., 2011).	6
Figure 2.1 (a,b) Concentrations and (c,d) isotopic compositions of four inorganic P (P _i) pools (H ₂ O-P _i , NaHCO ₃ -P _i , NaOH-P _i , and HCl-P _i) in the control plot (without application of ¹⁸ O labeled P _i) (a, c) 55 d before and (b, d) 155 d after the start of the experiment. The dark grey lines indicate equilibrium $\delta^{18}\text{O}_P$ composition calculated from measured water $\delta^{18}\text{O}_w$ values and temperature at the time of sampling, and the shaded regions correspond to that of daily average of the sampling month.	25
Figure 2.2 (a,b,c) Concentrations and (d,e) isotopic compositions of four inorganic P (P _i) pools (H ₂ O-P _i , NaHCO ₃ -P _i , NaOH-P _i , and HCl-P _i) in the experimental plot before and after application of ¹⁸ O labeled P _i (38‰) at (a) 1 d before, and (b,d) 18 d and (c, e) 155 d after the start of the experiment. The dark grey lines indicate equilibrium $\delta^{18}\text{O}_P$ composition calculated from measured pore-water $\delta^{18}\text{O}_w$ values and temperature at the time of sampling, and the shaded regions correspond to the daily average of the sampling month.....	28
Figure 2.3 Schematic diagrams showing P speciation and transformations. The relative length of an arrow corresponds to the extent of biological cycling of a particular P pool (H ₂ O-P _i , NaHCO ₃ -P _i , NaOH-P _i , and HCl-P _i). The dashed arrows (uni- or bidirectional) of different colors indicate transfer of P from one pool to another. Illustrations do not consider long-term reactions such as potential dissolution and remobilization of HCl-P _i	33
Figure 3.1 Flow diagram for the purification of P from sequentially extracted soil solution and precipitation of silver phosphate.....	55

Figure 3.2 ^{31}P solid state NMR spectra of bulk soils (from 0–7.5 and 7.5–15 cm depths). Spectra were acquired at the single-pulse magic angle spinning (MAS) condition at a spinning rate of 10 kHz, with a $\pi/6$ pulse and a pulse delay of 30 s. Approximately 3000 - 14000 scans were accumulated for these samples. 59

Figure 3.3 Concentrations (a, b, and c) and isotopic compositions (d, e, and f) of soil P_i pools (NaOH- P_i , HCl- P_i , and HNO_3 - P_i) as a function of depth. The dark grey lines indicate equilibrium $\delta^{18}\text{O}_\text{P}$ composition calculated from measured water $\delta^{18}\text{O}_\text{w}$ values and temperature at the time of sampling. 60

Figure 3.4 Concentration of total P, Fe, Al, and Ca in HCl (a, b, c, and d) and HNO_3 (f, g, h, and i) extracted solutions. The soil pH (e and f) was plotted to compare with the concentration profiles. Please note that both e and f are the same soil pH. Concentrations of these elements were measured by using inductively coupled plasma emission spectrometry (ICP-OES). 63

Figure 3.5 Scatter plots P with other elements that are associated or coupled with P: Fe (a, d), Al (b, e), and Ca (c, f) in 1 mol L^{-1} HCl extracted solution at shallow (a, b, and c) and deeper (d, e, and f) depth in the soil column. R^2 values refer to Pearson’s linear correlation. 64

Figure 3.6 The scatter plots P with other elements that are associated or coupled with P: Fe (a, d), Al (b, e), and Ca (c, f) in 10 mol L^{-1} HNO_3 extracted solution at shallow (a, b, and c) and deeper (d, e, and f) soil column. R^2 values refer to Pearson’s linear correlation. 64

Figure 4.1 Map of East Creek and locations of water and sediment core sampling sites (adapted from Stout et al., 2016). 87

Figure 4.2 Concentrations of P_i and P_o in water samples collected from sites in the wetland region near the bay (A, B, and C) and the agriculture-dominated region in the headwater (J, K, and L) (a) and isotope values of dissolved P_i in water samples from the sites near the agricultural fields (b). The dark dotted line indicates equilibrium $\delta^{18}\text{O}_\text{P}$ composition calculated from measured water $\delta^{18}\text{O}_\text{w}$ values and temperature at the time of sampling and the shaded region corresponds to that of monthly temperature average of the sampling month. 92

Figure 4.3 Phosphate (P _i) pools in the suspended particulate matter in creek water at sites in the wetland region near the bay (A, B, and C) and the agriculture-dominated region in the headwater (J, K, and L) (a) and their corresponding isotopic compositions (b). The equilibrium isotope values and range are the same as in Figure 4.2.....	94
Figure 4.4 Water oxygen isotope ratios in the pore water at selected depths from sites in the wetland region near the bay (A, B, and C) and the agriculture-dominated region in the headwater (J, K, and L). Depth < 0 cm means the surface water in the creek. The line traces are showing the trends and not actual fitting results.....	95
Figure 4.5 Concentrations and isotopic compositions (sites in the wetland region near the bay (A, B, and C) (i) and the agriculture-dominated region in the headwater (J, K, and L) (ii)) of pore water phosphate. The dark dotted line indicates equilibrium $\delta^{18}\text{O}_\text{P}$ composition calculated from measured pore water $\delta^{18}\text{O}_\text{W}$ values and temperature at the time of sampling and the shaded region corresponds to that of monthly temperature average of the sampling month.	97
Figure 4.6 Concentrations of sediment P _i pools (H ₂ O-P _i , NaHCO ₃ -P _i , NaOH-P _i , and HNO ₃ -P _i) in the river bed sediment (0–2 cm) in the wetland region near the bay (A, and C) and the agriculture-dominated region in the headwater (J, K, and L).	99
Figure 5.1 Major mineral phases in the pristine sediments from 0–1, 12–15 and 30–32 cm depth. Please note that except pyrite, Fe and P bearing minerals were below detection limit of XRD diffraction.....	123
Figure 5.2 Mossbauer spectra at 10 K: (a) Modeled spectrum of 0–1 cm with various Fe-minerals (Py = pyrite; I = Ilmenite, PS = phyllosilicate, Al-H = aluminum hematite, sp-OM-P = small-particle Fe-oxide with OM and P coatings), (b) comparison showing the absence of sp-OM-P sextet in the 0.5 N HCl-treated 0–1 cm sample (green trace), and (c) comparison of 0–1 and 30–32 cm showing little or no sp-OM-P sextet in the 30–32 cm sediment.	124

Figure 5.3 Variable temperature spectra of pristine sediment from 0-1 cm. Spectra at various temperatures were obtained to gain insights into semi-quantitative Fe mineral distribution. Inset in (b) shows the sextet that was apparent at 35 K spectra. P = Pyrite ((low-spin (LS) Fe(II)) content is fixed based on chemical composition and XRD derived pyrite content. PS Fe(II) is mostly clay because vivianite is less than a % of the total Fe (based on 0.5 N HCl extractable P). PS = phyllosilicate; I = Ilmenite; Al-H = Aluminum substituted hematite; sp = small-particle; OM = organic matter..... 126

Figure 5.4 Concentration and corresponding $\delta^{18}\text{O}_p$ values of P pools in the sediment: (a) Ferric Fe-bound P dominates sediment P pools and (b) $\delta^{18}\text{O}_p$ values of ferric Fe-bound and authigenic P. The dotted line represents the equilibrium $\delta^{18}\text{O}_p$ values (per ref 70) at the site using August temperature (per ref 69) and pore water $\delta^{18}\text{O}_w$ values and the shaded region for the entire year. The dashed line is equilibrium $\delta^{18}\text{O}_p$ values per ref 71. All isotope values in this paper are reported to Vienna Standard Mean Ocean Water (VSMOW). 129

Figure 5.5 Concentration and corresponding $\delta^{18}\text{O}_p$ values of porewater P. Dotted and dashed lines represent the equilibrium $\delta^{18}\text{O}_p$ values calculated using measured water $\delta^{18}\text{O}_w$ values and temperature, following refs 70 and 71, respectively. The arrows from mean $\delta^{18}\text{O}_p$ values of authigenic and ferric Fe-bound P indicate direction of isotope excursion due to biological cycling..... 136

Figure 5.6 P cycling near sediment-water interface interpreted from isotope data. Please note ? symbol indicates uncertainty of data and * indicates that both reactions may not necessarily be highly redox-sensitive if some of this ferric Fe-bound P is associated with ferric iron in clays (otherwise there would be no ferric Fe-bound P found at depth in these sediments). 140

Figure 6.1 Location of the sediment sampling sites in the Chesapeake Bay. 156

Figure 6.2 Mineralogical composition of sediment at 2 to 3 cm depth from site N. The sediment predominantly consists of quartz, muscovite, feldspar group minerals, chlorite, and pyrite..... 160

Figure 6.3 Concentrations of P, Fe, Ca, and S in sites N (a, b, c, and d), M (e, f, g, and h), and S (i, j, k, and l) sediments. The sediment samples were digested in a Katanax K1 fluxer and concentrations were measured using inductively coupled plasma optical emission spectrometer (ICP-OES). 161

Figure 6.4 Concentration of exchangeable, ferric Fe-bound (Fe-P), authigenic apatite (Ca-P), and detrital P pools in the sediments from a) North (N); b) middle (M); and c) South (S) sites of the Bay. 162

Figure 6.5 Isotopic compositions of Fe-P and Ca-P pools in the sediments from a) North (N); b) middle (M); and c) South (S) sites of the Chesapeake Bay. Thick dotted lines at sites N and M represents the equilibrium isotopic compositions (as per (Longinelli and Nuti, 1973)) calculated using August temperature (Reeburgh, 1969) and porewater oxygen isotope values and the shaded region for the entire year. The dashed line is equilibrium isotopic compositions calculated as per Chang and Blake, 2015 (Chang and Blake, 2015). 164

ABSTRACT

The Chesapeake Bay and its watershed suffer from varying degrees of water quality issues fueled by both point and non-point nutrient sources. Methodological limitations on source tracking and identification of the specific phosphorus (P) pools that can be biologically cycled (or remain recalcitrant) in both the short and long terms are the major obstacles preventing accurate assessment of the nutrient loads that could impact water quality. This research utilized phosphate oxygen isotope ratios, mineralogical (XRD and micro-XRD), microscopic (SEM), elemental, and spectroscopic (^{31}P NMR and ^{57}Fe Mössbauer) methods to characterize P speciation and investigate mechanisms and pathways of P transformations in the Chesapeake Bay and its watershed.

In an agricultural soil, short-term transformation of externally applied P to a less or non-bioavailable P pool was tracked by using ^{18}O labeled phosphate. This enabled identification of sources and precipitation pathways of acid extractable P pools. In East Creek, a tidal tributary of the Chesapeake Bay, impact of P loading primarily from agricultural runoff was reflected on the pathways and intensity of P cycling: both input flux higher than microbial cycling and remineralization (degradation of organic P) contributed to higher pore water P_i in the headwater region. In the wetland region, on the other hand, porewater P_i was completely cycled. In the Chesapeake Bay sediments, ferric Fe-bound and authigenic P pools were the two major P sinks, regardless of bottom water hypoxia. Regeneration of P_i from organic matter degradation was found to be the predominant, if not sole, pathway for

authigenic P precipitation. Overall, this work generated new insights into the sources, stability, and transformations of various P pools in soils, waters, and sediments under different biogeochemical conditions. These findings are expected to be useful to watershed nutrient management plans as well as to widen source- and pathway- based research in the Chesapeake Bay and other watersheds.

Chapter 1

INTRODUCTION AND RESEARCH OBJECTIVES

1.1 Chesapeake Bay and its water quality issues

The Chesapeake Bay is located in the Mid Atlantic coastal region of the United States. It is the largest estuary in the United States, spans approximately 320 km in length, and ranges from 5 to 55 km in width (CBF, 2016). The maximum water depth is > 45 m with an average depth of 10 m (CBP, 2012). The Chesapeake Bay watershed covers a total area of about 166,000 km² that including portions of Maryland, Pennsylvania, Virginia, West Virginia, Delaware, New York, and the District of Columbia (Fig 1.1) and is populated by ~17 million people. The major land uses in the watershed are forest (60%) and agriculture (28%) and remaining land uses include residential (4%), water (4%), wetland (3%), and barren land (1%). The five major rivers (Susquehanna, Potomac, Rappahannock, York, and James) discharge about 90% of the total fresh water to the bay (CBP, 2012). The watershed provides habitat to more than 2,700 species of plants and animals. The tidal wetlands also provide shelter and habitat for fish, birds, crabs, and many other species.

The Chesapeake Bay is one of the most biologically productive estuaries in the United States (Babbin and Ward, 2013). In the mesohaline region of Chesapeake Bay, mean summer productivity can exceed 4 g C m⁻² day⁻¹ (Malone, 1991). The relatively high primary productivity in the bay is associated with riverine discharge of nutrients from both point and non-point sources (Boesch et al., 2001). Every year, the bay receives an estimated 9.74×10^6 kg of phosphorus (P) and 1.32×10^8 kg of

nitrogen (N) from its watershed, mainly through the Susquehanna and Potomac Rivers (Ator et al., 2011). Increased nutrient levels in the bay have several environmental impacts including increased algal blooms and turbidity and decreased dissolved oxygen, submerged aquatic vegetation, and fishery production. During high productive seasons, decomposition of organic matter (primarily biomass from primary producers) in the water column and sediments consumes oxygen leading to periodic and sustained hypoxic ($<2.0 \text{ mg O}_2 \text{ L}^{-1}$) or anoxic ($<0.2 \text{ mg O}_2 \text{ L}^{-1}$) conditions. These water quality issues impact both the environment and economy in the region.

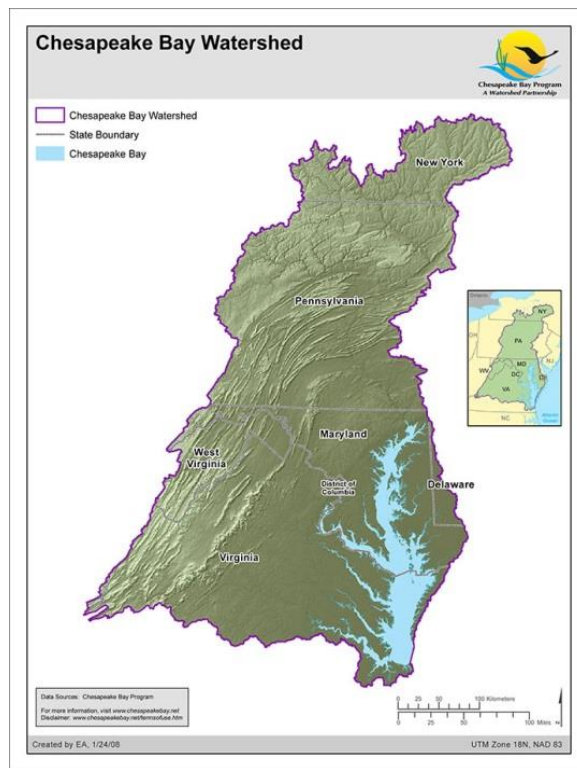


Figure 1.1 Map of the Chesapeake Bay watershed (Andrews, 2008).

Hypoxia in the Chesapeake Bay dates back to 1950s (Hagy et al., 2004). While research on the cause and extent of hypoxia has been conducted since then, interactions between physical and biological processes and their roles in spatial and seasonal development of hypoxia are not well known (Kemp et al., 1992; Boynton & Kemp, 2000). For example, early summer hypoxia in the bottom water is strongly correlated with physical processes such as allochthonous nutrient input, freshwater inflow, and stratification strength (Boynton et al., 1990; Boynton & Kemp, 2000; Hagy et al., 2004; Murphy et al., 2011). However, late summer hypoxia is found to be related to eutrophication and is fueled by autochthonous (recycled) nutrients (Boynton et al., 1990; Testa & Kemp, 2012). Interestingly, the monthly mean ratio (1985–2010) of dissolved inorganic nitrogen to phosphorus (DIN:DIP) in the bay is higher than the Redfield ratio (i.e., 16 for N/P) in all seasons except mid-summer (Fig 1.2) (Prasad et al., 2010). This indicates that P is the limiting nutrient for early summer eutrophication. Therefore, a better understanding of P sources and cycling in the bay and its watershed could provide much sought-after information on how P contributes to the bay water quality.

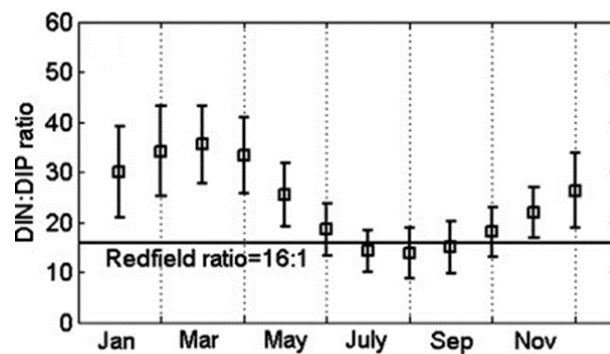


Figure 1.2 Change in DIN:DIP ratio during early spring and late spring eutrophication in the Chesapeake Bay (Prasad et al., 2010).

1.1.1 Sources of phosphorus in the Chesapeake Bay

Several point and nonpoint sources supply P to the Chesapeake Bay. Point sources include primarily municipal waste water treatment plants and industrial sources while nonpoint sources include agricultural farms, soils, and other geological sources (Ator et al., 2011). Quantification of P sources and their temporal and spatial variations provides key information useful to prepare and implement management practices to improve the bay water quality. In one such attempt to quantify P mass flux, Boynton et al. (1995) integrated data on P inputs, outputs, and recycling and subsequently developed a total phosphorus (TP) budget for the entire bay (Fig 1.3). Based on this budget combined inputs from point and diffuse sources account for ~ 68% TP, and interestingly this mass balance calculation indicate net import ~ 27% of TP from the ocean to the Bay. Phosphorus loss through sediment burial was the primary sink (94%) and exceeded terrestrial and atmospheric inputs (Boynton et al., 1995). However, sediments serve not only as a P sink, but also as a P source as P may be released into the water column, especially under hypoxic or anoxic conditions in the bottom water or sediment column. In fact, the remobilization of P was estimated to comprise 25 to 30% up to even >100% in the Bay (Cornwell et al., 1996; Anschutz et al., 1998).

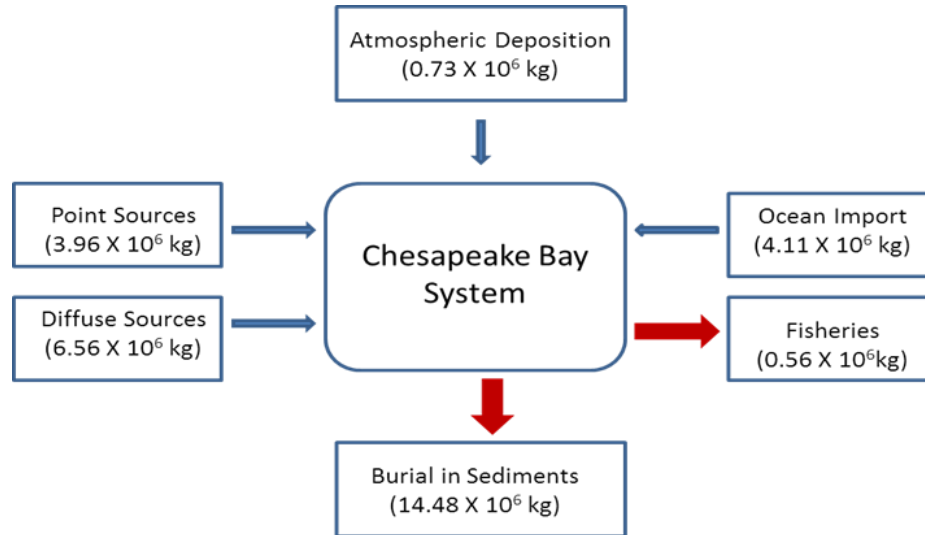


Figure 1.3 P budget in the Chesapeake Bay (after Boynton et al., 1995).

1.1.2 Phosphorus cycling in agricultural soils

Understanding of P cycling in soils is not straightforward due to complex interactions and transformations among multiple P species and biotic and abiotic processes (Frossard et al., 2011), the intensity of these processes varies both in space and time (Fig 1.4). Plant and microbial uptake of P are two dominant biological processes that control soil P concentration. In addition, abiotic processes such as sorption of P onto Al and Fe oxides and precipitation as Ca-P minerals readily decrease available P in soils (Griffin et al., 2003). Fertilizer application and plant uptake affect P dynamics in agricultural soils. For example, continuous cropping without external P input decreases bioavailable P pools in soils (Olsen et al., 1954) and may provoke transfer of P from relatively recalcitrant P pools to labile pools and transformation of organic P (P_o) into inorganic P (P_i) to replenish bioavailable P pools. On the other hand, if fertilizers or animal wastes are continuously applied, bioavailable P could be maintained at sufficient (or excess) levels for plant needs. For

example, soil solution P concentration could reach as high as $\sim 30 \mu\text{mol L}^{-1}$ in fertilized soils (Pierzynski, 1991). The excess P, primarily bioavailable P, may eventually transform into moderately available to unavailable recalcitrant and residual P pools (Barrow, 1984). Over time, recalcitrant and residual P may continue to build up in soils (Lahmen et al., 2005; Read et al., 1977). Thus, understanding the processes that promote the build-up of recalcitrant/residual P pools and distribution of bioavailable P pools in soils provides information useful to identify the fate of applied P in soils as well as to optimize fertilizer application.

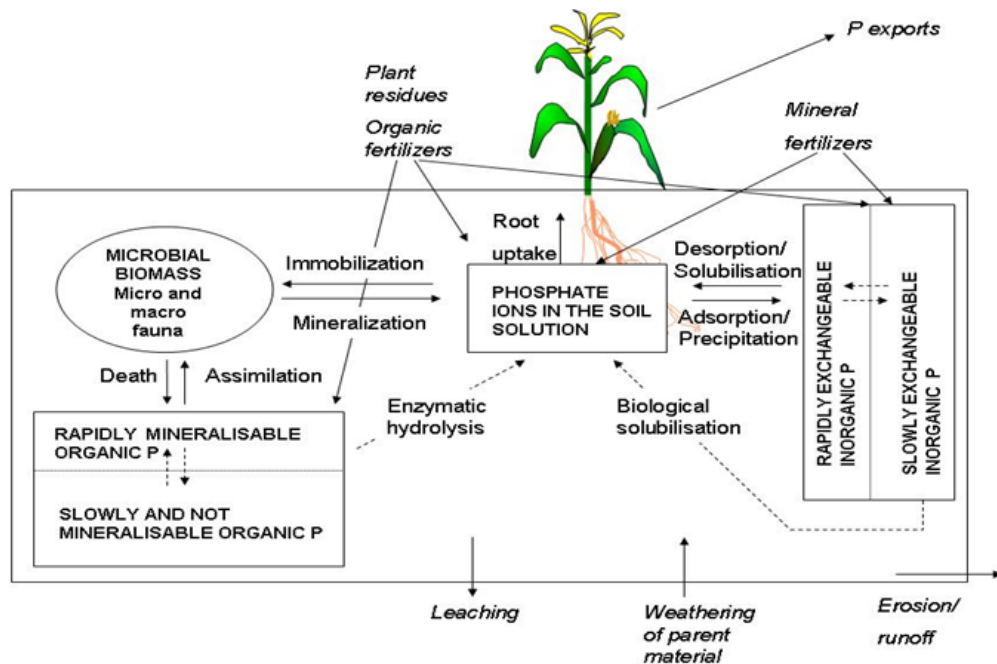


Figure 1.4 P cycling in soil-plant system (Frossard et al., 2011).

1.1.3 Phosphorus cycling in sediments

Sediment plays important role in the overall nutrient dynamics of shallow water such as Bay (Kemp & Boynton, 1984). P flux calculations at the bay show that sedimentary P release, primarily in summer months, contributes a major internal P load to the water column (Boynton et al., 1990, 1995; Cowan & Boynton, 1996; Testa & Kemp, 2012) and supplies a significant portion of phytoplankton P demand (Koop et al., 1990; Cowan & Boynton, 1996). Sediment P processes in the bay are controlled by several factors including nutrient loading, bottom water oxygen concentration, quality and quantity of organic matter, and temperature (Kemp & Boynton, 1984; Cowan & Boynton, 1996; Testa & Kemp, 2012). For example, sediment P flux is inversely related to the degree of nutrient loading from fresh water and bottom water oxygen concentration (Kemp & Boynton, 1984; Boynton et al., 1990).

Because of differential reactivity of sedimentary P pools in response to changing biogeochemical conditions, P speciation can provide important insights on the fate and cycling of P in sediment. Sequential extraction is the most commonly used method to separate sedimentary P pools and have been used to develop qualitative understanding on the selective mobilization or remineralization of a particular P pool. The SEDEX method, originally developed by Ruttенburg (1992) to determine P concentrations in operationally-defined sediment P pools, is widely used in marine sediments (Ruttенburg, 1992; Ruttенburg & Berner, 1993; Jaisi & Blake, 2010). Application of the SEDEX method has enabled identification of ferric Fe-bound P as the predominant P pool in the Patuxent River estuary, which may undergo internal cycling in anoxic sediments (Jordan et al., 2008). The SEDEX method, in combination with phosphate oxygen isotope ratios ($\delta^{18}\text{O}_\text{P}$), has recently been used to trace sources and biogeochemical processes within the sediment column in Peru Margin (Jaisi &

Blake, 2010) and allowed identification of three generations of authigenic phosphates coexisting in the sediments.

1.2 Research objectives

This dissertation includes five research objectives aimed to investigate biogeochemical cycling of P in the Chesapeake Bay and its watershed. Major research objectives and the key questions addressed in each chapter are listed below:

Objective 1. To identify transformation of P pools in an agricultural soil

- I. How do soil P pools vary in response to external application of P and plant uptake?
- II. What mechanisms control the transformation of available P into non-available P over time?
- III. Can phosphate oxygen isotopic ratios be used to identify the pathways of P transformation?

Objective 2. To identify the sources and mechanisms of formation of acid extractable P pools in an agricultural soil

- I. What are the sources of acid extractable P pools?
- II. What are the pathways and mechanisms forming acid extractable P pools?

Objective 3. To understand the impact of P loading on the pathways of P cycling in creek sediment in a watershed dominated by agricultural runoff

- I. What is the impact of P loading on P speciation in water column and sediment P pools?
- II. What are the differences in the pathways of P cycling in the headwater dominated by agricultural runoff and a wetland at the mouth of a creek?

Objective 4. To identify the relative importance of remineralization (i.e., coupled C-P cycling) versus remobilization (i.e., coupled Fe-P cycling) pathways for the precipitation of authigenic apatite P in the Chesapeake Bay

- I. What are the sources of P that precipitate into authigenic P in mid-Bay sediments under the seasonally hypoxic bottom water?
- II. What factors control the degree of remineralization or remobilization in the sediments?

Objective 5. To determine the relative dominance of coupled Fe-P cycling and C-P cycling pathways in sediments in response to bottom water hypoxia in the Chesapeake Bay

- I. How does bottom water hypoxia impact redistribution of P pools in sediments?
- II. Can ferric iron P and authigenic P pools retain their source signatures in the sediments?

REFERENCES

- Andrews, E. 2008. Map: Chesapeake Bay watershed. *Chesapeake Bay Program* Available at http://www.chesapeakebay.net/maps/map/chesapeake_bay_watershed1.
- Anschutz, P., Zhong, S., Sundby, B., Mucci, A., & Gobeil, C. 1998. Burial efficiency of phosphorus and the geochemistry of iron in continental margin sediments. *Limnology and Oceanography* **43**, 53–64.
- Ator, S.W., Brakebill, J.W., & Blomquist, J.D. 2011. Sources, fate, and transport of nitrogen and phosphorus in the Chesapeake Bay watershed: An empirical model.
- Babbin, A.R., Ward, B.B. 2013. Controls on nitrogen loss processes in Chesapeake Bay sediments. *Environmental Science & Technology* **47**, 4189–4196.
- Barrow, N.J. 1984. Modelling the effects of pH on phosphate sorption by soils. *European Journal of Soil Science Journal of Soil Science* **35**, 283–297.
- Boesch, D.F., Brinsfield, R.B., & Magnien, R.E. 2001. Chesapeake bay eutrophication. *Journal of Environmental Quality* 30(2), 303–320.
- Boynton, W.R., Garber, J.H., Summers, R., & Kemp, W.M. 1995. Inputs, transformations, and transport of nitrogen and phosphorus in Chesapeake Bay and selected tributaries. *Estuaries* **18**, 285–314.
- Boynton, W.R., & Kemp, W.M. 2000. Influence of river flow and nutrient loading on selected ecosystem processes and properties in Chesapeake Bay. p. 269–298. *In* J, H. (ed.), *Estuarine science: a synthetic approach to research and practice*. Island Press, Washington, DC.
- Boynton, W.R., Kemp, W.M., Barnes, J.M., Cowan, J.L.W., Stammerjohn, S.E., Matteson, L.L., Rohland, F.M., & Marvin, M. 1990. Long-term characteristics and trends of benthic oxygen and nutrient fluxes in the Maryland portion of Chesapeake Bay. p. 239–354. *In* *New Perspectives in the Chesapeake System: A Research and Management Partnership*. Chesapeake Research Consortium Publication No. 137, Baltimore, MD.

- Chesapeake Bay Foundation. 2016. Chesapeake Bay watershed geography and facts. [<http://www.cbf.org/about-the-bay/more-than-just-the-bay/chesapeake-bay-watershed-geography-and-facts#overview>] Accessed July 11, 2016.
- Chesapeake Bay Program. 2012. Frequently asked questions. [<http://www.chesapeakebay.net/faq>] Accessed June 3, 2016.
- Cornwell, J., Conley, D., Owens, M., & Stevenson, J.C. 1996. A sediment chronology of the eutrophication of Chesapeake Bay. *Estuaries* **19**, 488–499.
- Cowan, J.W., & Boynton, W. 1996. Sediment-water oxygen and nutrient exchanges along the longitudinal axis of Chesapeake Bay: Seasonal patterns, controlling factors and ecological significance. *Estuaries* **19**, 562–580.
- Frossard, E., Achat, D.L., Bernasconi, S.M., Fardeau, J., Jansa, J., Morel, C., Randriamanantsoa, L., Sinaj, S., & Oberson, A. 2011. Phosphorus in action (E Bünemann, A Oberson, and E Frossard, Eds.). Springer Berlin Heidelberg, Berlin, Heidelberg.
- Griffin, T.S., Honeycutt, C.W., & He, Z. 2003. Changes in soil phosphorus from manure application. *Soil Science Society of America Journal* **67**, 645–653.
- Hagy, J.D., Boynton, W.R., Keefe, C.W., & Wood, K. V. 2004. Hypoxia in Chesapeake Bay, 1950–2001: Long-term change in relation to nutrient loading and river flow. *Estuaries* **27**, 634–658.
- Jaisi, D.P., & Blake, R.E. 2010. Tracing sources and cycling of phosphorus in Peru Margin sediments using oxygen isotopes in authigenic and detrital phosphates. *Geochimica et Cosmochimica Acta* **74**, 3199–3212.
- Jordan, T.E., Cornwell, J.C., Boynton, W.R., & Anderson, J.T. 2008. Changes in phosphorus biogeochemistry along an esturine salinity gradient: The iron conveyor belt. *American Society of Limnology and Oceanography* **53**, 172–184
- Kemp, M.W., & Boynton, W.R. 1984. Spatial and temporal coupling of nutrient inputs to estuarine primary production: The role of particulate transport and decomposition. *Bulletin of Marine Science* **35**, 522–535.
- Kemp, W.M., Sampou, P.A., Garber, J., Turtle, J., & Boynton, W.. 1992. Seasonal depletion of oxygen from bottom waters of Chesapeake Bay: roles of benthic and planktonic respiration and physical exchange processes. *Marine Ecology Progress Series* **85**, 137–152.

- Koop, K., Boynton, W.R., Wulff, F., & Carman, R. 1990. Sediment- water oxygen and nutrient exchanges along a depth gra- dent in the Baltic Sea. *Mar Ecol Prog Se* **63**, 65–77.
- Lehmann, J., Lan, Z., Hyland, C., Sato, S., Solomon, D., & Ketterings, Q.M. 2005. Long-term dynamics of phosphorus forms and retention in manure-amended soils. *Environmental Science & Technology* **39**, 6672–6680.
- Malone, T.C. 1991. River flow, phytoplankton production and oxygen depletion in Chesapeake Bay. *Geological Society, London, Special Publications Geological Society, London, Special Publications* **58**, 83–93.
- Murphy, R., Kemp, W.M., & Ball, W. 2011. Long-term trends in Chesapeake Bay seasonal hypoxia, stratification, and nutrient loading. *Estuaries and Coasts* **34**, 1293–1309.
- Olsen, S.R., Cole, C. V, Watanabe, F.S., & Dean, L.A. 1954. Estimation of available phosphorus by extraction with sodium bicarbonate. *USDA Circ. 939, U.S. Govt. Print. Office, Washington, D.C.*
- Pierzynski, G.M. 1991. The chemistry and mineralogy of phosphorus in excessively fertilized soils. *Critical Reviews in Environmental Control* **21**, 265–295.
- Prasad, M.B.K., Sapiano, M.R.P., Anderson, C.R., Long, W., & Murtugudde, R. 2010. Long-term variability of nutrients and chlorophyll in the Chesapeake Bay: A retrospective analysis, 1985–2008. *Estuaries and Coasts* **33**, 1128–1143.
- Read, D.W.L., Warder, F.G., Spratt, E.D., & Bailey, L.D. 1977. Residual effects of phosphorus fertilizer. I. For wheat grown on four chernozemic soil types in Saskatchewan and Manitoba. *Canadian Journal of Soil Science* **57**, 255–262.
- Ruttenberg, K.C. 1992. Development of a sequential extraction method for different forms of phosphorus in marine sediments. *Limnology and Oceanography* **37**, 1460–1482.
- Ruttenberg, K.C., & Berner, R.A. 1993. Authigenic apatite formation and burial in sediments from non-upwelling, continental margin environments. *Geochimica et Cosmochimica Acta* **57**, 991–1007.
- Testa, J.M., & Kemp, W.M. 2012. Hypoxia-induced shifts in nitrogen and phosphorus cycling in Chesapeake Bay. *Limnology and Oceanography* **57**, 835–850.

Chapter 2

TRANSFORMATION OF PHOSPHORUS POOLS IN AN AGRICULTURAL SOIL: AN APPLICATION OF OXYGEN-18 LABELING IN PHOSPHATE

2.1 Abstract

Phosphorus is a key ingredient for fertilizers, and there is no other substitute for P in sustaining life and food production. Excess P in soils may be fixed and become agronomically inactive or removed because of leaching and soil erosion. In this research, we aimed to explore how a particular P pool transforms into another pool by using ^{18}O labeled phosphate in an agricultural soil. We analyzed the changes in concentrations and oxygen isotope ratios ($\delta^{18}\text{O}_\text{P}$) of four inorganic (P_i) pools (H_2O , NaHCO_3 , NaOH , and HCl) along with soil chemistry to understand the roles of different biogeochemical processes changing isotopic composition. By monitoring $\delta^{18}\text{O}_\text{P}$ values of four P pools, an active transformation from $\text{H}_2\text{O}-\text{P}_\text{i}$ and $\text{NaHCO}_3-\text{P}_\text{i}$ to $\text{NaOH}-\text{P}_\text{i}$ and $\text{HCl}-\text{P}_\text{i}$ was identified. Transformation of originally bioavailable P to unavailable P such as $\text{HCl}-\text{P}_\text{i}$ allow us to conclude that a suite of $\text{HCl}-\text{P}_\text{i}$ with different $\delta^{18}\text{O}_\text{P}$ values could be precipitated from the originally cycled or bioavailable P pools. Thus, isotope technique allowed tracking of short-term transformation of readily bioavailable P to a less or non-bioavailable P pool and to discriminate biological and chemical reactions during transformation. These findings support the burgeoning applications of $\delta^{18}\text{O}_\text{P}$ as a tracer of P cycling in soil and are expected to be useful for fertilizer application as well as nutrient management in soils.

2.2 Introduction

Phosphorus is one of the most essential macronutrients for all living beings. Despite its occurrence at ~0.09 wt. % in Earth's crust and being a non-renewable resource, P is a sole source of fertilizer for food production. Increasing global demand for P after the agricultural revolution has rapidly depleted P reserves on the Earth (Cordell et al., 2009). By virtue of P chemistry, it mostly remains as sorbed (or occluded) species in soil, thus limiting the ability of plants to uptake all P applied to soil. This process results in the build-up of P in soil as "recalcitrant P" (extractable P by reagents used in sequential extraction but not directly bioavailable) and "residual P" (nonextractable P by sequential extraction reagents) pools that are not available for plants (Read et al., 1977). Researchers have claimed that long-term recovery of P applied to soils may be as high as 90%, assuming that fixed P in the soil may change slowly into available forms (Syers et al., 2008). However, this scenario may be less applicable to agricultural soils where fertilizers and animal wastes are constantly added, often beyond crop P uptake levels. In these soils, the concentrations of available P pools do not decrease to the level that promotes release of P from residual or recalcitrant P pools.

Phosphorus dynamics in soils are controlled to a significant extent by the complex interactions among competing biotic and abiotic reactions and processes. Sequential chemical extraction methods have long been used to differentiate operationally discrete P pools in soils such as bioavailable and recalcitrant P pools, and determine supplemental P requirements for plants (Chang & Jackson, 1957; Shelton & Coleman, 1968; Hedley et al., 1982; Tiessen et al., 1984; He et al., 2012). The most commonly used sequential extraction method developed by Hedley et al. (1982), separates soil P pools into $\text{H}_2\text{O-P}_i$, $\text{NaHCO}_3\text{-P}_i$, NaOH-P_i , and HCl-P_i (Hedley

et al., 1982; Tiessen et al., 1984; Negassa & Leinweber, 2009). Among these pools, $\text{H}_2\text{O-P}_i$ and $\text{NaHCO}_3\text{-P}_i$ are considered bioavailable (Olsen et al., 1954; Bowman et al., 1978; Tiessen et al., 1983), but NaOH-P_i can be moderately bioavailable in the long-term or unavailable depending on relative P concentrations in different P pools and efficiency of specific plants to take up NaOH-P_i (Tiessen et al., 1983; Sharpley, 1985; Zhang & MacKenzie, 1997). The HCl-P_i pool is not directly bioavailable, at least for crop plants. There are, however, several indirect mechanisms that plant roots may act on to dissolve and thus access HCl-P_i , for example by manipulating specific microorganisms on their roots or through induction of metabolic processes such as P starvation-induced organic acid production (Guo et al., 2000; Richardson, 2001; Khan & Joergensen, 2009; Richardson & Simpson, 2011). The extent to which these mechanisms operate in agricultural soils and mobilize non-bioavailable P is expected to be low or insignificant, particularly due to application of fertilizers and manures often in excess of plant needs.

Phosphate O isotope ratios ($\delta^{18}\text{O}_\text{P}$) have increasingly been applied to understand the physicochemical and biological pathways of P cycling and fate of P in agricultural and non-agricultural soils (Larsen et al., 1989; Johansen et al., 1990; Zohar et al., 2010; Angert et al., 2012; Tamburini et al., 2012). In biological systems, rapid O isotope exchange between water and phosphate results in an equilibrium isotopic composition controlled by ambient water O isotope ratios ($\delta^{18}\text{O}_\text{w}$) and temperature (Longinelli & Nuti, 1973; Blake et al., 1997; Paytan et al., 2002; Jaisi et al., 2010; Jaisi & Blake, 2010; Joshi et al., 2015). However, in abiotic systems isotope exchange between water and phosphate, including sorption, desorption, mineral transformation, and subsurface transport is negligible at low temperature ($<70^\circ\text{C}$) and

circumneutral pH (Lecuyer et al., 1999; O'Neil et al., 2003; Jaisi et al., 2010; Jaisi, 2013; Li & Jaisi, 2015). These fundamentally distinct properties of $\delta^{18}\text{O}_\text{P}$ in abiotic and biotic reactions provide the potential means to apply this as a tracer to study complex P interactions between abiotic and biotic processes in soils and other environments.

The ^{18}O -enrichment as well as natural abundance studies have greatly helped to elucidate the roles of microbial cycling in different soil P pools (Larsen et al., 1989; Johansen et al., 1990; Zohar et al., 2010; Weiner et al., 2011; Angert et al., 2011). Laboratory synthesized ^{18}O -labeled P_i has been used to identify the changes in $\delta^{18}\text{O}_\text{P}$ during biological cycling at the interface and to develop indirect proxies for microbial activity (Jaisi et al., 2011; Stout et al., 2014). Sequential extraction of P pools and measurement of their corresponding $\delta^{18}\text{O}_\text{P}$ values in sediments (Jaisi & Blake, 2010) and soils (Zohar et al., 2010; Tamburini et al., 2012; Amelung et al., 2015) have enabled identification of sources as well as biogeochemical processes for the formation of specific P pool. Overall, these studies have provided enough evidence for successful application of isotope tools to differentiate P pools in soils. The objectives of this research, therefore, are to develop a mechanistic understanding of (i) the formation of fixed P (Fe- and Al- oxide-bound P pool and precipitated P as Ca-apatite) and ii) the interplay of biotic and abiotic reactions involved in soil P cycling, and (iii) investigate potential routes of precipitation of HCl-P_i with a range of isotope compositions. To realize these objectives, we applied ^{18}O labeled P_i in soil and tracked O-isotope compositions of different P_i pools with time. Our results show a rapid but step-wise P transformation in soil that eventually converts originally bioavailable P into unavailable Ca-P minerals.

2.3 Materials and methods

2.3.1 Site description and soil characterization

The site selected for ^{18}O labeled P_i tracer study was the Agricultural Experiment Station in Newark, DE (latitude $39^\circ 40'$ N longitude $75^\circ 45'$ W) at the University of Delaware. This site is located on the Piedmont Plateau and the dominant soil order is Ultisol (80–90%) (Pautler & Sims, 2000). It has been used for corn (*Zea mays* L.) and soybean [*Glycine max* (L.) Merr.] fertility research for decades and has always received phosphate fertilizer ($\sim 200 \text{ kg ha}^{-1}$). It is chisel ploughed ($\sim 30 \text{ cm}$ depth) every year before the start of a growing season. The water table is about $\geq 0.5 \text{ m}$ below the ground surface and therefore the major part of biologically active soil remains mostly unsaturated. It is drip irrigated, as needed, during the growing season. The site receives an annual rainfall of $\sim 120 \text{ cm}$, which in general, is spread evenly throughout the months, and average topsoil temperature in the cold winter months is $2 \pm 1^\circ\text{C}$ and in the warm summer months $23 \pm 2^\circ\text{C}$ (Delaware Environmental Observing System, 2014).

To quantify P_i pools and their corresponding isotopic compositions in the soil after application of ^{18}O labeled P, soil cores were collected at the start, middle, and end of the experiment using a Hoffer soil sampler (2.54 cm i.d.) at an interval of 2 cm up to a total depth of 80 to 125 cm. The control plot that did not receive ^{18}O labeled P was sampled before and at the end of the experiment at an interval of 7.5 cm. No other fertilizers were applied to either of the field plots. We took three to four soil cores at each sampling time and combined core slices sectioned from the same depth intervals. A fraction of the core was put inside an airtight tube immediately after slicing to extract soil pore water for measurement of water O isotope ratios ($\delta^{18}\text{O}_w$). Soil

temperature was measured by inserting a stem thermometer at selected soil depths into intact soil. The collected soil cores were freeze dried, ground thoroughly, and size separated ($<200\ \mu\text{m}$) and then analyzed for physical and chemical properties. This included the grain size distribution, pH, organic C content, Mehlich-3 P, total P, and concentrations of elements that are relevant to P cycling (Fe, Al, and Ca) (Table 2.1). We used Mehlich-3, a widely used soil test method in agronomy particularly to identify P requirements for optimum crop yield, to compare results obtained from sequential extraction. Mehlich-3 extraction reagents included $0.2\ \text{mol L}^{-1}\ \text{CH}_3\text{COOH}$, $0.25\ \text{mol L}^{-1}\ \text{NH}_4\text{NO}_3$, $0.015\ \text{mol L}^{-1}\ \text{NH}_4\text{F}$, $0.013\ \text{mol L}^{-1}\ \text{HNO}_3$, and $0.001\ \text{mol L}^{-1}$ ethylenediaminetetraacetic acid (Mehlich, 1984). Pristine soil (before sequential extraction) as well as residual soil after the last step of sequential extraction (i.e. after $1\ \text{mol L}^{-1}\ \text{HCl}$ treatment) were dissolved using microwave digestion to identify total and residual P and other elements that are relevant for P cycling (Fe, Al, and Ca) (Table 2.2). The concentrations of P and these elements in solution were measured by using inductively coupled plasma emission spectrometry.

2.3.2 Application of ^{18}O labeled phosphate and soil sampling

The ^{18}O -labeled P_i was synthesized by reacting PCl_5 (Sigma- Aldrich) with ^{18}O labeled water (Melby et al., 2011; Stout et al., 2014). After synthesis, the P_i concentration of the solution was diluted (to $250\ \mu\text{mol L}^{-1}$) and pH was neutralized (pH 6.6) to be the same as the field soil pH. A calibrated fixed spray nozzle was used to apply labeled P_i (38.0‰) on a rectangular area (4.6 by 1.8 m) at the rate of $\sim 110\ \text{kg ha}^{-1}$, a rate within the ranges of fertilization practices being used in the region. Soil samples were collected, as above six different times (4, 18, 31, 64, 96, and 155 d),

chosen based on the rate of isotope exchange identified from the pilot experiment in the same field. The soil cores were processed using the method described above.

Table 2.1 Physical and Chemical properties of soils collected from four depths.

Depth	pH [‡]	Density	Total P [§]	M3-P [¶]	OM	Sand	Silt	Clay
cm		g cm ⁻³	mg kg ⁻¹			%		
0-7.5	6.3	1.03	914.35 ±0.03 [†]	212.71 ±0.30	2.5	15	61	24
22.5-30	6.3	1.17	692.62 ±0.03	142.73 ±0.02	1.7	13	59	28
37.5-45	5.7	1.08	469.1 ±0.01	48.96 ±0.01	1.4	9	61	30
75-82.5	5.3	1.09	488.27 ±0.05	74.36 ±0.05	1.4	11	57	32

‡ Soil pH values were measured at a 1:1 soil/water ratio

§ Total P was measured after microwave digestion of soil by using inductively coupled plasma optical emission spectrometry.

¶ Mean ± standard deviation

2.3.3 Extraction of soil phosphate pools

To differentiate and quantify four different P pools (H₂O-P_i, NaHCO₃-P_i, NaOH-P_i, and HCl-P_i) in the control and experimental soils, we applied the sequential extraction technique originally developed by Hedley et al. (1982) and revised by Tiessen et al. (1984) with slight modifications. Our modifications were aimed at restricting the redistribution of extracted P onto residual solid surfaces. This included additional extraction steps with 0.5 mol L⁻¹ NaHCO₃ and/or H₂O after a particular reagent was used for extracting targeted P pool (analogous to the method of Ruttenberg, 1992). The concentration of P_i in each pool that are relevant for P cycling was measured by using the phosphomolybdate blue method (Murphy & Riley, 1962). Total P was measured after persulfate digestion (Rowland & Haygarth, 1997), and the organic P (P_o) was calculated as the difference between TP and P_i. Extracted

supernatants for a particular P pool were then combined and stored at 4 °C before processing and purification for Ag₃PO₄ precipitation.

Table 2.2 Elemental concentration of P, Fe, Al, and Ca in soils at different depths measured by inductively coupled plasma optical emission spectrometry before and after sequential extraction.

Depth	Before extraction				After extraction			
	P	Fe	Al	Ca	P	Fe	Al	Ca
cm	mg kg ⁻¹				mg kg ⁻¹			
0-2	1013	16841	16425	1240	180	11603	8135	142
2-4	883	16400	12222	1264	205	12967	7875	145
4-6	824	16317	14360	1081	213	13359	9701	155
8-10	849	17502	13957	1115	213	13274	11948	201
10-12	868	17553	16573	1152	197	12544	8992	143
14-16	918	18814	20728	1289	237	15848	12707	199
36-38	369	23352	17308	713	195	18346	13176	170
56-58	329	24164	19233	775	170	17667	10074	110
74-76	347	25977	21015	834	174	17387	11310	122

2.3.4 Sample purification and measurement of phosphate oxygen isotope ratios

All P pools were further processed to remove contaminants and concentrate the P_i before being converted to Ag₃PO₄ for isotope analyses. Given that different P pools contain a variable amount of P_o, particularly in NaHCO₃ (8–27%) and NaOH (12–30%) extractions (Table 2.3), P_o has to be removed because any hydrolysis of P_o compounds incorporates the light water O-isotope with negative fractionation factors (Liang & Blake, 2006, 2009) in the released P_i and thus compromises the original P_i O-isotope signature. Hence, we used non-ionic, macro-porous DAX 8 Superlite resin

to remove dissolved organic matter (Tamburini et al., 2010). The DAX resin is moderately polar and is good for separation and removal of surfactants, fulvic and humic acids, and other hydrophobic organic compounds with molecular weight up to 150,000. Soil extracts from shallow depths required two DAX resin treatments. In selected samples, we measured TP and P_i (by colorimetry) before and after resin treatment to compare the efficiency of DAX resin to trap organic matter as well as to identify any P_i loss (Table 2.3). The clear solution thus produced was further processed to reduce its volume and to concentrate P_i by the magnesium induced coprecipitation (MagIC) method (Karl & Tien, 1992). It was important to generate finely dispersed $Mg(OH)_2$ colloids to maximize trapping P_i in MagIC and to maintain homogeneous dispersion of colloids throughout the reaction. The MagIC suspension was centrifuged and pellets were separated. We measured the concentration of P_i in the residual supernatant after a 1.0 to 1.5 log order decrease in volume (by evaporation) to ensure removal of P_i by MagIC. The MagIC pellets were dissolved in $0.5 \text{ mol L}^{-1} \text{ HNO}_3$ by vortexing the mixture before and right after the addition of acid to maximize the dissolution and to minimize time action of acid. In selected samples, we used ^{18}O -spiked acid to test residual P_o hydrolysis during MagIC pellet dissolution. The dissolved solution from selected pools ($\text{NaHCO}_3\text{-P}$ and NaOH-P pools) was passed one more time through DAX 8 resin to trap residual organic compounds.

Precipitation of ammonium phosphomolybdate (APM) and subsequent steps followed the methods described in Jaisi and Blake (2010, 2014) and were finally precipitated as Ag_3PO_4 , the ultimate analyte for O isotope measurement. For this step, MagIC dissolved samples were evaporated to attain final concentration of ~ 500 to $1000 \text{ } \mu\text{mol L}^{-1}$ before APM precipitation. The acidic APM precipitation allowed

removing contaminants that are soluble in low pH. Precipitates were removed, washed, dissolved, and precipitated as magnesium ammonium phosphate (MAP) at high pH, where contaminants soluble at high pH were washed off. The MAP crystals were then dissolved, pH neutralized, and further treated with a cation resin to remove cations. A separate P standard and a replicate sample for which ^{18}O labeled water (with final $\delta^{18}\text{O}_w$ values = 50.0‰) was spiked in all reagents were processed in parallel with samples to test the validity of sample processing and to identify hydrolysis of P_o during sample treatment, if any.

Table 2.3 Organic P concentration in NaHCO_3 and NaOH extracted pools before and after the DAX 8 Superlite resin treatment.

Depth cm	Total organic P			
	NaHCO_3		NaOH	
	Before	After	Before	After
4–6	26	6	28	2
14–16	27	3	29	6

A Thermo-Chemolysis Elemental Analyzer (TC/EA) coupled to a Delta V continuous flow isotope ratio monitoring mass spectrometer (IRMS, Thermo-Finnigan; precision of 0.3‰) was used to measure $\delta^{18}\text{O}_P$ values. The measured $\delta^{18}\text{O}_P$ values were calibrated against YR1-1aR2 and YR3-2 standards that were originally calibrated using a conventional fluorination method (Vennemann et al., 2002). The yield of O during pyrolysis was calculated based on the mass and O content in Ag_3PO_4 precipitate and those with acceptable yield (>90%) were included for isotope analyses. We used several prong tests to identify successful removal of dissolved organic carbon

(DOC) from the samples (Jaisi and Blake, 2010). First, the results from isotope-enriched water spiked samples did not show any significant difference in $\delta^{18}\text{O}_\text{P}$ values means no significant hydrolysis occurred. If there was extraneous O incorporation, there should be corresponding change in the $\delta^{18}\text{O}_\text{P}$ values. This is because, due to the unusually large fractionation factors (Liang and Blake, 2006, 2009; Jaisi et al., 2010), and much lighter isotopic composition of water, organic P hydrolysis could be easily identified from corresponding changes in isotope values. Second, comparing theoretical O yield to the Ag_3PO_4 samples to that of phosphate oxygen isotope standards (in the form of Ag_3PO_4) gives strong evidence on any presence of extraneous material including DOC. Any N contamination (from DOC or inorganic sources) is clearly seen in IRMS chromatogram because of the same mass of N_2 and CO, and yet N_2 elutes faster than CO. Third, the presence of C and N contaminants in selected Ag_3PO_4 precipitates was also tested in the elemental analyzer (which is used for C and N isotopes) because the elemental analyzer has a greater sensitivity to detect small masses. This test did not show any of C and N content. The few samples that showed the presence of C and N were rejected and not included for isotope analysis. The $\delta^{18}\text{O}_\text{P}$ values given here are reported relative to the Vienna Standard Mean Oceanic Water (in ‰).

2.4 Results and Discussion

2.4.1 Soil properties

The key soil properties from four different soil depth intervals are shown in Table 2.1. As expected, organic matter content and concentrations of total and Mehlich-3 P were high in surface soils and decreased with depth. The surface soil was

slightly acidic (pH 6.3) from long-term fertilizer application and the acidity was found to increase (5.3 to 5.7) in deeper soil horizons (37.5–45 and 75.0–82.5 cm). Based on sand, silt, and clay content, the soil at 0 to 7.5 cm depth horizon belongs to the silt loam class, whereas deeper soils are silty clay loam, according to the USDA soil classification system.

2.4.2 Phosphate pools and isotopic compositions in the control site

Concentrations of four extracted P_i pools and their isotopic compositions in the control plot are shown in Figure 2.1. As expected, P_i concentrations of almost all pools were high at the shallow depth (0–21.5 cm), decreased sharply below it (e.g., the sum of all extractable P_i pools decreased by 57% at ~40 cm), and became relatively constant for depths ≥ 40 cm. This trend in P concentration is consistent with several other silty and clay loamy agricultural soils in Delaware (Mozaffari & Sims, 1994) and indicates most active P cycling is limited to shallow depth (<40 cm) due to several factors including tilling, P application, uptake and recycling of P pools by microorganisms and crops in the soil.

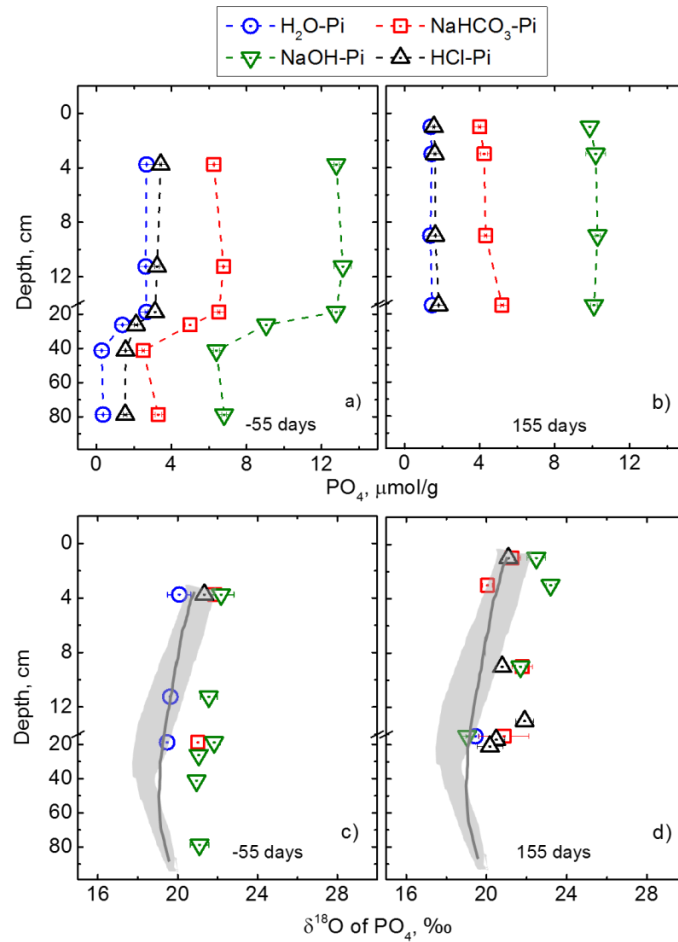


Figure 2.1 (a,b) Concentrations and (c,d) isotopic compositions of four inorganic P (P_i) pools (H_2O - P_i , $NaHCO_3$ - P_i , $NaOH$ - P_i , and HCl - P_i) in the control plot (without application of ^{18}O labeled P_i) (a, c) 55 d before and (b, d) 155 d after the start of the experiment. The dark grey lines indicate equilibrium $\delta^{18}O_P$ composition calculated from measured water $\delta^{18}O_w$ values and temperature at the time of sampling, and the shaded regions correspond to that of daily average of the sampling month.

In general, relative order of P_i concentrations was $NaOH$ - $P_i > NaHCO_3$ - $P_i > HCl$ - $P_i > H_2O$ - P_i in all soil depths (Fig. 2.1a and 2.1b). The highest amount of P_i in $NaOH$ fraction among all P pools indicates that this pool (i.e., tightly bound P to Fe and Al minerals) (Hedley et al., 1982; Tiessen et al., 1984; Wagar et al., 1986), is the

major sink of P in this soil. This result is consistent with similar studies in other acidic and circumneutral pH soils (Tiessen et al., 1984; Beck & Sanchez, 1994; Zhang & MacKenzie, 1997; Guo et al., 2000). Overall, the sum of all sequentially extracted P_i accounted for ~76 to 84% of TP in the soil, measured from microwave digestion of the soil (Table 2.2). The residual P (i.e., P remaining in the soil after sequential extraction) accounted for about 15 to 25% of TP at shallow depths (0–16 cm) and ~50% at deeper depths (36–76 cm). This indicates a relatively small fraction of TP was present as P_o and residual P in shallow depth. Because the concentration of the residual P pool did not change significantly at different sampling times, the formation or removal of P from this pool was considered negligible.

The isotopic compositions of $\text{NaHCO}_3\text{-}P_i$ and $\text{NaOH-}P_i$ were consistently similar for the entire depth (0–80 cm) (Fig. 2.1c and 2.1d). If significant P_o hydrolysis occurred during our sample processing and contributed to $\delta^{18}\text{O}_P$ values, we should be able to see a corresponding change (towards lighter isotope composition), particularly in shallow depth because of high P_o content in $\text{NaHCO}_3\text{-}P_i$ and $\text{NaOH-}P_i$ pools. This result alternatively proves that the methods used to remove P_o compounds (Table 2.3) and as well as ^{18}O water spiking tests were sufficient to avoid P_o hydrolysis.

The $\delta^{18}\text{O}_P$ values of $\text{H}_2\text{O-}P_i$ were found to be lighter by 1.5 to 2.0‰ than the other three pools (Fig. 2.1c). We calculated equilibrium $\delta^{18}\text{O}_P$ by using the Longinelli and Nuti (1973) equation from (i) measured water isotope composition ($\delta^{18}\text{O}_w = -3.8$ to -5.2 ‰) and measured temperature ($4.5\text{--}6.0^\circ\text{C}$) at different depths on the sampling date (shown by line traces), and ii) ambient soil temperature for the sampling month in the past 5 yr ($2.3 \pm 5.5^\circ\text{C}$) (Delaware Environmental Observatory System, 2014) shown by the gray zone. The $\delta^{18}\text{O}_P$ values of $\text{H}_2\text{O-}P_i$ lie within the ranges of equilibrium

isotopic composition. It means this P_i pool was fully cycled by microorganisms even in winter when soil temperature is low and even frozen on several days. Similar results of complete equilibration, however, have been found in other soils in subtropical and temperate climate zones in Israel and Switzerland (e.g., Zohar et al., 2010; Tamburini et al., 2012).

2.4.3 Phosphate pools and isotopic compositions in oxygen-18- labeled inorganic phosphorus applied site

Sequentially extracted soil P pools 1 d before and 18 d after the application of ^{18}O labeled P_i showed an immediate increase in concentration of H_2O-P_i and $NaHCO_3-P_i$ pools by 236 and 29%, respectively, at 0 to 2 cm (Fig. 2.2a and 2.2b), confirming that the applied P_i readily partitioned into at least these two pools. Interestingly, there was also a small increase in $NaOH-P_i$ (~10%) and no detectable change in the $HCl-P_i$ pool. Soil P pools at a depth ≥ 4 cm were less impacted by the application of labeled P_i than those on the surface, and the general depth- P_i concentration trend remained essentially similar to the pre-application stage.

By 155 d, labeled P_i was found to be redistributed in all four pools (H_2O-P_i , $NaHCO_3-P_i$, $NaOH-P_i$, and $HCl-P_i$; Fig. 2.2c). For example, at the 0 to 2 cm depth, concentration of H_2O-P_i decreased by ~50% (compared to 18 d after labeled P_i application), while $NaOH-P_i$ increased by ~10% but $NaHCO_3-P_i$ and $HCl-P_i$ did not show any appreciable change. Although no major change was observed in the $NaHCO_3-P_i$ pool, this pool was expected to be more dynamic because it behaves as an intermediate P pool for exchange between $NaOH-P_i$ and H_2O-P_i pools (Beck & Sanchez, 1994; Waldrip-Dail et al., 2009). A similar increase in the $NaOH-P_i$ pool was found in ^{33}P labeled and soil incubation studies in the time frame spanning from

several days to months (Daroub et al., 2000; Waldrip-Dail et al., 2009) as well as long-term (>25 yr) research in externally P applied agricultural soils (Lehmann et al., 2005). These results are consistent with the fact that this pool is considered to be the major P_i sink in agricultural soils (Beck & Sanchez, 1994; Richards et al., 1995; Zhang & MacKenzie, 1997).

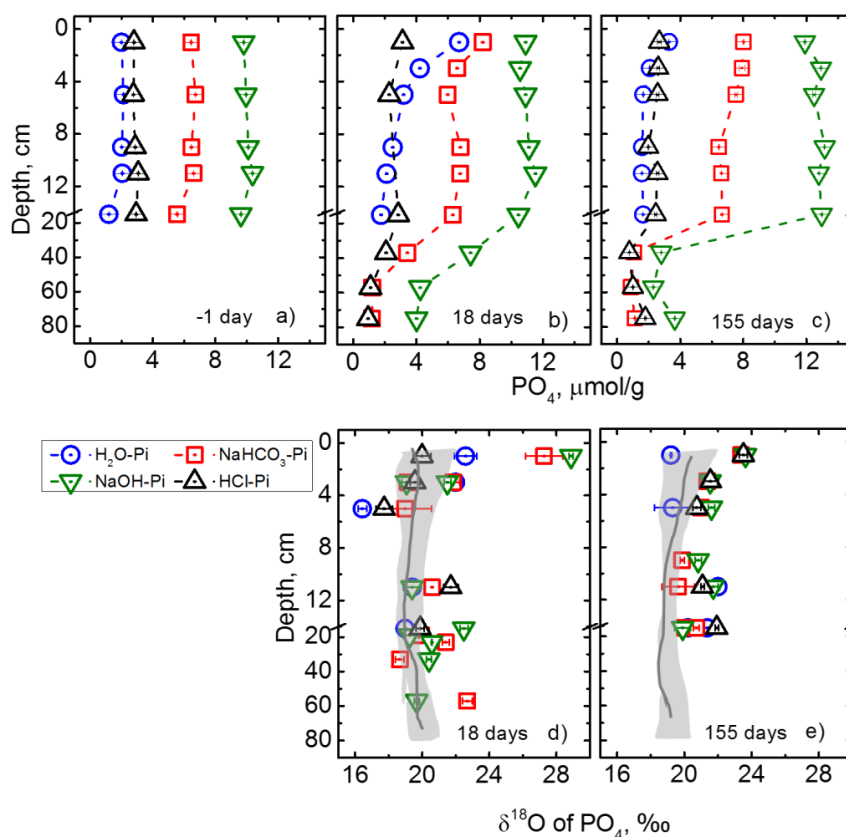


Figure 2.2 (a,b,c) Concentrations and (d,e) isotopic compositions of four inorganic P (P_i) pools ($H_2O\text{-}P_i$, $NaHCO_3\text{-}P_i$, $NaOH\text{-}P_i$, and $HCl\text{-}P_i$) in the experimental plot before and after application of ^{18}O labeled P_i (38‰) at (a) 1 d before, and (b,d) 18 d and (c, e) 155 d after the start of the experiment. The dark grey lines indicate equilibrium $\delta^{18}O_P$ composition calculated from measured pore-water $\delta^{18}O_w$ values and temperature at the time of sampling, and the shaded regions correspond to the daily average of the sampling month.

In vertical profile, a clear trend in the changes in P concentrations was observed by 155 d. For example at 2 to 4 cm depth, $\text{NaHCO}_3\text{-P}_i$ and NaOH-P_i pools increased by 20 and 22%, respectively (compared with 18 d after labeled P_i application), suggesting vertical transport or leaching of applied P_i into deeper soil horizons, albeit a few cm below top soil. All soil P_i pools sharply decreased below ~40 cm depth and remained relatively constant and similar to the control plot at deeper (≥ 40 cm) soil depths.

The isotope composition of different P pools showed an interesting trend. Consistent with the build-up of $\text{H}_2\text{O-P}_i$, $\text{NaHCO}_3\text{-P}_i$, and NaOH-P_i pools over 18 d after ^{18}O labeled P_i application, there were corresponding changes in $\delta^{18}\text{O}_\text{P}$ values of these pools (Fig. 2.2d). Isotope ratios and mass balance calculated from measured concentrations and $\delta^{18}\text{O}_\text{P}$ values of different P pools before and after the application of labeled P_i showed that the new $\delta^{18}\text{O}_\text{P}$ values of $\text{H}_2\text{O-P}_i$, $\text{NaHCO}_3\text{-P}_i$, and NaOH-P_i pools (in 18 d) should be ~33, 26, and 25‰, respectively. Measured $\delta^{18}\text{O}_\text{P}$ values of $\text{H}_2\text{O-P}_i$ were ~10‰ lighter than the calculated value, suggesting that the biological uptake and cycling of this P pool resulted in its lighter (i.e., approach towards equilibrium) isotopic composition. Interestingly, the measured $\delta^{18}\text{O}_\text{P}$ values of $\text{NaHCO}_3\text{-P}_i$ were similar to the calculated values, indicating that the labeled P_i partially transferred into this P pool without much biological cycling by this sampling time. The measured $\delta^{18}\text{O}_\text{P}$ values of NaOH-P_i were slightly heavier than the calculated value but within narrow ranges.

The isotopic compositions of $\text{H}_2\text{O-P}_i$, $\text{NaHCO}_3\text{-P}_i$, and NaOH-P_i pools at 155 d (~5 mo) after labeled P_i application showed complex P dynamics in the soil (Fig. 2.2e). For example, the $\delta^{18}\text{O}_\text{P}$ values of $\text{H}_2\text{O-P}_i$ at 0 to 2 cm were found to be in

equilibrium with the measured water O isotope values and soil temperature at the time of sampling. Similarly, $\delta^{18}\text{O}_\text{P}$ values of both $\text{NaHCO}_3\text{-P}_i$ and NaOH-P_i were lighter than those at 18 d after labeled P_i application (Fig. 2.2d) but still were 2 to 3‰ heavier than equilibrium $\delta^{18}\text{O}_\text{P}$ values. These results indicated that these pools were derived from P pools that became progressively lighter than the original $\delta^{18}\text{O}_\text{P}$ values of the labeled P_i (see below).

The trend in the evolution of $\delta^{18}\text{O}_\text{P}$ values of HCl-P_i after labeled P_i application was different from other P pools. For example, it remained essentially constant with depth in the soil (before application of ^{18}O labeled P_i) and did not follow the calculated depth-equilibrium trend. After the application of ^{18}O labeled P_i , $\delta^{18}\text{O}_\text{P}$ values of the HCl-P_i pool remained relatively uninfluenced for a long time and then increased by $\sim 3.5\%$ at 155 d (Fig. 2.2e). This indicates precipitation of Ca-P minerals from P pools derived from labeled P_i . This raises an interesting point on sources and pathways of HCl-P_i (see below).

The majority of isotope data for the $\text{NaHCO}_3\text{-P}_i$, NaOH-P_i , and HCl-P_i pools showed similar trends with depth, except several of them showed wide fluctuation, albeit largely within equilibrium values if these data were extrapolated to the surface. This extrapolation is relevant because shallow soils (<30 cm) were physically mixed due to tilling (in the previous season before the application of labeled P_i) and hence could have leached to deeper soils. However, a similar trend in deeper (as deep as 80 cm) soils potentially indicated the formation of new $\text{NaHCO}_3\text{-P}_i$ and NaOH-P_i pools at these depths. This, in turn, indicates differential reactivity of different P pools across soil depth in response to their availability to plants and soil microorganisms and phase transformations that may form or consume a specific P pool.

2.4.4 Dynamics of concentrations and isotopic compositions of phosphorus pools: Interplay of biotic and abiotic reactions

An in-depth temporal analysis of distinct isotope excursion of H₂O-P_i, NaHCO₃-P_i, NaOH-P_i, and HCl-P_i pools can provide additional information on the sources or biogeochemical processes involved on the formation as well as transformation of these P pools. The rate of change of $\delta^{18}\text{O}_\text{P}$ values of the H₂O-P_i pool was found to be faster than that of the other P pools, as expected, as a result of faster isotope exchange with water, and this pool approached equilibrium isotopic composition. This is consistent with the fact that H₂O-P_i is the most bioavailable pool. Diverse communities of microorganisms play an active role in soil P cycling (e.g., Richardson, 2001; Khan and Joergensen, 2009; Richardson and Simpson, 2011), and quantifying their individual activity is difficult. However, all microorganisms catalyze P_i-H₂O O isotope exchange, and this activity is reflected in corresponding changes in $\delta^{18}\text{O}_\text{P}$ values (Blake et al., 2001, 2005; Stout et al., 2014), particularly when $\delta^{18}\text{O}_\text{P}$ values of the starting P pool are off from equilibrium isotopic composition, and thus it has been proposed as an indirect proxy for microbial activity. Our results are consistent with these past studies and add to the fact that isotope exchange could be used to understand the relative bioavailability and cycling of different P pools in soils.

The rate of isotope excursion of NaHCO₃-P_i pool was slower than that of H₂O-P_i, and still 2 to 3‰ heavier than that of equilibrium $\delta^{18}\text{O}_\text{P}$ values at 155 d. These results are consistent with those obtained from controlled laboratory sorption-desorption experiments (Jaisi et al., 2010; Li and Jaisi, 2015) showing that this pool is taken up by biota after H₂O-P_i is drawn first and that NaHCO₃-P_i is bioavailable (Olsen et al., 1954; Bowman et al., 1978; Tiessen et al., 1983). Given that biological cycling tends not to accumulate NaHCO₃-P_i but changes its $\delta^{18}\text{O}_\text{P}$ values, an almost

constant concentration but different isotopic composition provides evidence that this pool is biologically recycled and speciated again, at least partly, as $\text{NaHCO}_3\text{-P}_i$. This, in turn, highlights the importance to understand P cycling, which is a more important parameter for nutrient management than P speciation.

The isotope composition of NaOH-P_i at 18 and 155 d after labeled P_i application (Fig. 2.2 d and 2.2e) was essentially similar but still 2 to 3‰ heavier than that of equilibrium $\delta^{18}\text{O}_\text{P}$ values. The NaOH-P_i is considered moderately bioavailable depending on the soil P conditions and plant efficiency of P uptake (Tiessen et al., 1983; Zhang & MacKenzie, 1997; Guo et al., 2000). We interpret the heavier isotopic composition of the NaOH-P_i pool as being due to the transformation of other P_i pools (that have relatively heavier $\delta^{18}\text{O}_\text{P}$ values such as $\text{H}_2\text{O-P}_i$ or $\text{NaHCO}_3\text{-P}_i$) to the NaOH-P_i pool. This means that a portion of the $\text{H}_2\text{O-P}_i$ and $\text{NaHCO}_3\text{-P}_i$ pools transformed into NaOH-P_i while these pools underwent active microbial cycling and their $\delta^{18}\text{O}_\text{P}$ values approached equilibrium (lighter) isotopic composition. It is, however, important to emphasize that actual microbial cycling of the NaOH-P_i pool itself is less likely change $\delta^{18}\text{O}_\text{P}$ values of the residual NaOH-P_i pool because microbial uptake removes P and most likely transforms it into the $\text{H}_2\text{O-P}_i$ and/or $\text{NaHCO}_3\text{-P}_i$ pool. A schematic diagram showing the varying rate of isotope excursion of the different P pools towards equilibrium isotopic composition and the formation of new P pools during this excursion is included in Fig 2.3. As indicated, a suite of biological processes and chemical reactions (isotope exchange and ion exchange, respectively; Jaisi et al., 2011) change the original isotope identity of $\text{H}_2\text{O-P}_i$ and $\text{NaHCO}_3\text{-P}_i$ pools. These processes also change the isotopic composition of the newly formed P_i pool as several generations of P_i accumulate and coexist with time. For example, HCl-P_i can

be formed from three other P_i pools at any time during their excursion towards equilibrium isotopic composition. These explanations are consistent with results from a previous study (Jaisi & Blake, 2010) where several generations of Ca-P minerals precipitating at different times were found to coexist in a sediment.

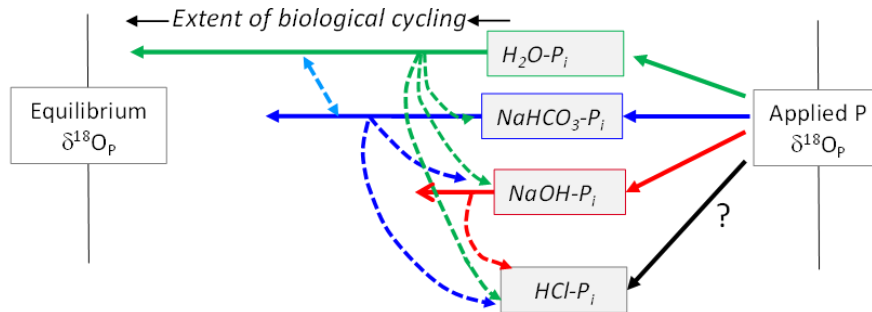


Figure 2.3 Schematic diagrams showing P speciation and transformations. The relative length of an arrow corresponds to the extent of biological cycling of a particular P pool (H_2O-P_i , $NaHCO_3-P_i$, $NaOH-P_i$, and $HCl-P_i$). The dashed arrows (uni- or bidirectional) of different colors indicate transfer of P from one pool to another. Illustrations do not consider long-term reactions such as potential dissolution and remobilization of $HCl-P_i$.

The results obtained from this study can be summed up to generalize the P cycling pathway as follows. Externally applied P disturbs the chemical equilibria of existing soil P pools as it speciates first into dissolved and weakly sorbed P (H_2O-P_i and $NaHCO_3-P_i$) pools. These two P_i pools are actively taken up and recycled by microorganisms and plants. Depending on the extent of microbial cycling and the length of time a particular P pool cycles, it is important to emphasize that the original isotopic composition of externally applied P could be (i) overprinted as it approaches

equilibrium isotopic composition or ii) partially or fully retained if it transforms into recalcitrant P pools. This generalization deduced from our results is consistent with several past studies (e.g., Jaisi and Blake, 2010; Stout et al., 2014) and adds new important information that (i) bioavailable P ($\text{H}_2\text{O-P}_i$ and $\text{NaHCO}_3\text{-P}_i$) pools are partially transformed into the NaOH-P_i pool and are finally precipitated as Ca-P minerals (HCl-P_i pool), and (ii) even if the concentration of a particular P pool is constant with time (without net loss or gain), it may still undergo significant biological cycling (i.e., formation or removal). This brings up a unique application of isotope tools to discriminate these changes.

2.4.5 Variable sources and pathways of hydrochloric acid extractable inorganic phosphorus

The HCl extractable P pool corresponds to crystalline Ca-P minerals such as apatite, and the formation of HCl-P_i at the expense of other P pools has been interpreted from its changing concentration with time (McKenzie et al., 1992; Richards et al., 1995; Lehmann et al., 2005). Pathways that lead to the formation of HCl-P_i can be better understood by comparing $\delta^{18}\text{O}_P$ values of the $\text{NaHCO}_3\text{-P}_i$, and NaOH-P_i pools (i.e. $\sim 27 \pm 1$ and $29 \pm 0.1\%$, respectively) in 18 d and then among the $\text{NaHCO}_3\text{-P}_i$, NaOH-P_i and HCl-P_i pools at 155 d (Fig. 2.2d and 2.2e). Lighter $\delta^{18}\text{O}_P$ values of $\text{NaHCO}_3\text{-P}_i$ than NaOH-P_i suggests that the labeled P_i probably did not instantly transfer to the NaOH-P_i pool and a portion of $\text{NaHCO}_3\text{-P}_i$ continued to be biological cycled after being transformed to NaOH-P_i (Fig. 2.3). Please note that $\delta^{18}\text{O}_P$ values of $\text{NaHCO}_3\text{-P}_i$ and NaOH-P_i in the soil before ^{18}O labeled P_i application (control plot) were essentially the same (21.5 ± 0.3 and $21.8 \pm 0.4\%$, respectively, for 0–21 cm depth; Fig. 2.1c). Interestingly, before 155 d $\delta^{18}\text{O}_P$ values of HCl-P_i

remained constant ($20 \pm 1\%$), meaning that it did not pick up any derivative of labeled P_i . Furthermore, any residual or undissolved fertilizer applied in the field in previous growing seasons should not contribute to a change in $\delta^{18}O_P$ values of HCl- P_i because the farm never received rock fertilizer that has limited solubility. Any increase in $\delta^{18}O_P$ values is only possible if HCl- P_i originated from any derivative of ^{18}O labeled P_i . Because H_2O - P_i and $NaHCO_3$ - P_i almost attained equilibrium isotopic composition by 155 d, the $\sim 3.5\%$ offset of HCl- P_i from equilibrium isotopic composition suggests NaOH- P_i as the most likely precursor phase for HCl- P_i . These results collectively indicate an active and stepwise transformation of H_2O - P_i and $NaHCO_3$ - P_i to NaOH- P_i , and finally to the HCl- P_i pool. Furthermore, these results provide strong evidence of Ca-P mineral precipitation at slightly acidic to circumneutral pH in the field. Interestingly, the concentration of the HCl- P_i pool did not increase in 155 d, but the isotopic composition provided evidence of new Ca-P mineral precipitation. This, however, cautions the interpretation of loss or gains on P pools based solely on sequential extraction data and at the same time highlights the importance of the isotope tool to identify phase transformation. Overall, these results show a P transformation pathway of different P pools and highlight the application of isotopes to identify these reactions and processes.

Given that a suite of $\delta^{18}O_P$ values of HCl- P_i could precipitate in a soil history (dotted arrows in Fig. 2.3) and because $\delta^{18}O_P$ values of the Ca-P mineral are locked in (Jaisi and Blake, 2010), interpretation of $\delta^{18}O_P$ values of HCl- P_i requires some caution. For example, $\delta^{18}O_P$ values near equilibrium could be misinterpreted as bioavailable HCl- P_i if the potential sources or pathways for this P pool are not taken into account. The HCl- P_i is not directly bioavailable to plants and microorganisms and

is not expected to be bioavailable in the agricultural soil in this study due to high H₂O-P_i and NaHCO₃-P_i pools (>6 μmol g⁻¹) (Table 2.1, Fig 2.1a and 2.1b), it is important to note that δ¹⁸O_P values of HCl-P_i close to equilibrium (in this and other past studies) do not necessarily mean that this particular P_i pool is cycled by microorganisms but rather suggests that HCl-P_i is precipitated from biologically cycled P pools.

2.5 Conclusions and implications

The mechanisms and pathways of P cycling that generate fixed P (held by Al and Fe oxides or Ca-P minerals) in soils are poorly understood. In this research, we applied ¹⁸O labeled P in an agricultural soil and traced the movement of P in four different soil P_i pools (H₂O- P_i, NaHCO₃- P_i, NaOH- P_i, and HCl- P_i). The results showed active transformation of applied P in soil from bioavailable to precipitated Ca-P minerals. This is a unique observation, and no previous studies have identified the rate and pathway of this reaction or have explicitly identified the formation of HCl-P_i. Overall, our results indicate precipitation of Ca-P minerals in agricultural soil from fertilizer P, not apatite from geogenic (sedimentary or any other geological) origin.

In many agricultural soils, surplus P exists as legacy P and contributes to nonpoint source P pollution (e.g., Leytem et al., 2003; Sharpley et al., 2013). The fate of excess P both from current and legacy sources is required to identify the appropriate P load reduction needed to meet the water quality goals specified for different watersheds. A better understanding of P pool dynamics, particularly their formation and transformation, provides key information that could be used to identify susceptibility of a particular P pool to leaching and thus potentially contaminating surface and subsurface waters. Our results provide important insights into the fate of externally applied P in a soil and soil P dynamics over time. Findings from this study

can be utilized to improve existing P management practices or develop new P management plans for agricultural soils. Overall, in the long term, this may help shift the current mineral phosphate-based agricultural economy to an economy that has a sustainable phosphate cycle.

2.6 Acknowledgement

This research was supported by a research grant from the US Department of Agriculture (NIFA award 2012-67019-19320). We thank Kiran Upreti, Michael Scharf, Awet Negusse, and Yuge Bai for their help with soil core recovery and water extraction.

REFERENCES

- Amelung, W., P. Antar, I. Kleeberg, Y. Oelmann, L. Lucke, F. Alt, H. Lewandowski, S. Patzhold, and J.A.M. Bar. 2015. The $\delta^{18}\text{O}$ signatures of HCl-extractable soil phosphates: Methodological challenges and evidence of the cycling of biological P in arable soil.
- Angert, A., T. Weiner, S. Mazeh, and M. Sternberg. 2012. Soil phosphate stable oxygen isotopes across rainfall and bedrock gradients. *Environ. Sci. Technol.* 46(4): 2156–62.
- Angert, A., T. Weiner, S. Mazeh, F. Tamburini, E. Frossard, S.M. Bernasconi, and M. Sternberg. 2011. Seasonal variability of soil phosphate stable oxygen isotopes in rainfall manipulation experiments. *Geochim. Cosmochim. Acta* 75(15): 4216–4227.
- Beck, M.A., and P.A. Sanchez. 1994. Soil phosphorus fraction dynamics during 18 years of cultivation on a Typic Paleudult. *Soil Sci. Soc. Am. J.* 58(5): 1424–1431.
- Blake, R.E., J.C. Alt, and A.M. Martini. 2001. Oxygen isotope ratios of PO_4 : An inorganic indicator of enzymatic activity and P metabolism and a new biomarker in the search for life. *Proc Natl Acad Sci . USA* 98(5): 2148–2153.
- Blake, R.E., J.R. O’Neil, and G.A. Garcia. 1997. Oxygen isotope systematics of biologically mediated reactions of phosphate: I. Microbial degradation of organophosphorus compounds. *Geochim. Cosmochim. Acta* 61(20): 4411–4422.
- Blake, R.E., J.R. O’Neil, and A. V. Surkov. 2005. Biogeochemical cycling of phosphorus: Insights from oxygen isotope effects of phosphoenzymes. *Am. J. Sci.* 305: 596–620.
- Bowman, R.A., S.R. Olsen, and F.S. Watanabe. 1978. Greenhouse evaluation of residual phosphate by four phosphorus methods in neutral and calcareous soils. *Soil Sci. Soc. Am. J.* 42(3): 451–454.
- Chang, S.C., and M.L. Jackson. 1957. Fractionation of soil phosphorus. *Soil Sci.* 84: 133–144.

- Cordell, D., J.-O. Drangert, and S. White. 2009. The story of phosphorus: Global food security and food for thought. *Glob. Environ. Chang.* 19(2): 292–305.
- Daroub, S.H., F.J. Pierce, and B.G. Ellis. 2000. Phosphorus fractions and fate of phosphorus-33 in soils under plowing and no-tillage. *Soil Sci. Soc. Am. J.* 64: 170–176.
- Delaware Environmental Observing System. 2014. DEOS data services. [Database.] DEOS, Univ. of Delaware, Newark. <http://www.deos.udel.edu/>(accessed 9 Dec. 2014).
- Guo, F., R.S. Yost, N. V Hue, C.I. Evensen, and J.A. Silva. 2000. Changes in phosphorus fractions in soils under intensive plant growth. *Soil Sci. Soc. Am. J.* 64: 1681–1689.
- He, Z., Z.N. Senwo, and I.A. Tazisong. 2012. Long-term dynamics of labile and stable phosphorus following poultry litter application to pasture soils. *Commun. Soil Sci. Plant Anal.* 43(22): 2835–2850.
- Hedley, M.J., W.B. Stewart, and B.S. Chauwan. 1982. Changes in inorganic and organic soil phosphorus fractions induced by cultivation practices and by laboratory incubations. *Soil Sci. Soc. Am. J.* 46: 970–976.
- Jaisi, D.P. 2013. Stable isotope fractionations during reactive transport of phosphate in packed-bed sediment columns. *J. Contam. Hydrol.* 154: 10–9.
- Jaisi, D.P., and R.E. Blake. 2010. Tracing sources and cycling of phosphorus in Peru Margin sediments using oxygen isotopes in authigenic and detrital phosphates. *Geochim. Cosmochim. Acta* 74(11): 3199–3212.
- Jaisi, D.P., and R.E. Blake. 2014. Advance in using oxygen isotope ratios of phosphate to understand phosphorus cycling in the environment. *Adv. Agron.* 125:1–53.
- Jaisi, D.P., R.K. Kukkadapu, and R.E. Blake. 2010. Fractionation of oxygen isotopes in phosphate during its interactions with iron oxides. *Geochim. Cosmochim. Acta* 74(4): 1309–1319.
- Jaisi, D.P., R.K. Kukkadapu, L.M. Stout, T. Varga, and R.E. Blake. 2011. Biotic and abiotic pathways of phosphorus cycling in minerals and sediments: Insights from oxygen isotope ratios in phosphate. *Environ. Sci. Technol.* 45(15): 6254–61.

- Johansen, H.S., V. Middelboe, and S. Larsen. 1990. Delabelling of ^{18}O enriched phosphate added to soil as a function of biological activity in the soil. In: Stable isotopes in plant nutrition, soil fertility and environmental studies. Vienna.
- Joshi, S.R., R.K. Kukkadapu, D.J. Burdige, M.E. Bowden, D.L. Sparks, and D.P. Jaisi. 2015. Organic matter remineralization predominates phosphorus cycling in the Mid-bay sediments in the Chesapeake Bay. *Environ. Sci. Technol.* 49(10): 5887–5896.
- Karl, D.M., and G. Tien. 1992. MagIC: A sensitive and precise method for measuring dissolved phosphorus in aquatic environments. *Limnol. Oceanogr.* 37(1): 105–116.
- Khan, K.S., and R.G. Joergensen. 2009. Changes in microbial biomass and P fractions in biogenic household waste compost amended with inorganic P fertilizers. *Bioresour. Technol.* 100(1): 303–309.
- Larsen, S., V. Middelboe, and H.S. Johansen. 1989. The fate of ^{18}O labelled phosphate in soil-plant systems. *Plant Soil* 117(1): 143–145.
- Lecuyer, C., P. Grandjean, and S.M.F. Sheppard. 1999. Oxygen isotope exchange between dissolved phosphate and water at temperatures $< 135^\circ\text{C}$: Inorganic versus biological fractionations. *Geochim. Cosmochim. Acta* 63(6): 855–862.
- Lehmann, J., Z. Lan, C. Hyland, S. Sato, D. Solomon, and Q.M. Ketterings. 2005. Long-term dynamics of phosphorus forms and retention in manure-amended soils. *Environ. Sci. Technol.* 39(17): 6672–6680.
- Leytem, A.B., J.T. Sims, and F.J. Coale. 2003. On-farm evaluation of a phosphorus site index for Delaware. *J. Soil Water Conserv.* 58(2): 89–97.
- Li, H., and D.P. Jaisi. 2015. An isotope labeling technique to investigate atom exchange during phosphate sorption and desorption. *Soil Sci. Soc. Am. J.* 79: 1340–1351.
- Liang, Y., and R.E. Blake. 2006. Oxygen isotope signature of P_i regeneration from organic compounds by phosphomonoesterases and photooxidation. *Geochim. Cosmochim. Acta* 70(15): 3957–3969.
- Liang, Y., and R.E. Blake. 2009. Compound and enzyme-specific phosphodiester hydrolysis mechanisms revealed by $\delta^{18}\text{O}$ of dissolved inorganic phosphate: Implications for marine P cycling. *Geochim. Cosmochim. Acta* 73(13): 3782–3794.

- Longinelli, A., and S. Nuti. 1973. Revised phosphate-water isotopic temperature scale. *Earth Planet. Sci. Lett.* 19(3): 373–376.
- McKenzie, R.H., J.W.B. Stewart, J.F. Dormaar, and G.B. Schaalje. 1992. Long-term crop rotation and fertilizer effects on phosphorus transformations: II. In a Luvisolic soil. *Can. J. Soil Sci.* 72(4): 581–589.
- Mehlich, A. 1984. Mehlich 3 soil test extractant: A modification of Mehlich 2 extractant. *Commun. Soil Sci. Plant Anal.* 15(12): 1409–1416.
- Melby, E.S., D.J. Soldat, and P. Barak. 2011. Synthesis and detection of oxygen-18 labeled phosphate. *PLoS One* 6(4): e18420.
- Mozaffari, M., and J.T. Sims. 1994. Phosphorus availability and sorption in an Atlantic Coastal plain watershed dominated by animal-based agriculture. *Soil Sci.* 157(2).
- Murphy, J., and J.P. Riley. 1962. A modified single solution method for the determination of phosphate in natural waters. *Anal. Chim. Acta* 27(0): 31–36.
- Negassa, W., and P. Leinweber. 2009. How does the Hedley sequential phosphorus fractionation reflect impacts of land use and management on soil phosphorus: A review. *J. Plant Nutr. Soil Sci.* 172(3): 305–325.
- Olsen, S.R., C. V Cole, F.S. Watanabe, and L.A. Dean. 1954. Estimation of available phosphorus by extraction with sodium bicarbonate. *USDA Circ.* 939, U.S. Govt. Print. Off. Washington, D.C.
- O'Neil, J.R., T.W. Vennemann, and W.F. McKenzie. 2003. Effects of speciation on equilibrium fractionations and rates of oxygen isotope exchange between (PO₄)^{aq} and H₂O. *Geochim. Cosmochim. Acta* 67(13): 3135–3144.
- Pautler, M.C., and J.T. Sims. 2000. Relationships between soil test phosphorus, soluble phosphorus, and phosphorus saturation in Delaware soils. *Soil Sci. Soc. Am. J.* 64: 765–773.
- Paytan, A., Y. Kolodny, A. Neori, and B. Luz. 2002. Rapid biologically mediated oxygen isotope exchange between water and phosphate. *Global Biogeochem. Cycles* 16(1): 13–18.
- Read, D.W.L., F.G. Warder, E.D. Spratt, and L.D. Bailey. 1977. Residual effects of phosphorus fertilizer. I. For wheat grown on four chernozemic soil types in Saskatchewan and Manitoba. *Can. J. Soil Sci.* 57(3): 255–262.

- Richards, J.E., T.E. Bates, and S.C. Sheppard. 1995. Changes in the forms and distribution of soil phosphorus due to long-term corn production. *Can. J. Soil Sci.* 75(3): 311–318.
- Richardson, A.E. 2001. Prospects for using soil microorganisms to improve the acquisition of phosphorus by plants. *Funct. Plant Biol.* 28(9): 897–906.
- Richardson, A.E., and R.J. Simpson. 2011. Soil microorganisms mediating phosphorus availability update on microbial phosphorus. *Plant Physiol.* 156(3): 989–96.
- Rowland, A.P., and P.M. Haygarth. 1997. Determination of total dissolved phosphorus in soil solutions. *J. Environ. Qual.* 26: 410–415.
- Sharpley, A.N. 1985. Phosphorus cycling in unfertilized and fertilized agricultural soils. *Soil Sci. Soc. Am. J.* 49: 905–911.
- Ruttenberg, C. 1992. Development of a sequential extraction for different forms of phosphorus in marine sediments. *Limnol. Oceanogr.* 37: 1460–1482.
- Sharpley, A., H.P. Jarvie, A. Buda, L. May, B. Spears, and P. Kleinman. 2013. Phosphorus legacy: Overcoming the effects of past management practices to mitigate future water quality impairment. *J. Environ. Qual.* 42(5): 1308–1326.
- Shelton, J.E., and N.T. Coleman. 1968. Inorganic phosphorus fractions and their relationship to residual value of large applications of phosphorus on high phosphorus fixing soils. *Soil Sci Soc Am Proc* 32: 91–94.
- Stout, L.M., S.R. Joshi, T.M. Kana, and D.P. Jaisi. 2014. Microbial activities and phosphorus cycling: An application of oxygen isotope ratios in phosphate. *Geochim. Cosmochim. Acta* 138(0): 101–116.
- Syers, J.K., A.E. Johnson, and D. Curtin. 2008. Efficiency of soil and fertilizer phosphorus use: Reconciling changing concepts of soil phosphorus behaviour with agronomic information. *FAO Fertil. Plant Nutr. Bull.*: 123.
- Tamburini, F., S.M. Bernasconi, A. Angert, T. Weiner, and E. Frossard. 2010. A method for the analysis of the $\delta^{18}\text{O}$ of inorganic phosphate extracted from soils with HCl. *Eur. J. Soil Sci.* 61(6): 1025–1032.
- Tamburini, F., V. Pfahler, E.K. Bünemann, K. Guelland, S.M. Bernasconi, and E. Frossard. 2012. Oxygen isotopes unravel the role of microorganisms in phosphate cycling in soils. *Environ. Sci. Technol.* 46(11): 5956–62.

- Tiessen, H., J.W.B. Stewart, and C. V Cole. 1984. Pathways of phosphorus transformations in soils of differing pedogenesis. *Soil Sci. Soc. Am. J.* 48: 853–858.
- Tiessen, H., J.W.B. Stewart, and J.O. Moir. 1983. Changes in organic and inorganic phosphorus composition of two grassland soils and their particle size fractions during 60–90 years of cultivation. *J. Soil Sci.* 34(4): 815–823.
- Vennemann, T.W., H.C. Fricke, R.E. Blake, J.R.O. Neil, and A. Colman. 2002. Oxygen isotope analysis of phosphates : A comparison of techniques for analysis of Ag_3PO_4 . *Chem. Geol.* 185: 321–336.
- Wagar, B.I., J.W.B. Stewart, and J.O. Moir. 1986. Changes with time in the form and availability of residual fertilizer phosphorus in chemozemic soils. *Can. J. Soil Sci* 66: 105–119.
- Waldrip-Dail, H., Z. He, S.M. Erich, and W.C. Honeycutt. 2009. Soil phosphorus dynamics in response to poultry manure amendment. *Soil Sci.* 174(4).
- Weiner, T., S. Mazeh, F. Tamburini, E. Frossard, S.M. Bernasconi, T. Chiti, and A. Angert. 2011. A method for analyzing the $\delta^{18}\text{O}$ of resin-extractable soil inorganic phosphate. *Rapid Commun. Mass Spectrom.* 25(5): 624–628.
- Zhang, T.Q., and A.F. MacKenzie. 1997. Changes of soil phosphorous fractions under long-term corn monoculture. *Soil Sci. Soc. Am. J.* 61: 485–493.
- Zohar, I., A. Shaviv, T. Klass, K. Roberts, and A. Paytan. 2010. Method for the analysis of oxygen isotopic composition of soil phosphate fractions. *Environ. Sci. Technol.* 44(19): 7583–8.

Chapter 3

SOURCES AND MECHANISMS OF FORMATION OF ACID EXTRACTABLE PHOSPHORUS POOLS IN AN AGRICULTURAL SOIL

3.1 Abstract

Phosphorus (P) is a finite resource and an essential nutrient for sustaining life and agricultural production. Transformation of readily available P into unavailable P to plants requires additional cost to replenish this P to maintain crop production. Together these factors translate into lower agronomic benefits (food prices), loss of excess P in soil to runoff and degradation of water quality. Therefore, understanding the mechanisms and pathways of the formation of residual P pools in soils could be helpful in developing new biological approaches and technologies to inhibit the formation of unavailable P thus maximize P availability to plants. In this research, we used phosphate oxygen isotope ratios ($\delta^{18}\text{O}_\text{P}$) along with solid-state NMR, micro-XRD, and general soil chemistry techniques to identify the sources and precipitation pathways of two acid extractable P pools, namely 1 mol L⁻¹ HCl-P and 10 mol L⁻¹ HNO₃-P in an agricultural soil. Our results show that the concentrations of acid extractable P pools are high at the shallow depth soil samples and sharply decrease below the agronomically active soil depth. The $\delta^{18}\text{O}_\text{P}$ values of the HNO₃-P_i pool are similar to that of NaOH-P_i, suggesting linkage between these two P pools, especially under high soil acidity and high concentrations of Al and Fe. Furthermore, $\delta^{18}\text{O}_\text{P}$ values of HCl-P_i in deeper soils, where the effect of soil tilling or physical mixing is absent, are similar to the shallow depth soil. One plausible mechanism for this result is

that particle bound P leaches from top soil to the deeper soils. Overall, these findings provide an improved understanding on the sources and fate of acid extractable P in agricultural soils and better insights into the buildup of legacy P in soils.

3.2 Introduction

Phosphorus is a non-renewable resource (occurs at ~0.09 wt % in Earth's crust) and a required components of fertilizer for food production. Series of studies have raised concern that the increased exploitation of P, after the agricultural revolution, has reduced the P reserves on Earth (Cordell et al., 2009). As a result, the pressure to economize P such as by using less P in fertilizer, or recycling P from variety of waste sources, as well as more efficient use the available P has increased in the past decades (Morse et al., 1998; Balmér, 2004; Franz, 2008). Consequently series of research efforts and technological developments are being undertaken towards recycling P from human waste and sewage sludge in wastewater treatment plants, rationing P application in agricultural soils based on soil P concentration, reducing leaching and runoff, and research on various methods to enhance P uptake from soils including manipulation of symbiotic fungi and microorganisms on plant roots (Guo et al., 2000; Richardson, 2001; Khan & Joergensen, 2009; Richardson & Simpson, 2011; Gaxiola et al., 2011). These progresses have either regulated or commercialized P, or have been the area of increased research interest.

Sequential chemical extraction methods are widely used to differentiate operationally discrete bioavailable and recalcitrant P pools in soils to determine supplemental P requirements for plants (Chang & Jackson, 1957; Shelton & Coleman, 1968; Hedley et al., 1982; Tiessen et al., 1984; He et al., 2012). The non-bioavailable soil P pools extracted by reagents used in the sequential extraction are often referred

as ‘recalcitrant P’ whereas non-extractable P is considered ‘residual P’. Soil mineralogy and pH are the important properties that control the form of P pools in soils. In general, application of commercial P fertilizers or manure promotes precipitation of Ca-P minerals, which are often the dominant recalcitrant P forms, especially in alkaline pH soils. In highly weathered soil, where high concentrations of Al and Fe oxide minerals are present or the pH is low, P is a strongly sorbed species on to these minerals and to phyllosilicate minerals. These reactions are conducive to the formation of residual P pools that have limited or no availability to plants and microorganisms. In fact, long-term application of fertilizers and manures has found to increase both recalcitrant and residual P pools in soils (Wager et al., 1986; Guo et al., 2000; Lehmann et al., 2005). However, research on the pathway of formation as well as composition of the residual P pool is limited and nor the identity of these P pools is known well.

Advances in the understanding of soil P dynamics, particularly the interactions among P pools and biogeochemical processes that facilitate or restrict these interactions, is limited largely due to lack of appropriate analytical methods of investigation (Jaisi & Blake, 2014). While a series of innovative research tools have been used to understand P dynamics (Kruse et al., 2015), research on soil P biogeochemistry is lagging compared to other important bio-elements (e.g., C, N, S, and Fe). Thus our understanding of the links between specific biological activities and chemical signatures, as well as links between inorganic P (P_i) and other macronutrients in different environments, is limited. Spiking of ^{32}P and ^{33}P radionuclides into soil systems or otherwise controlled experiments have been used to quantify dissolved and sorbed P species, and to understand P uptake, cycling, and transformations (e.g.,

Friesen & Blair, 1988; Frossard & Sinaj, 1997; Bühler et al., 2003; Achat et al., 2009; Frossard et al., 2011). Although this method has long been used under field simulated laboratory conditions, the field application of radioisotopes is restricted due to safety and regulatory requirements. Furthermore, radioisotopes have several limitations. For example, they cannot be used for long-term P dynamic research (due to shorter half-lives: 25.34 days for ^{33}P and 14.26 days for ^{32}P); spiking radioisotopes disturbs P speciation and thus the results obtained may not reflect actual field processes. On the other hand, natural abundance of stable isotopes is capable of discriminating soil P speciation both in the short and long-term soil processes. Fundamentally distinct properties of phosphate oxygen isotope ratios ($\delta^{18}\text{O}_\text{P}$) in abiotic and biotic reactions make this tool more reliable tracer of P to study the physicochemical and biological P cycling pathways and fate of P in agricultural and non-agricultural soils (Larsen et al., 1989; Johansen et al., 1990; Zohar et al., 2010a; Angert et al., 2012; Tamburini et al., 2012; Joshi et al., 2016). For example, oxygen isotopic composition of phosphate remains constant during sorption, desorption, transport, and mineral transformation, except for short-term kinetic fractionation among P pools, at low temperature ($<70\text{ }^\circ\text{C}$) and circumneutral pH (Lecuyer et al., 1999; O'Neil et al., 2003; Jaisi et al., 2010; Jaisi, 2013; Wang et al., 2015). However, during biological processes rapid O-isotope exchange between P_i and ambient H_2O often results in complete isotope exchange and produces temperature-dependent equilibrium O-isotope fractionation (Longinelli & Nuti, 1973; Blake et al., 1997; Paytan et al., 2002; Jaisi et al., 2010; Jaisi & Blake, 2010; Joshi et al., 2015). These specific properties of $\delta^{18}\text{O}_\text{P}$ in abiotic and biotic reactions provide the potential means to apply this tool to develop the mechanistic understanding on the formation of recalcitrant P pools and interplay of biotic and

abiotic reactions involved in soil P cycling. Isotopes, however, have been underutilized as a geochemical indicator of P cycling in natural systems (Jaisi & Blake, 2014).

In this research, we used a stable isotope method, which goes beyond classical operationally defined P pool speciation, along with solid state NMR and micro-XRD techniques with an aim to develop mechanistic understanding of the formation of acid extractable P (referred to hereafter as acid-P) pools. In this communication we termed both 1 mol L⁻¹ HCl P as well as 10 mol L⁻¹ HNO₃ extractions as ‘acid-P’ pools, a new terminology because it partly overlaps existing terminologies (‘recalcitrant’ or ‘residual’ P) being used in the literature. We analyzed soils in a continuum from surface to beyond agronomic-relevant depth in a long-term agronomy research field. Based on results, we discussed potential pathways of phase transformation among P pools and ultimate formation of acid-P pools in an agricultural soil.

3.3 Materials and methods

3.3.1 Site description and soil sampling

A site classically used for corn and soybean fertility research at the Agricultural Experiment Station in Newark, DE at the University of Delaware was used for this research. The details about the study site and agronomic practices are described in Joshi et al. (2016). In brief, the water table is about 0.5 m or more below the surface and therefore the major part of biologically active and agronomically relevant soil is unsaturated. Every year the soil is chisel-plowed (~30 cm) before cropping. It is drip irrigated as needed during crop growing seasons.

To quantify P_i pools and their isotopic compositions, soil cores were retrieved from the experimental site using a Hoffer soil sampler (2.54 cm id) at intervals of 2.0 cm up to a total depth of 105 cm. We collected three to four soil cores and combined core slices from the same depth intervals and homogenized before processing and analysis. A fraction of the soil core was immediately placed inside an airtight container to quantify soil water content and to measure water $\delta^{18}O_w$ values. Soil temperature at different soil depths was measured by inserting a stem thermometer at targeted depths. The soil cores were freeze dried, and then ground thoroughly before size separation (<200 μm) to avoid incomplete extraction of targeted P pools and to be consistent with smaller size fractions recommended in literature for sequential extraction (e.g., Hedley et al., 1982; Psenner et al., 1988; Ruttenberg, 1992). The soil pH was measured without size separation to be closer to field conditions. The size separated samples were then analyzed for physical and chemical properties and processed for isotope measurements.

3.3.2 Soil characterization

The physical and chemical properties of the soil samples were measured to differentiate the most biologically and agronomically active top soil (0–20 cm), intermediate-depth soil (20–40 cm) and a deeper soil (>40 cm) largely beyond the active biological and agronomical activities. The soil pH was measured following the procedure described in Thomas (1996). Briefly, 10 g of soil sample was mixed with 10 mL of de-ionized (DI) water (pH=6.8) in 1:1 soil to water ratio (w/w). It was mixed thoroughly in a reciprocator shaker for 10 min and pH was measured using Orion[®] glass electrodes. To measure the Mehlich-3 P pool, a common soil P test in agronomy, the soil samples from different depths were extracted by using Mehlich-3 reagents (0.2

mol L⁻¹ CH₃COOH, 0.25 mol L⁻¹ NH₄NO₃, 0.015 mol L⁻¹ NH₄F, 0.013 mol L⁻¹ HNO₃, and 0.001 mol L⁻¹ EDTA) (Mehlich, 1984). Soils before the start of sequential extraction were dissolved using the microwave digestion method to identify total P and concentrations of other elements that are relevant to P speciation (Fe, Al, and Ca). The concentrations of P, Al, Ca, and Fe were measured by using inductively coupled plasma optical emission spectrometer (ICP-OES) in the Soil Testing Laboratory at the University of Delaware.

Variations in soil mineralogical composition across the soil depth were analyzed by using X-ray diffraction (XRD) (Empyrean, with CuK_α radiation $\lambda = 1.54056 \text{ \AA}$). We chose five soil depths (0–2, 8–10, 20–22, 50–52, 82.5–90, and 97.5–105 cm) for XRD analysis based on preliminary results on P, Fe, Al and Ca concentrations and pH changes. To understand the selective removal of minerals and changes in concentration of amorphous minerals during sequential extraction, soil residues were analyzed (i) after 0.5 mol L⁻¹ NaOH extraction but before HCl extraction, (ii) after HCl extraction, and (iii) after HNO₃ extraction separately in XRD. Diffraction data were processed by using the JADE 9.1.5 program (Materials Data Inc.) and the PDF4+ database (inorganic crystal structure database, ICSD) was used to fit the XRD peaks and identify mineral composition. We used ZnO, a NIST certified standard, as the internal standard for quantitative analyses of soil minerals and amorphous mineral content because ZnO peaks do not interfere with that of minerals from the soil. However, to our surprise, ZnO appeared to react with residual nitrate (from the reagent HNO₃) in solid-phase and generated new peaks in the soil residue after HNO₃ treatment. To circumvent this problem, we repeated XRD data collection

using Al_2O_3 as a new internal standard and performed the quantitative analyses of crystalline and amorphous minerals.

3.3.3 ^{31}P Solid-State NMR Spectroscopy

Solid state NMR was employed to directly determine the P speciation of soil samples. Solid-state $^{31}\text{P}\{^1\text{H}\}$ single pulse (SP) magic-angle-spinning (MAS) NMR spectra for several soil samples were collected on a 500 MHz Bruker AVIII solid-state spectrometer (11.7 T), at operating frequency of 202.5 MHz for ^{31}P , and 500.1 MHz for ^1H . A Bruker 4.0 mm HX double resonance probe was used for all solid-state NMR experiments. All the powder samples were packed into the rotor and spun at the MAS frequency of 10 kHz. The ^{31}P 30° pulse length was 0.8 μs , and the relaxation delay was 30 s.

3.3.4 Extraction of soil phosphate pools

Acid-P pools (HCl-P and HNO_3 -P) in soils were extracted using the most common operationally defined sequential extraction technique originally developed by Hedley et al. (1982) and revised by Tiessen et al. (1984) with slight modifications (Joshi et al., 2016). In brief, the soil samples were directly extracted by 0.5 mol L^{-1} NaHCO_3 for 16 hr in 1:100 soil to solution ratio. In order to avoid carryover of the residual P extracted by NaHCO_3 but not removed from soils, the soil was washed by 0.5 mol L^{-1} NaHCO_3 and H_2O (e.g., Ruttenberg, 1992). Then, the residual soil was extracted by 0.5 mol L^{-1} NaOH for 16 hr followed by 0.5 mol L^{-1} NaHCO_3 and H_2O washes, as before. The residual soil after NaOH extraction was extracted further by 1 mol L^{-1} HCl for 16 hr followed by separate 0.5 mol L^{-1} NaHCO_3 and H_2O washes, as before. The extracted solutions during washing steps were individually quantified for

P_i concentrations to ensure no carryover of P_i to next pool. Finally, the soil residue after HCl extraction was treated with $10 \text{ mol L}^{-1} \text{ HNO}_3$ in a 1:25 soil to solution ratio. The NaHCO_3 -P pool was discarded and not further analyzed, whereas NaOH-P, HCl-P, and HNO_3 -P pools were processed further for analysis. Concentrations of P_i and total P (TP) in each extract were measured by using phosphomolybdate blue method (Murphy & Riley, 1962) directly and after persulfate digestion (Rowland & Haygarth, 1997), respectively. Organic P (P_o) concentration was calculated as the difference between TP and P_i . In addition, the concentrations of Fe, Al, and Ca, in HCl and HNO_3 extracted solutions were measured by using ICP-OES in the Soil Testing Laboratory. Extracted supernatants for each P pool were combined and stored at 4°C before processing and purification for silver phosphate (Ag_3PO_4) precipitation.

3.3.5 Purification of extracted solution for isotope analysis

The extracted P pools were processed to remove residual reagents, cations and anions and compounds that were extracted along with P during various treatments and to concentrate P_i before it was converted to silver phosphate for the measurement of isotope ratios. A schematic diagram of the purification and precipitation methods is shown in Figure 3.1. The NaOH and HCl extracted solutions were first evaporated to reduce volume, and then P_i in the solutions was concentrated by using the magnesium induced co-precipitation (MagIC) method (Karl & Tien, 1992). Residual cations extracted by HCl as well as from Mg and NH_4 added during MagIC treatment were removed by passing the solution (after dissolving $\text{Mg}(\text{OH})_2$ pellets in $1 \text{ mol L}^{-1} \text{ HNO}_3$) through cation-exchange resin (AG50W-X8, BioRad). The volume of HNO_3 extracted solution ($\sim 100 \text{ mL}$) did not require MagIC treatment and P_i in this solution was

concentrated by evaporation (below 70 °C) only. Both extracted solutions were processed further for purification before Ag_3PO_4 precipitation.

Precipitation of ammonium phosphomolybdate (APM) and subsequent steps followed the methods described in Liang and Blake (2006) and Jaisi and Blake (2010, 2014) as outlined step by step in schematic diagram (Figure 3.1). The APM precipitation at low pH and separation of APM precipitates removed ions and contaminants that are soluble at low pH. We used 0.1 μm polysulfone filters (Pall Scientific) to separate APM precipitates and rinsed the precipitates with 5% NH_4NO_3 solution before dissolving in citrate solution. Magnesium ammonium phosphate (MAP) was precipitated from this solution at high pH. The MAP crystals were separated by filtration (as above) and rinsing. This step removed ions and contaminants that were soluble at high pH. The MAP dissolved solution, after pH adjustment to neutral, was passed through a vertical fixed-bed column packed with cation-exchange resin to remove cations (primarily Mg^{2+} and NH_4^+) and achieve P_i in protonated forms (HPO_4^{2-} and $\text{H}_2\text{PO}_4^{2-}$). The solution was further evaporated down to ~ 5 mL to enrich P_i for complete precipitation in a customized beaker. Finally Ag_3PO_4 was precipitated by adding silver amine solution in the concentrated P_i solution. A pair of separate phosphate standards with different $\delta^{18}\text{O}_\text{P}$ values was processed in parallel with soil extracts to validate the sample processing protocol as well as to confirm the reliability of isotope values. In selected samples, the presence and potential hydrolysis of the residual P_o was checked by spiking a sample split with ^{18}O -enriched water. Yield of Ag_3PO_4 precipitate was compared to that of P_i content in the starting solution and those with acceptable yield ($>90\%$) were used for isotope analyses.

3.3.6 Measurement of phosphate oxygen isotope ratios

A Thermo-Chemolysis Elemental Analyzer (TC/EA) coupled to a Delta V continuous flow isotope ratio monitoring mass spectrometer (IRMS, Thermo-Finnigan, Germany; precision of 0.3‰) was used to measure $\delta^{18}\text{O}_\text{P}$ values of precipitated Ag_3PO_4 at the Laboratory, University of Delaware. Each run sequence included an internal phosphate standard, benzoic acid, and two isotope standards (YR1a and YR3-2 with $\delta^{18}\text{O}_\text{P}$ values of -5.49 and $+33.63$ ‰, respectively) at first, and two isotope standards at the middle and the end of a run, each at least in triplicate. Yield of oxygen in Ag_3PO_4 was calculated based on theoretical O in the mineral (15.4%) and data with acceptable yield ($>90\%$) were used for analyses (and presented in this communication). All accepted isotope $\delta^{18}\text{O}_\text{P}$ values were calibrated against YR1a and YR3-2 standards that were originally calibrated using a conventional fluorination method (Vennemann et al., 2002) and are reported relative to the Vienna standard mean oceanic water (VSMOW) standard in units of permil (‰).

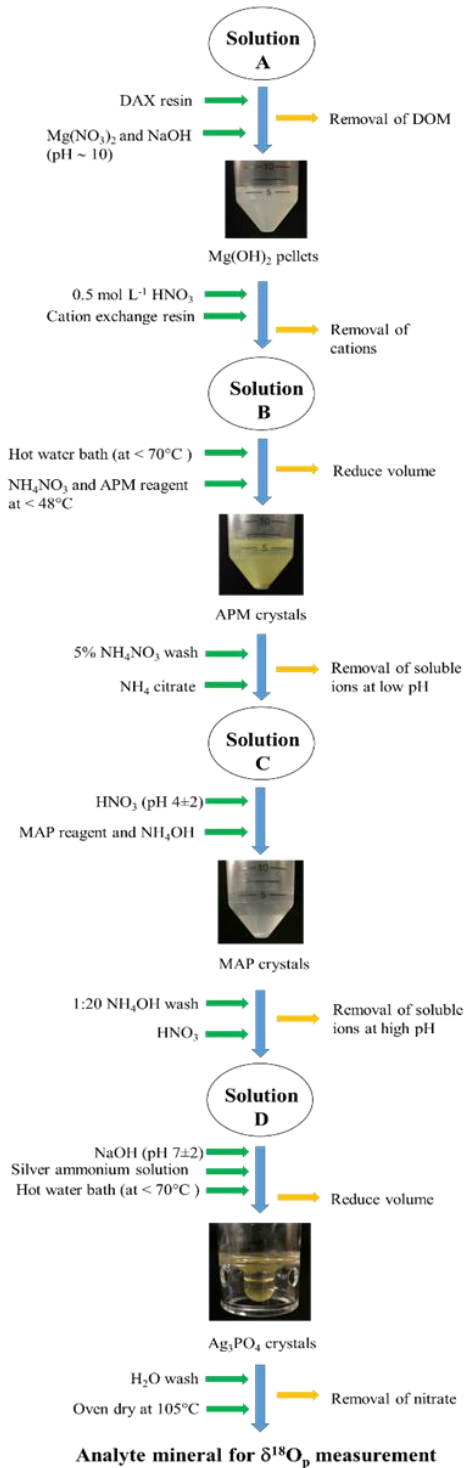


Figure 3.1 Flow diagram for the purification of P from sequentially extracted soil solution and precipitation of silver phosphate.

3.4 Results

3.4.1 Soil pH and elemental compositions

The soil pH and concentrations of total P, Mehlich-3 P, Fe, Al, and Ca from six soil depth intervals (0–2, 8–10, 20–22, 50–52, 82.5–90 and 97.5–105 cm) before sequential extraction of P pools are shown in Table 3.1. Soil pH, an important parameter that determines P speciation in soils, decreased with an increase in soil depths. For example, the soil samples were slightly acidic (pH= ~6.6 to 6.5) in agronomically active upper soil depths and soil acidity decreased by 0.25 units in the intermediate depths. In the deeper soil horizon (82.5–90 cm), the soil acidity further decreased to 5.3. Interestingly, change in soil acidity in the intermediate depth was steady. In surface soil, concentrations of total P, Mehlich-3 P and Ca was high, reflecting the impact of long-term fertilizer application, but their concentrations decreased in the deeper soil horizons. However, the concentrations of Fe and Al increased with increases in soil depths (see more details below).

Table 3.1 Selected soil properties at six different depth intervals in the study site.

Depth (cm)	pH	P (M-3) (mg/kg)	TP (mg/kg)	Al (g/kg)	Fe (g/kg)	Ca (g/kg)
0–2	6.62	192	785	16.7	18.6	1.1
8–10	6.63	163	805	20.9	21.5	1.3
20–22	6.58	¥	848	21.2	20.4	1.3
50–52	5.75	91	307	21.4	25.3	0.7
82.5–90	5.35	54	532	23.1	26.1	0.8
97.5–105	5.82	17	516	13.1	26.5	0.4

¥ absence of data

3.4.2 Mineralogical composition of soils

Quantitative analyses of mineralogical composition using micro-XRD in soils, soil residues after NaOH extraction but before HCl extraction, and after HCl and HNO₃ extraction (each from 0–2, 8–10, 20–22, 50–52, 82.5–90, and 97.5–105 cm depth) included minerals predominantly of quartz, feldspar, mica, kaolinite, and amorphous minerals (Table 3.2). There was a slight variation among the relative content of these minerals with soil depth. Comparative analyses during different extraction steps allowed us to identify selective removal of minerals as well as changes in concentration of amorphous minerals during sequential extractions. For example, comparison of minerals in soil residues before and after HCl extraction, and after HNO₃ extraction shows the removal of mica and kaolinite by 1 to 3, and 2 to 5%, respectively. On the other hand, amorphous minerals in soil residues increased by more than 20% after HNO₃ extraction. It is likely a sample processing artefact that the increase in amorphous mineral content after harsher reagent treatment is due to the precipitation of ions extracted by reagents but still attached to the residual minerals during freeze-drying.

Table 3.2 Mineralogical compositions of soil residues i) after NaOH extraction, ii) HCl extraction, and iii) after HNO₃ extraction at six different depth intervals.

Depth (cm)	Quartz			Mica			Feldspar			Kaolinite			Smectite			Amorphous		
	NaOH	HCl	HNO ₃	NaOH	HCl	HNO ₃	NaOH	HCl	HNO ₃	NaOH	HCl	HNO ₃	NaOH	HCl	HNO ₃	NaOH	HCl	HNO ₃
	(%)			(%)			(%)			(%)			(%)			(%)		
0–2	66	68	54	9.3	10	6.8	18	14	12	6.6	5.0	2.5	0.2	0.2	¥	¥	3.0	25
8–10	69	64	56	12	9.0	7.8	14	19	17	5.0	6.8	3.3	0.1	0.2	¥	¥	1.2	16
20–22	67	61	59	8.2	9.8	7.2	15	15	13	4.0	5.6	4.2	0.6	0.2	0.1	5.3	7.8	16
50–52	61	62	46	11	11	8.7	18	14	13	6.5	6.7	3.9	0.6	0.2	¥	2.9	6.3	28
82.5–90	63	58	44	12	11	8.5	14	13	13	7.2	8.2	3.8	0.6	0.2	¥	3.6	9.9	30
97.5–105	57	61	53	8.3	9.9	6.4	10	9.5	8.3	5.4	6.1	3.8	0.6	¥	¥	2.9	13	29

¥ below detection limit

3.4.3 ³¹P NMR results on the composition of phosphorus minerals

Solid-state ³¹P NMR allows direct characterization of the solid-state P speciation in soils and sediments by analyzing the chemical shifts of P nuclei in samples. Figure 3.2 shows the ³¹P solid state NMR results of selected soils samples. Spectrum for soil collected at 0 to 7.5 cm yields a major peak at 2.6 ppm, indicative of the presence of apatite mineral phase, and a minor broad peak at -5 ppm, which may be ascribed to mineral surface adsorbed phosphate. Different from this sample, the soil collected at 7.5 to 15 cm shows a much broad feature, which is more difficult to interpret.

According to the signal-to-noise ratio, it is obvious that both soil samples contain low total P. Due to the relatively low P content, the identification of P minerals precipitated in soils has largely been elusive. The P pool extracted by using 1 mol L⁻¹ HCl, operationally defined P pool, was considered as primary minerals, such as apatite (Tiessen et al., 1984). Soil state ³¹P-NMR and X-Ray diffraction methods identified Ca phosphate phases such as di-calcium and tri-calcium phosphate (DCP and TCP) in poultry litter amended with Al (Hunger et al., 2004; 2008). On the other hand, using P K-edge XANES spectroscopy only hydroxylapatite (HAP) was identified in Ca amended litter (Maguire et al., 2006). However, apatite phase mineral, thermodynamically stable mineral, have not been detected before in unamended litter and soils.

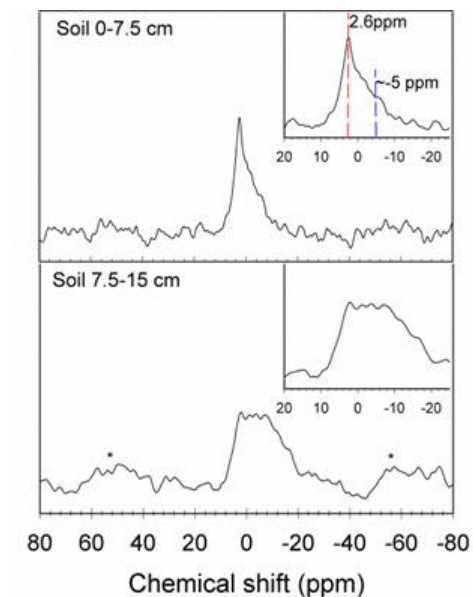


Figure 3.2 ^{31}P solid state NMR spectra of bulk soils (from 0–7.5 and 7.5–15 cm depths). Spectra were acquired at the single-pulse magic angle spinning (MAS) condition at a spinning rate of 10 kHz, with a $\pi/6$ pulse and a pulse delay of 30 s. Approximately 3000 - 14000 scans were accumulated for these samples.

3.4.4 Concentrations and isotopic compositions of P pools

Concentrations and isotopic compositions of NaOH- P_i , HCl- P_i and HNO_3 - P_i pools at different depth intervals are shown in Figure 3.3. As shown, NaOH extracted the highest amount of P_i compared to acid- P_i pools (e.g., at shallow depth greater than 6 times). Overall, the general trend of P_i pools was similar (i.e., high at the shallow soil depth (0–20 cm), decreased sharply below it and became relatively constant for deeper soil depths (≥ 40 cm)). However, concentrations among P_i pools were different. For example, at the shallow depth HCl- P_i was ~60% higher compared to the concentration of HNO_3 - P_i . This means that HCl- P_i is the dominant acid extractable P pool that may have formed due to excess P from fertilizer application. In the deeper soils, the concentrations of both acid- P_i pools were similar.

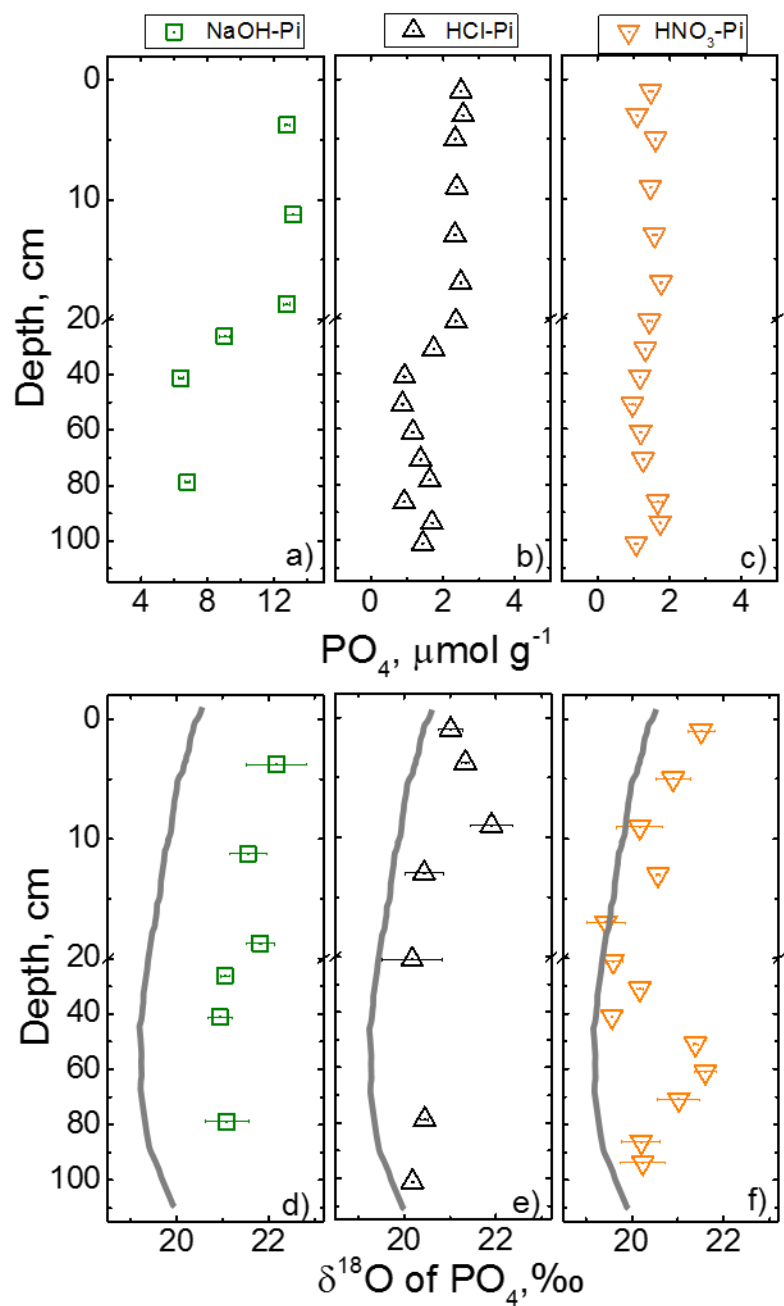


Figure 3.3 Concentrations (a, b, and c) and isotopic compositions (d, e, and f) of soil P_i pools (NaOH-P_i, HCl-P_i, and HNO₃-P_i) as a function of depth. The dark grey lines indicate equilibrium δ¹⁸O_P composition calculated from measured water δ¹⁸O_w values and temperature at the time of sampling.

The isotopic compositions of NaOH-P_i, HCl-P_i and HNO₃-P_i pools show that the $\delta^{18}\text{O}_\text{P}$ values of all three P_i pools varied within a narrow range, between 19.5 to 22‰, for the entire depth (0–105 cm) studied. Interestingly, general trends of $\delta^{18}\text{O}_\text{P}$ values of P_i pools as a function of depth were unique, and all values were slightly heavier (~1–2‰) than the equilibrium isotopic composition calculated by using the Longinelli and Nuti (1973) equation based on measured water isotope composition and measured temperature. Particular difference in the variation in isotope values could be classified at three different depths, i.e., shallow (<20 cm), intermediate (20–40 cm) and deep (>40 cm) soils. For example, at shallow depth, $\delta^{18}\text{O}_\text{P}$ values of NaOH-P_i were ~22‰ which gradually decreased towards deeper soil and became ~21‰. On the other hand, at 0 to 2 cm depth interval, $\delta^{18}\text{O}_\text{P}$ values of HCl-P_i steadily became heavier from surface to ~10 cm (~22‰), and then became lighter, to ~21‰, by 15 cm and remained within 20 to 21‰ for the remaining depth. The isotopic composition of HNO₃-P_i was opposite (mirror-image) to the trend of HCl-P_i, albeit with a slightly wider range, between 19.5 to 21.9‰, with heavier isotopic compositions near the surface and again at 50 to 60 cm. At the intermediate depths, $\delta^{18}\text{O}_\text{P}$ values of HNO₃-P_i were within the equilibrium isotopic compositions.

3.4.5 Concentrations of P, Fe, Al, and Ca in acid extraction

Concentration profiles of total P, Fe, Al, and Ca in 1 mol L⁻¹ HCl and 10 mol L⁻¹ HNO₃ extracted solutions along with soil pH are shown in Figure 3.4. At the shallow depth, overall concentration profiles of P, Fe, Al, and Ca were similar in both HCl and HNO₃ extracted solutions. However, as soil acidity increased in the intermediate and deep soils, concentrations of Fe and Al increased while P concentration decreased. HCl extracted higher amounts of P compared to HNO₃ at

shallow depths whereas in the deeper soil the concentrations were similar. In the entire profile, HCl and HNO₃ extracted similar amounts of Fe and Al. On the other hand, changes in soil acidity with depth had a negligible effect on Ca concentration, the reason for this being unclear. The depth averaged concentration of Ca in HCl extracted solution was $15.2 \pm 2.6 \mu\text{mol g}^{-1}$ which is more than a log order higher than Ca concentration in HNO₃ extracted solution (i.e., $2.1 \pm 0.3 \mu\text{mol g}^{-1}$).

Concentrations of P and other elements (Fe, Al, and Ca) in HCl and HNO₃ extracted solutions from the shallow and deeper depth samples were plotted in scatter diagrams and results are shown in Figures 3.5 and 3.6. As intermediate depth lies in the transitional zone where pH gradually decreases by ~1.5 units, correlation analysis was quite variable, as expected, and thus not included. In HCl extracts, R² values (Pearson's linear correlation) between P and Fe, Al, and Ca were close to zero suggesting there is not any correlation between P and other elements (Fe, Al and Ca) in both shallow and deep soil columns. This result is odd and does not follow the reciprocal relationship that is apparent in the concentration profile of Fe and Al with P (Figure 3.5). However, in the HNO₃ extract, there was a strong positive correlation between P and other elements (Fe, Al, and Ca) in both shallow and deeper soils. At the shallow depth, R² values between P and Fe, Al, and Ca were 0.86, 0.98, and 0.60, respectively. Similarly, in the deeper soils, R² values between P and Fe, Al, and Ca were 0.72, 0.74, and 0.67, respectively.

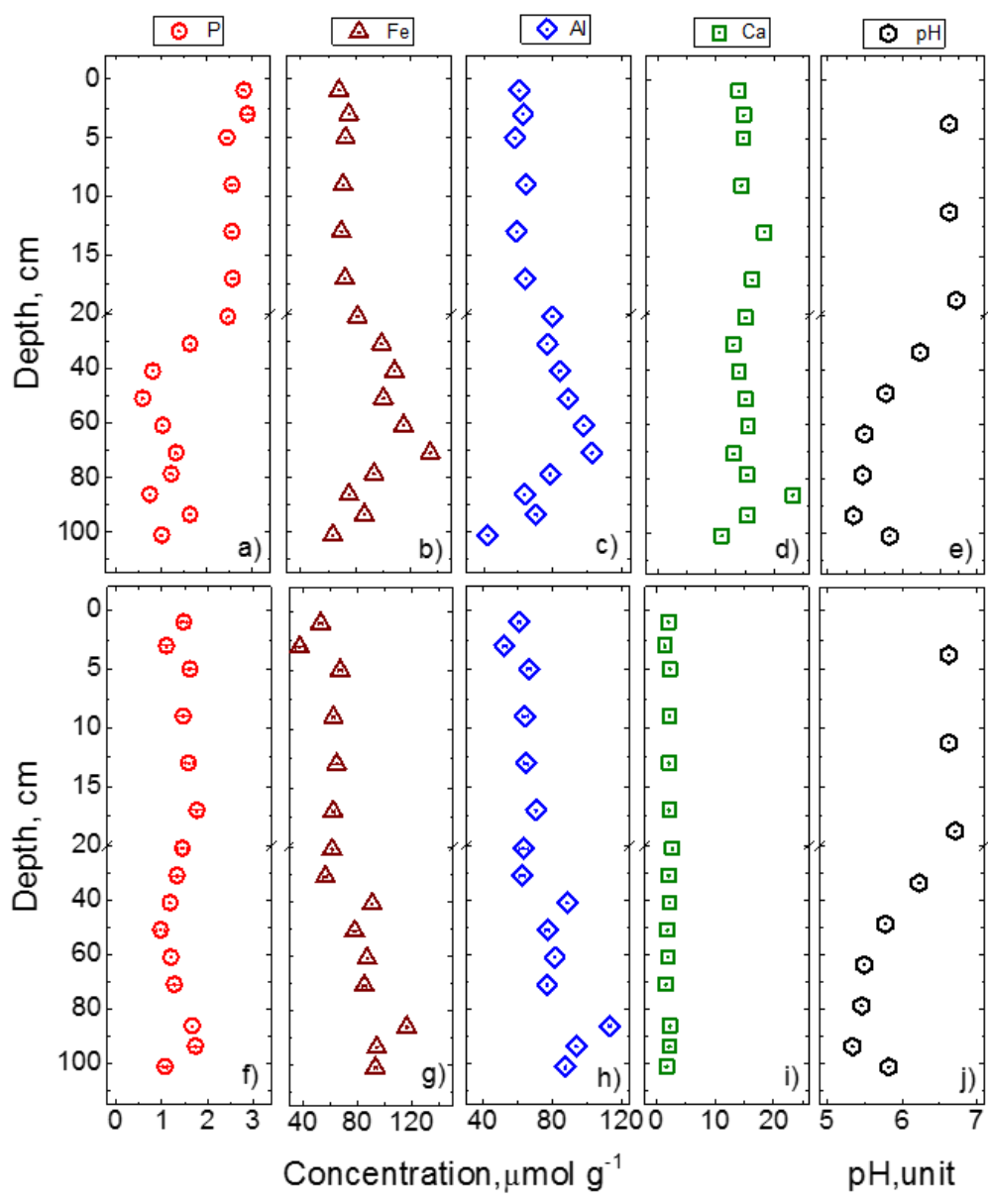


Figure 3.4 Concentration of total P, Fe, Al, and Ca in HCl (a, b, c, and d) and HNO₃ (f, g, h, and i) extracted solutions. The soil pH (e and f) was plotted to compare with the concentration profiles. Please note that both e and f are the same soil pH. Concentrations of these elements were measured by using inductively coupled plasma emission spectrometry (ICP-OES).

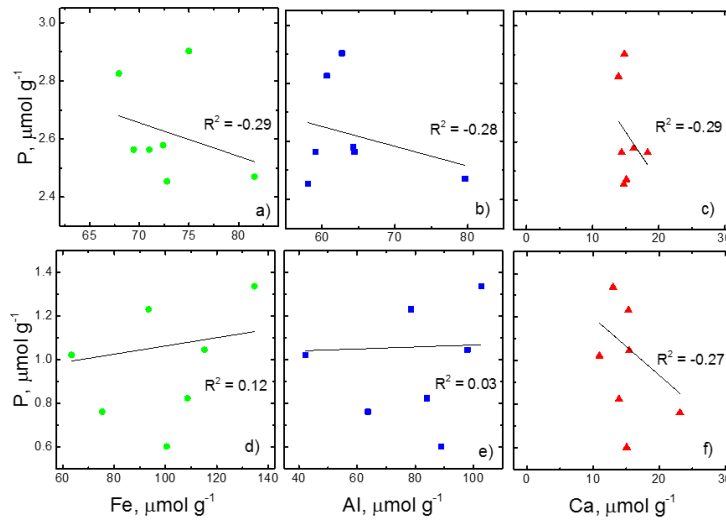


Figure 3.5 Scatter plots P with other elements that are associated or coupled with P: Fe (a, d), Al (b, e), and Ca (c, f) in 1 mol L⁻¹ HCl extracted solution at shallow (a, b, and c) and deeper (d, e, and f) depth in the soil column. R² values refer to Pearson's linear correlation.

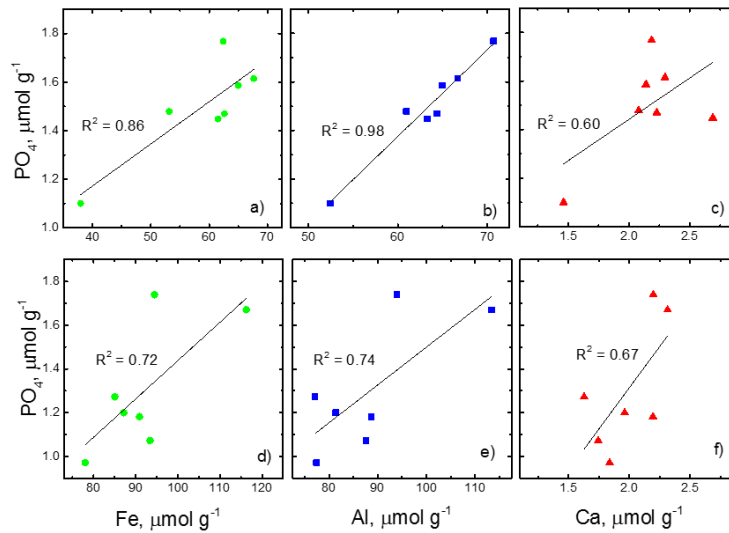


Figure 3.6 The scatter plots P with other elements that are associated or coupled with P: Fe (a, d), Al (b, e), and Ca (c, f) in 10 mol L⁻¹ HNO₃ extracted solution at shallow (a, b, and c) and deeper (d, e, and f) soil column. R² values refer to Pearson's linear correlation.

3.5 Discussion

3.5.1 Sources of acid extractable P pools

Fertilizer application plays an important role in buildup of soil P pools and active plant uptake changes P dynamics. Thus, identification of P sources that precipitate or transform into acid-P pools not only allows quantitative understanding of these P pools in the residual fraction remaining after sequential fractionation but also provides insights into the sources that transform into acid-P pools. Given that there are several potential P sources (such as soil P pools, microbial P pool, and organic P pool) within soil that may contribute to the formation of the HCl-P and HNO₃-P pools and complex interactions among biotic and abiotic processes including P transformation within soil P pools may generate these P pools, intricacies among these processes complicate the differentiation of P sources. Long-term application of fertilizer at shallow depth (i.e., agronomically active top soil) leads to increased TP, soil P pools (NaOH, HCl, and HNO₃) and Mehlich-3 P, consistent with past studies (e.g., Lehman et al., 2005). Comparing individual P pools, TP content in the soil in our study sites is more than 50% higher than mean soil test in New Castle county soils (Pautler & Sims, 2000). At the shallow depth, Mehlich-3 P content is very high (~192 mg kg⁻¹; Table 3.1) which is more than 6 times higher than the average agronomic soil test phosphorus (STP; i.e., Mehlich-1) in the region (~30 mg kg⁻¹; Pautler & Sims, 2000). Similarly, the NaOH-P_i pool accounted for > 50% of TP content of soils (see Table 3.1 and Figure 3.3 a). This P_i pool, which is considered as P tightly bound to Fe and Al minerals (Hedley et al., 1982; Tiessen et al., 1984; Wager et al., 1986), is the major sink of P in slightly acidic soils (Tiessen et al., 1984; Guo et al., 2000; Joshi et

al., 2016). These results suggest shallow depth soils are highly P saturated and may promote precipitation or formation of acid-P pools.

The isotopic compositions of acid-P pools provide further evidence of their potential sources in an agricultural soil. The $\delta^{18}\text{O}_\text{P}$ values of HCl-P_i in the soil varied within a narrow range (between 20.2–21.9‰) over the entire depth (0–105 cm) but were slightly heavier than the calculated depth-equilibrium trend (Figure 3.3e). In contrast the isotopic compositions of HCl-P_i in non-agricultural and agricultural soils measured so far have been found to include a wider range (between 5.6–21.3‰) depending upon P sources and biogeochemical processes on the formation of these P pools (Zohar et al., 2010b; Angert et al., 2011, 2012; Tamburini et al., 2012; Joshi et al., 2016). Also note that the $\delta^{18}\text{O}_\text{P}$ values of HCl-P_i from geological sources should be much lighter (Ayliffe et al., 1992; Jaisi and Blake, 2010; Angert et al., 2012; Tamburini et al., 2012). For example, volcanic apatite minerals have the lowest range of isotopic compositions (5.3–7.0‰; Taylor, 1968; Mizota et al., 1992). The isotope values become heavier during weathering and dissolution/re-precipitation of primary apatite from draining meteoric waters (Singer et al., 1991). However, biological cycling will change the P pool composition (most likely to NaHCO₃-P_i or NaOH-P_i) as well as the isotope composition of these pools (Joshi et al., 2016). These lines of evidences suggest that the HCl-P_i pool extracted from the study site even at higher depths (105 cm) is not of geogenic (source rock under the soil horizons) origin but rather precipitated from anthropogenic P sources (i.e., applied P for crops in soils). Interestingly, $\delta^{18}\text{O}_\text{P}$ values of HCl-P_i are very similar to that of NaOH-P_i (Figure 3.3d) even though there are some mismatches at certain depths. This suggests that NaOH-P_i acts as the potential precursor P pool which may precipitated or transformed into HCl-

P_i. Given that HCl-P_i and NaOH-P_i pools have two distinct P forms (as HCl-P_i includes amorphous or crystalline Ca-P minerals and NaOH-P_i includes strongly sorbed, occluded and precipitated P with Fe and Al oxides), it is intuitive to discuss the potential mode of this transformation.

The $\delta^{18}\text{O}_\text{P}$ values of HNO₃-P_i in the soil varied within a narrow range (between 19.5–21.9‰) over the entire depth (0–105 cm) (Figure 3.3f). Although these values are heavier near the surface and at 50 to 60 cm, they were within the calculated equilibrium isotopic compositions at the intermediate depths. This result suggests that at the intermediate depths, microbially cycled P or a certain fraction of this P pool is potentially transferred into the HNO₃-P_i pool. In fact, $\delta^{18}\text{O}_\text{P}$ values of HNO₃-P_i are more similar to that of NaOH-P_i pools (Figures 3.3d, f) and show a similar trend with depth, suggesting NaOH-P_i pools offer a stronger potential precursor for the HNO₃-P_i pool (see below for additional evidence from elemental composition). NaOH-P (i.e., tightly bound P to Fe and Al minerals) is the major sink of P in the soil, which is considered as moderately bioavailable or unavailable depending upon soil P conditions and plant efficiency of P uptake (Tiessen et al., 1983; Zhang & MacKenzie, 1997; Guo et al., 2000). This P pool acts as an intermediate between dissolved or loosely sorbed (H₂O-P and NaHCO₃-P) and acid-P (HCl-P and HNO₃-P) pools.

Evaluation of the relationship of P with Fe, Al, and Ca in HCl and HNO₃ extracted solutions provides additional insights into potential sources and modes of transformation. High concentration of Ca in HCl extracted solution over the entire soil depth indirectly supports that HCl dissolves primarily crystalline Ca-P minerals such as apatite. The concentration of phytate in HCl extracted solution is expected to be low (Mingjing Sun; personal communication). This result is consistent with the literature

that suggests HCl-P corresponds to crystalline Ca-P minerals such as apatite (Tiessen et al., 1983; Tiessen & Moir, 1993). Several other studies using the P K-edge XANES method on soil residue with or without HCl extraction also support removal of Ca-P by HCl (e.g., Beauchemin et al., 2003; Kar et al., 2011; McLaren et al., 2015).

Although HCl dissolves primarily Ca-P minerals, high concentration of Fe and Al in HCl extracted solutions (Figure 3.4b, c, d) suggest dissolution of additional soil minerals (primarily not associated with Ca) by HCl. Similar results have been reported in the literature (e.g., McLaren et al., 2015). This could be some crystalline Fe and Al oxides or silicates that are not extracted by 0.5 mol L⁻¹ NaOH. Similarly, HNO₃ extracts a high amount of Fe and Al and a negligible amount of Ca (Figure 3.4g, h, i). However, the overall trends of extracted Fe, Al, and Ca were similar, suggesting potential dissolution of secondary clay minerals and Fe and Al minerals during extraction. Dissolution of clay minerals, mica and kaolinite, is also supported with quantitative micro-XRD by a consistent decrease during HNO₃ extraction (Table 3.2). Furthermore, the amount of amorphous mineral content increased in the residual minerals after NaOH to HCl to HNO₃ extractions. This could likely result from the supersaturation of ions and corresponding precipitation of extracted solution during freeze-drying before XRD measurement. Given that fate of P in soils is controlled by amorphous minerals and those with high reactive surface area, absence of an appropriate method to quantify these minerals limits quantitative understanding of the composition of these minerals that are not extracted by 0.5 mol L⁻¹ NaOH but dissolve in 1 mol L⁻¹ HCl, and the residual minerals that dissolve in 10 mol L⁻¹ HNO₃.

3.5.2 Mechanisms of P transformation and formation of acid extractable P

Isotopic compositions of P_i pools ($\text{NaOH-}P_i$, $\text{HCl-}P_i$, and $\text{HNO}_3\text{-}P_i$) and concentrations of P, Fe, Al, and Ca in HCl and HNO_3 extracted solutions provide mechanistic insights into P transformation or precipitation of acid-P pools. Continuous application of P fertilizer increases the HCl-P pool and the formation of this P pool at the expense of other P pools has been interpreted from its changing concentration with time (McKenzie et al., 1992; Richards et al., 1995; Lehmann et al., 2005). However, identifying the pathways and mechanisms that lead to the formation of HCl-P has been either interpreted or empirically defined because of the inability of concentration-based data to identify the mechanism. Recently, using ^{18}O -labeled phosphate in an agricultural soil, active P transformation of readily available P ($\text{H}_2\text{O-}P_i$ and $\text{NaHCO}_3\text{-}P_i$) into moderately available ($\text{NaOH-}P_i$) and finally into P precipitates such as apatite ($\text{HCl-}P_i$) in soil was identified (Joshi et al., 2016). As discussed above, our results from this study are consistent with Joshi et al. (2016) and confirm that the $\text{NaOH-}P_i$ pool is primarily transformed and precipitated as $\text{HCl-}P_i$. This extends the application of natural abundance of isotopes to address P pool transformation.

Strong acids extract P primarily occluded within more crystalline Fe and Al minerals and P retained in primary or secondary silicate minerals. A high concentration of $\text{HNO}_3\text{-}P_i$ in our study site suggests that continuous application of P fertilizer resulted in the formation of a highly recalcitrant P pool. Similar isotopic compositions of $\text{HNO}_3\text{-}P_i$ and $\text{NaOH-}P_i$ pools suggest $\text{NaOH-}P_i$ as the primary pool that transformed or precipitated as $\text{HNO}_3\text{-}P_i$ in the shallow and deeper soils. The near absence of Ca in $\text{HNO}_3\text{-}P_i$ but higher concentrations of Al and Fe that are positively correlated with P (Figures 3.5 and 3.6) is consistent with the interpretation that $\text{NaOH-}P_i$, but not $\text{HCl-}P_i$, transforms into $\text{HNO}_3\text{-}P_i$. Thus it is intuitive to imagine that over

time slow adsorption of P in Fe and Al oxide and clay minerals, controlled primarily by diffusion processes, crystallinity, and particle morphology (Parfitt, 1989; Torrent et al., 1992; Arai & Sparks, 2007) makes a fraction of this P pool unavailable for the NaOH reagent. Both neither the slow transformation of the NaOH-P_i pool and surface precipitation (Arai & Sparks, 2007) alter its original isotopic composition, except minor kinetic fractionation (Jaisi et al., 2010), which are expected to be insignificant in soil environments. Given that the NaOH-P_i pool is largely not bioavailable, transforming it into an even more recalcitrant P pool locks in its isotopic signatures (e.g., Jaisi & Blake, 2010; Joshi et al., 2015). A suite of physicochemical processes in soils might have promoted physical entrapment or occlusion of NaOH-P_i or precipitation of amorphous Fe and Al-P_i minerals, preserving the isotopic compositions of NaOH-P_i. Overall, it is reasonable based on the present and past observation to conclude that the HNO₃-P_i pool is transformed almost entirely from NaOH-P_i.

3.5.3 Leaching of phosphorus to deeper soil horizons

Irrespective of soil depth, isotopic compositions of HCl-P_i varied within a narrow range (between 20.2–21.9‰) but are largely lighter (by ~0.5–1‰) than the equilibrium isotopic composition (Figure 3.3 e). As $\delta^{18}\text{O}_\text{P}$ values of HCl-P_i are locked in and are not biologically cycled (Jaisi & Blake, 2010; Joshi et al., 2015), any biological cycling will remove P from HCl-P_i into other readily bioavailable forms. The similar isotopic compositions of HCl-P_i suggest physical movement of particle bound P from surface soil into deeper soil. This is similar to past studies which report significant amounts of P may be transported into deeper soil horizons in the dissolved or particulate forms (Sims et al., 1998; Heathwaite & Dils, 2000; McDowell &

Sharpley, 2001; de Jonge et al., 2004; Kleinman et al., 2015). Vertical transport is largely controlled by soil type and structure, physical disturbance of surface soil (e.g., tilling), sorption and desorption processes, and water transport mechanisms (de Jonge et al., 2004; Djodjic et al., 2004; Schelde et al., 2006; Kleinman et al., 2015; Toor & Sims, 2015). Although the leaching of P from surface soil into deeper soil is known from a series of field and laboratory column studies, mechanistic understanding of particular P pools and P forms (particulate, colloidal, and dissolved) and biogeochemical processes such as uptake and recycling of P during vertical transport of P is largely unknown. This is the first study that applied natural abundance of oxygen isotope ratios of soil P_i pools to identify the process of soil P leaching. Vertical profiles of $\delta^{18}O_P$ values of the HCl- P_i pool at shallow depth are impacted from physical mixing because the soil is chisel-ploughed (~30 cm) every year. There are three possibilities: i) HCl- P_i and HNO_3 - P_i are formed in shallow soil and later migrate in deeper soil, ii) transformation of NaOH- P_i occurred at different depths after NaOH- P_i migrated to those depths, and iii) downward movement of dissolved P underwent a series of transformations to form these P pools. In situ precipitation of HCl- P_i at different depths from the same P source will result in locking in of the $\delta^{18}O_P$ values. But any biological cycling such as that of dissolved P during vertical migration, will change the isotope composition towards equilibrium. Given that Ca-P minerals are not often in the nano- to colloidal- size range, the possibility of precipitated Ca-P minerals migrating downward in the soil column is relatively low. However, Fe and Al oxides are most commonly present in nano- to colloidal- size range, making it likely that NaOH- P_i and HNO_3 - P_i pools might have migrated as intact minerals or NaOH- P_i transformed into HNO_3 - P_i at certain depth. These lines of possibilities are consistent

with the implications made in several other controlled and field studies (e.g., Uusitalo et al., 2001; de Jonge et al., 2004; Jiang et al., 2015). However, further research focused on the mode and mechanism of transport in the soil column is required to constrain the mechanism and explicit understanding on the form of leaching of a specific P pool.

3.6 Conclusions and implications

Our understanding on the sources and mechanistic understanding of P that generates acid extractable P_i pools (i.e., HCl and HNO_3) in soils are poorly understood. These P pools constitute a significant proportion of the total P, generally >30% in moderately weathered soils, but could be >80% in soils that are strongly weathered or derived from volcanic parent material (Turner et al., 2005; Condon & Newman, 2011) and intermediate values are normally found in agricultural soils. Other studies claim that long-term recovery of P applied to soils may be as high as 90%, assuming that fixed P in the soil transfers into available forms (Syers et al., 2008), this condition is anticipated to be less likely in agricultural soils where external sources of easily bioavailable P are constantly added, often beyond the crop P removal rate. There are, however, several indirect mechanisms that plant roots may act on to dissolve and thus access acid-P pool, including release of protons and low-molecular-weight organic acids, microbial metabolites, or root exudates, or through symbiotic relationships with specific microorganisms but most often under P starvation or under low P conditions (Guo et al., 2000; Hinsinger, 2001; Richardson, 2001; Khan & Joergensen, 2009; Richardson & Simpson, 2011). Thus exploitation of these physicochemical or biological routes to extract recalcitrant P pools into plant available forms benefits both saving a declining natural resource as well as limiting P loss into

open waters. The paucity of research on the pathways of formation as well composition of the acid-P pool has limited our ability to fully understand P dynamics and thus provide scientific grounds for efficient management of soil P resources.

Understanding developed from this study on the sources, mechanisms, and pathways of HCl-P_i and $\text{HNO}_3\text{-P}_i$ formation in soil provides critical information that could be used either to minimize or slow down the transformation of P into more recalcitrant P pools or otherwise explore avenues to mobilize these P pools. On the methodological front, our results provide strong evidence that the stable isotope method goes beyond operationally defined P pool speciation and aids in developing mechanistic understanding on the formation of acid-P pools. It is hoped that application of new tracers that are more specific to reactions and processes will catalyze new research efforts and thus enhance our understanding from classically operationally-defined P pools to functionally-defined P speciation in soils.

REFERENCES

- Achat, D.L., Bakker, M.R., & Morel, C. 2009. Process-Based Assessment of Phosphorus Availability in a Low Phosphorus Sorbing Forest Soil using Isotopic Dilution Methods All rights reserved. No part of this periodical may be reproduced or transmitted in any form or by any means, electronic or mechani. *Soil Science Society of America Journal* **73**, 2131–2142.
- Angert, A., Weiner, T., Mazeh, S., & Sternberg, M. 2012. Soil phosphate stable oxygen isotopes across rainfall and bedrock gradients. *Environmental science & technology* **46**, 2156–62.
- Angert, A., Weiner, T., Mazeh, S., Tamburini, F., Frossard, E., Bernasconi, S.M., & Sternberg, M. 2011. Seasonal variability of soil phosphate stable oxygen isotopes in rainfall manipulation experiments. *Geochimica et Cosmochimica Acta* **75**, 4216–4227.
- Arai, Y., & Sparks, D.L. 2007. Phosphate reaction dynamics in soils and soil components: A Multiscale Approach. p. 135–179. In *Agronomy, D.L.S.B.T.-A.* in (ed.), Academic Press.
- Ayliffe, L.K., Lister, A.M., & Chivas, A.R. 1992. The preservation of glacial-interglacial climatic signatures in the oxygen isotopes of elephant skeletal phosphate. *Palaeogeography, Palaeoclimatology, Palaeoecology* **99**, 179–191.
- Balmér, P. 2004. Phosphorus recovery - an overview of potentials and possibilities. *Water Science and Technology* **49**, 185–190.
- Beauchemin, S., Hesterberg, D., Chou, J., Beauchemin, M., Simard, R.R., & Sayers, D.E. 2003. Speciation of phosphorus in phosphorus-enriched agricultural soils using X-Ray absorption near-edge structure spectroscopy and chemical fractionation Contribution no. 02-091(J). *Journal of Environmental Quality* **32**, 1809–1819.
- Blake, R.E., O’Neil, J.R., & Garcia, G.A. 1997. Oxygen isotope systematics of biologically mediated reactions of phosphate: I. Microbial degradation of organophosphorus compounds. *Geochimica et Cosmochimica Acta* **61**, 4411–4422.

- Bräuniger, T., Wormald, P., & Hodgkinson, P. 2002. Improved proton decoupling in NMR spectroscopy of crystalline solids using the SPINAL-64 sequence. *Monatshefte für Chemie / Chemical Monthly* **133**, 1549–1554.
- Bühler, S., Oberson, A., Sinaj, S., Friesen, D.K., & Frossard, E. 2003. Isotope methods for assessing plant available phosphorus in acid tropical soils. *European Journal of Soil Science* **54**, 605–616.
- Chang, S.C., & Jackson, M.L. 1957. Fractionation of soil phosphorus. *Soil Science* **84**, 133–144.
- Condron, L.M., & Newman, S. 2011. Revisiting the fundamentals of phosphorus fractionation of sediments and soils. *Journal of Soils and Sediments* **11**, 830–840.
- Cordell, D., Drangert, J.-O., & White, S. 2009. The story of phosphorus: Global food security and food for thought. *Global Environmental Change* **19**, 292–305.
- Djordjic, F., Börling, K., & Bergström, L. 2004. Phosphorus leaching in relation to soil type and soil phosphorus content. *Journal of Environmental Quality* **33**, 678–684.
- Franz, M. 2008. Phosphate fertilizer from sewage sludge ash (SSA). *Waste Management* **28**, 1809–1818.
- Friesen, D.K., & Blair, G.J. 1988. A dual radiotracer study of transformations of organic, inorganic and plant residue phosphorus in soil in the presence and absence of plants. *Soil Research* **26**, 355–366.
- Frossard, E., Achat, D.L., Bernasconi, S.M., Bünemann, E.K., Fardeau, J.C., Jansa, J., Morel, C., Rabeharisoa, L., Randriamanantsoa, L., Sinaj, S., Tamburini, F., & Oberson, A. 2011. The use of tracers to investigate phosphate cycling in soil/plant systems. p. 59–91. In Bünemann, E.K., Oberson, A., Frossard, E. (eds.), *Phosphorus in Action*. Springer Berlin Heidelberg.
- Frossard, E., & Sinaj, S. 1997. The isotope exchange kinetic technique: a method to describe the availability of inorganic nutrients. Applications to K, PO₄, SO₄ and Zn. *Isotopes Environ. Health Stud.* **33**, 61–77.
- Gaxiola, R.A., Edwards, M., & Elser, J.J. 2011. A transgenic approach to enhance phosphorus use efficiency in crops as part of a comprehensive strategy for sustainable agriculture. *Chemosphere* **84**, 840–845.

- Guo, F., Yost, R.S., Hue, N. V, Evensen, C.I., & Silva, J.A. 2000. Changes in phosphorus fractions in soils under intensive plant growth. *Soil Science Society of America Journal* **64**, 1681–1689.
- He, Z., Senwo, Z.N., & Tazisong, I.A. 2012. Long-term dynamics of labile and stable phosphorus following poultry litter application to pasture soils. *Communications in Soil Science and Plant Analysis* **43**, 2835–2850.
- Heathwaite, A.L., & Dils, R.M. 2000. Characterising phosphorus loss in surface and subsurface hydrological pathways. *Science of The Total Environment* **251–252**, 523–538.
- Hedley, M.J., Stewart, W.B., & Chauwan, B.S. 1982. Changes in inorganic and organic soil phosphorus fractions induced by cultivation practices and by laboratory incubations. *Soil Science Society of America Journal* **46**, 970–976.
- Hinsinger, P. 2001. Bioavailability of soil inorganic P in the rhizosphere as affected by root-induced chemical changes: a review. *Plant and Soil* **237**, 173–195.
- Hunger, S., Cho, H., Sim, J.T., & Sparks, D.L. 2004. Direct speciation of phosphorus in alum-amended poultry litter: Solid-state ³¹P-NMR investigation. *Environmental Science & Technology* **38**, 674–681.
- Hunger, S., Cho, H., Sim, J.T., & Sparks, D.L. 2008. Evidence for struvite in poultry litter: effect of storage and drying. *Journal of Environmental Quality* **37**, 1617–1625.
- Jaisi, D.P. 2013. Stable isotope fractionations during reactive transport of phosphate in packed-bed sediment columns. *Journal of contaminant hydrology* **154**, 10–9.
- Jaisi, D.P., & Blake, R.E. 2010. Tracing sources and cycling of phosphorus in Peru Margin sediments using oxygen isotopes in authigenic and detrital phosphates. *Geochimica et Cosmochimica Acta* **74**, 3199–3212.
- Jaisi, D.P., & Blake, R.E. 2014. Advances in using oxygen isotope ratios of phosphate to understand phosphorus cycling in the environment. p. 1–53. *In* Advances in Agronomy. Academic Press.
- Jaisi, D.P., Kukkadapu, R.K., & Blake, R.E. 2010. Fractionation of oxygen isotopes in phosphate during its interactions with iron oxides. *Geochimica et Cosmochimica Acta* **74**, 1309–1319.

- Jiang, X., Bol, R., Nischwitz, V., Siebers, N., Willbold, S., Vereecken, H., Amelung, W., & Klumpp, E. 2015. Phosphorus containing water dispersible nanoparticles in arable soil. *Journal of Environmental Quality* **44**, 1772–1781.
- Johansen, H.S., Middelboe, V., & Larsen, S. 1990. Delabelling of ^{18}O enriched phosphate added to soil as a function of biological activity in the soil. In: Stable isotopes in plant nutrition, soil fertility and environmental studies. Vienna.
- de Jonge, L.W., Moldrup, P., Rubæk, G.H., Schelde, K., & Djurhuus, J. 2004. Particle leaching and particle-facilitated transport of phosphorus at field scale. *Vadose Zone Journal* **3**, 462–470.
- Joshi, S.R., Kukkadapu, R.K., Burdige, D.J., Bowden, M.E., Sparks, D.L., & Jaisi, D.P. 2015. Organic matter remineralization predominates phosphorus cycling in the Mid-bay sediments in the Chesapeake Bay. *Environmental Science & Technology* **49**, 5887–5896.
- Joshi, S.R., Li, X., & Jaisi, D.P. 2016. Transformation of phosphorus pools in an agricultural soil: An application of oxygen-18 labeling in phosphate. *Soil Science Society of America Journal* **80**.
- Kar, G., Hundal, L.S., Schoenau, J.J., & Peak, D. 2011. Direct chemical speciation of P in sequential chemical extraction residues using P K-Edge X-Ray absorption near-edge structure spectroscopy. *Soil Science* **176**.
- Karl, D.M., & Tien, G. 1992. MagIC: A sensitive and precise method for measuring dissolved phosphorus in aquatic environments. *Limnology and Oceanography* **37**, 105–116.
- Khan, K.S., & Joergensen, R.G. 2009. Changes in microbial biomass and P fractions in biogenic household waste compost amended with inorganic P fertilizers. *Bioresource Technology* **100**, 303–309.
- Kleinman, P.J.A., Church, C., Saporito, L.S., McGrath, J.M., Reiter, M.S., Allen, A.L., Tingle, S., Binford, G.D., Han, K., & Joern, B.C. 2015. Phosphorus leaching from agricultural soils of the Delmarva Peninsula, USA. *Journal of Environmental Quality* **44**, 524–534.
- Kruse, J., Abraham, M., Amelung, W., Baum, C., Bol, R., Kühn, O., Lewandowski, H., Niederberger, J., Oelmann, Y., Rüger, C., Santner, J., Siebers, M., Siebers, N., Spohn, M., Vestergren, J., Vogts, A., & Leinweber, P. 2015. Innovative methods in soil phosphorus research: A review. *Journal of Plant Nutrition and Soil Science* **178**, 43–88.

- Larsen, S., Middelboe, V., & Johansen, H.S. 1989. The fate of ^{18}O labelled phosphate in soil-plant systems. *Plant and Soil* **117**, 143–145.
- Lecuyer, C., Grandjean, P., & Sheppard, S.M.F. 1999. Oxygen isotope exchange between dissolved phosphate and water at temperatures $< 135^\circ\text{C}$: Inorganic versus biological fractionations. *Geochimica et Cosmochimica Acta* **63**, 855–862.
- Lehmann, J., Lan, Z., Hyland, C., Sato, S., Solomon, D., & Ketterings, Q.M. 2005. Long-term dynamics of phosphorus forms and retention in manure-amended soils. *Environmental Science & Technology* **39**, 6672–6680.
- Li, W., Joshi, S.R., Hou, G., Burdige, D., Sparks, D.L., & Jaisi, D.P. 2014. Characterizing phosphorus speciation of Chesapeake Bay sediments using chemical extraction, ^{31}P NMR, and X-ray absorption fine structure spectroscopy. *Environmental Science & Technology* **49**, 203–211.
- Liang, Y., & Blake, R.E. 2006. Oxygen isotope signature of Pi regeneration from organic compounds by phosphomonoesterases and photooxidation. *Geochimica et Cosmochimica Acta* **70**, 3957–3969.
- Longinelli, A., & Nuti, S. 1973. Revised phosphate-water isotopic temperature scale. *Earth and Planetary Science Letters* **19**, 373–376.
- Maguire, R.O., Hesterberg, D., Gernat, A., Anderson, K., Wineland, M., & Grimes, J. 2006. Liming poultry manures to decrease soluble phosphorus and suppress the bacteria population. *Journal of Environmental Quality* **35**, 849–857.
- McDowell, R.W., & Sharpley, A.N. 2001. Approximating phosphorus release from soils to surface runoff and subsurface drainage. *Journal of Environmental Quality* **30**, 508–520.
- McKenzie, R.H., Stewart, J.W.B., Dormaar, J.F., & Schaalje, G.B. 1992. Long-term crop rotation and fertilizer effects on phosphorus transformations: II. In a Luvisolic soil. *Canadian Journal of Soil Science* **72**, 581–589.
- McLaren, T.I., Guppy, C.N., Tighe, M.K., Schefe, C.R., Flavel, R.J., Cowie, B.C.C., & Tadich, A. 2015. Validation of soil phosphate removal by alkaline and acidic reagents in a vertosol soil using XANES spectroscopy. *Communications in Soil Science and Plant Analysis* **46**, 1998–2017.
- Mehlich, A. 1984. Mehlich 3 soil test extractant: A modification of Mehlich 2 extractant. *Communications in Soil Science and Plant Analysis* **15**, 1409–1416.

- Mizota, C., Domon, Y., & Yoshida, N. 1992. Oxygen isotope composition of natural phosphates from volcanic ash soils of the Great Rift Valley of Africa and east Java, Indonesia. *Geoderma* **53**, 111–123.
- Morse, G.K., Brett, S.W., Guy, J.A., & Lester, J.N. 1998. Review: Phosphorus removal and recovery technologies. *Science of The Total Environment* **212**, 69–81.
- Murphy, J., & Riley, J.P. 1962. A modified single solution method for the determination of phosphate in natural waters. *Analytica Chimica Acta* **27**, 31–36.
- O'Neil, J.R., Vennemann, T.W., & McKenzie, W.F. 2003. Effects of speciation on equilibrium fractionations and rates of oxygen isotope exchange between (PO₄)^{aq} and H₂O. *Geochimica et Cosmochimica Acta* **67**, 3135–3144.
- Parfitt, R.L. 1989. Phosphate reactions with natural allophane, ferrihydrite and goethite. *Journal of Soil Science* **40**, 359–369.
- Pautler, M.C., & Sims, J.T. 2000. Relationships between soil test phosphorus, soluble phosphorus, and phosphorus saturation in Delaware soils. *Soil Science Society of America Journal* **64**, 765–773.
- Paytan, A., Kolodny, Y., Neori, A., & Luz, B. 2002. Rapid biologically mediated oxygen isotope exchange between water and phosphate. *Global Biogeochemical Cycles* **16**, 13–18.
- Psenner, R., Bostrom, B., Dinka, M., Petterson, K., Pucsko, R., Sager, A., & Mackenzie, F.T. 1988. No Title. *Arch. Hydrobiol, Beih Ergebn Limnol.* **30**, 98–103.
- Richards, J.E., Bates, T.E., & Sheppard, S.C. 1995. Changes in the forms and distribution of soil phosphorus due to long-term corn production. *Canadian Journal of Soil Science* **75**, 311–318.
- Richardson, A.E. 2001. Prospects for using soil microorganisms to improve the acquisition of phosphorus by plants. *Functional Plant Biology* **28**, 897–906.
- Richardson, A.E., & Simpson, R.J. 2011. Soil microorganisms mediating phosphorus availability update on microbial phosphorus. *Plant physiology* **156**, 989–96.
- Rowland, A.P., & Haygarth, P.M. 1997. Determination of total dissolved phosphorus in soil solutions. *Journal of Environmental Quality* **26**, 410–415.

- Ruttenberg, C. 1992. Development of a sequential extraction method for different forms of phosphorus in marine sediments. *Limnol. Oceanogr* **37**, 1460–1482.
- Schelde, K., de Jonge, L.W., Kjaergaard, C., Laegdsmand, M., & Rubæk, G.H. 2006. Effects of manure application and plowing on transport of colloids and phosphorus to tile drains. *Vadose Zone Journal* **5**, 445–458.
- Shelton, J.E., & Coleman, N.T. 1968. Inorganic phosphorus fractions and their relationship to residual value of large applications of phosphorus on high phosphorus fixing soils. *Soil Sci Soc Am Proc* **32**, 91–94.
- Sims, J.T., Simard, R.R., & Joern, B.C. 1998. Phosphorus loss in agricultural drainage: Historical perspective and current research. *Journal of Environmental Quality* **27**, 277–293.
- Singer, A., Silber, A., & Szafrank, D. 1991. Nodular-silica-phosphate minerals of the Har Peres pyroclastics, Golan Heights. *Neues. jb. Miner. Mh., H.* **8**, 337–354.
- Syers, J.K., Johnson, A.E., & Curtin, D. 2008. Efficiency of soil and fertilizer phosphorus use: Reconciling changing concepts of soil phosphorus behaviour with agronomic information. *FAO Fertilizer and Plant Nutrient Bulletin*, 123.
- Tamburini, F., Pfahler, V., Bünemann, E.K., Guelland, K., Bernasconi, S.M., & Frossard, E. 2012. Oxygen isotopes unravel the role of microorganisms in phosphate cycling in soils. *Environmental science & technology* **46**, 5956–62.
- Taylor, H.P. 1968. The oxygen isotope geochemistry of igneous rocks. *Contributions to Mineralogy and Petrology* **19**, 1–71.
- Thomas, G.W. 1996. Soil pH and soil acidity. In Sparks, D.L. (ed.), *Method of soil analysis*. Soil Science Society of America, Madison, WI.
- Tiessen, H.J., & Moir, O. 1993. Characterization of available P by sequential extraction. p. 75–86. In Carter, M.R. (ed.), *Soil sampling and methods of analysis*. Canadian Soil Science Society., Lewis Publ., Boca Raton, FL.
- Tiessen, H., Stewart, J.W.B., & Cole, C. V. 1984. Pathways of phosphorus transformations in soils of differing pedogenesis. *Soil Science Society of America Journal* **48**, 853–858.
- Tiessen, H., Stewart, J.W.B., & Moir, J.O. 1983. Changes in organic and inorganic phosphorus composition of two grassland soils and their particle size fractions during 60–90 years of cultivation. *Journal of Soil Science* **34**, 815–823.

- Toor, G.S., & Sims, J.T. 2015. Managing phosphorus leaching in Mid-Atlantic soils: Importance of legacy sources. *Vadose Zone Journal* **14**.
- Torrent, J., Schwertmann, U., & Barron, V. 1992. Fast and slow phosphate sorption by goethite-rich natural materials. *Clays and Clay Minerals* **40**, 14–21.
- Turner, B.L., Cade-Menun, B.J., Condon, L.M., & Newman, S. 2005. Extraction of soil organic phosphorus. *Talanta* **66**, 294–306.
- Uusitalo, R., Turtola, E., Kauppila, T., & Lilja, T. 2001. Particulate phosphorus and sediment in surface runoff and drainflow from clayey soils. *Journal of Environmental Quality* **30**, 589–595.
- Vennemann, T.W., Fricke, H.C., Blake, R.E., Neil, J.R.O., & Colman, A. 2002. Oxygen isotope analysis of phosphates : A comparison of techniques for analysis of Ag₃ PO₄. *Chemical Geology* **185**, 321–336.
- Wager, B.I., Stewart, J.W.B., & Moir, J.O. 1986. Changes with time in the form and availability of residual fertilizer phosphorus on chernozemic soils. *Canadian Journal of Soil Science* **66**, 105–119.
- Wang, D., Xie, Y., Jaisi, D.P., & Jin, Y. 2016. Effects of low-molecular-weight organic acids on the dissolution of hydroxyapatite nanoparticles. *Environmental Science: Nano*.
- Zhang, T.Q., & MacKenzie, A.F. 1997. Changes of soil phosphorous fractions under long-term corn monoculture. *Soil Science Society of America Journal* **61**, 485–493.
- Zohar, I., Shaviv, A., Klass, T., Roberts, K., & Paytan, A. 2010a. Method for the analysis of oxygen isotopic composition of soil phosphate fractions. *Environmental science & technology* **44**, 7583–8.
- Zohar, I., Shaviv, A., Young, M., Kendall, C., Silva, S., & Paytan, A. 2010b. Phosphorus dynamics in soils irrigated with reclaimed waste water or fresh water - A study using oxygen isotopic composition of phosphate. *Geoderma* **159**, 109–121.

Chapter 4

DISTINCT PATHWAYS OF PHOSPHORUS CYCLING IN THE UPSTREAM AND DOWNSTREAM SECTIONS OF A CREEK IN AN AGRICULTURAL RUNOFF DOMINATED WATERSHED

4.1 Abstract

Phosphorus (P) loss from agricultural fields is a major non-point P source that causes environmental problems such as eutrophication in open waters. However, the effects of active P load from agricultural fields as well as legacy P in the watershed on build-up of sediment P pools and the impact on biogeochemical cycling of P are poorly understood largely due to methodological limitations that constrain and track P sources and biogeochemical processes. This, in fact, has been a major obstacle preventing the accurate assessment of nutrient loads released to open waters and ecosystems. In this study, we analyzed concentrations and phosphate oxygen isotope ratios ($\delta^{18}\text{O}_\text{P}$) in dissolved and suspended particulate matter P in the surface water, pore water, and sediment P pools in river bed along two district zones (agricultural runoff dominated headwater and wetland dominated mouth) of East Creek, a tidal tributary of the Chesapeake Bay. Our results show high concentrations of dissolved inorganic (P_i) and organic P (P_o) in the water column and pore water as well as high particulate and sediment P_i in the headwater region, suggesting the role of P loading from agricultural fields as well as from other potential legacy sources and biogeochemical processes that release P. Concentrations of all of these P pools in the wetland zone was low and the trend of pore water P concentration was in fact opposite

to that of the headwater region and impacted by advancing tides both in surface and subsurface waters. Isotopic compositions of pore water and sediment P pools suggested dominance of the remineralization pathway of P cycling in the headwater region and overall complete biological cycling of pore water P in the wetland region. New insights gained from these findings on the sources and cycling of P are expected to be helpful to control P loss and improve water quality issues in the Chesapeake Bay.

4.2 Introduction

Phosphorus loss from agricultural fields is considered as the major source of non-point P pollution in open waters. Most often, P applied as commercial fertilizer or animal waste is incompletely taken up by crops. In the Delmarva Peninsula, a long history of farming and extensive application of commercial fertilizer and manure beyond the crop requirement has resulted in the build-up of soil P [*Sims et al., 2000*]. Furthermore, intensive poultry production in the region also has added P in soils and resulted in the accumulation of legacy P in the soil and the watershed [*Kleinman et al., 2012; Sharpley et al., 2013*]. An increase in soil P, in turn, has increased the vulnerability of P loss by leaching and surface runoff. Depending on hydrologic connectivity, this P is carried downstream by rivers and released to larger water bodies such as lakes, estuaries, and bays, and can lead to further deterioration of water quality by contributing to surface water eutrophication and bottom water dead zones.

Most often, riverine systems are considered transport routes for nutrients and physicochemical and biogeochemical processes within the water column and sediments are largely ignored. Since sedimentary burial is the main mechanism of P removal from waters, understanding P sequestration by river bed sediments and the

eventual fate of buried P are important to identify the extent to which the sediments can be a temporal or long-term sink for P. Several past studies indicate the variable extent of P burial and mobilization. For example, only a small portion (1–5%) of particulate P (PP) entering the oceans is permanently buried in sediments [*Anschutz et al.*, 1998; *Benitez-Nelson*, 2000] primarily because a substantial amount of sedimentary PP can still be converted to soluble P that escapes to the water column [*Li et al.*, 2016a]. The extent of burial was found to be slightly higher (~30%) in the shallow Aarhus Bay in Denmark [*Jensen et al.*, 1995]. In a comparative study of sediments from the Atlantic, Canadian, and Portuguese continental margins and the anoxic region of the Chesapeake Bay, 20–30% of total P buried in the sediment was found to be remobilized to the overlying water [*Anschutz et al.*, 1998]. The extent of burial and remobilization, however, cannot be compared among rivers in different geographical regions without considering their hydrodynamics, salinity, sediment type, nutrient load, and degree of nutrient saturation on sediment sorption sites, among other factors. However, since P can be more effectively retained in freshwater sediments than in marine sediments [*Callender*, 1982; *Fox*, 1989; *Caraco et al.*, 1990; *Chambers and Odum*, 1990; *Jensen et al.*, 1995; *Jordan et al.*, 2008], it is important to understand the role of river bed sediment on P burial as well as the potential for exchange with the water column so that the long-term fate of P in the sediment can be better understood.

The fate of P transported by rivers also depends on the form of P. For example, PP in the suspended matter is the most dominant form of P in the water column, and likely deposits in the river bed sediments [*Svendsen et al.*, 1995; *Ballantine et al.*, 2009]. Similarly, over 90% of P transported by rivers to estuaries and coastal waters is

PP [Froelich *et al.*, 1988; Föllmi, 1996]. Thus, both current and legacy P in the sediment could be derived primarily from PP deposition [Sharpley *et al.*, 2013]. Dissolved P, however, may leach into deeper soils and be carried by subsurface water to rivers via shallow lateral flow or base flow. For example, shallow subsurface flow has been identified as a key pathway of P transport from heavily manure applied fields to ditches in the coastal plain of the Delmarva Peninsula [Kleinman *et al.*, 2007]. The biogeochemical processes within the sediment may release P_i into the pore water. The two major biogeochemical processes that increase sediment pore water P_i concentration are the remineralization of organic matter and the reductive dissolution of Fe(III) oxyhydroxide particles and subsequent release of P_i . The large gradients in pore water P concentration within the sediment column and between surface sediment and water column creates a diffusive flux of P into the surface waters [House and Denison, 2002]. Therefore, it is critical need to understand the biogeochemical processes including P redistribution within the river bed sediments to develop better assessment of the magnitude of P release across the sediment-water interface.

The impact of continued P loss from agricultural fields, both current as well as legacy P sources on the build-up of sediment P pools, and biogeochemical cycling of P are poorly understood. This, in fact, has been listed as a major obstacle preventing accurate assessment of nutrient loads released to the different open waters and ecosystems and devising appropriate watershed management plans [Sharpley *et al.*, 2013]. One major challenge in this assessment is the lack of inherent tracers for analyzing P sources and cycling [Karl, 2000]. Classical approaches for quantifying the role of different P sources such as mass flux and export budgets, temporal and spatial P concentrations, and other indirect tracers are unable to track P sources and identify

biogeochemical processes [Davies *et al.*, 2014] because the history of individual P sources can be muddled by both P cycling and mixing of P from different sources [Jaisi and Blake, 2014]. Phosphate oxygen isotope ratios of P pools could be a powerful tracer as this has been successfully applied to identify sources and cycling of P in soils and sediments [Jaisi and Blake, 2010; Zohar *et al.*, 2010; Angert *et al.*, 2011, 2012; Joshi *et al.*, 2015, 2016]. The objective of this study is to understand the impact of P loads in an agricultural runoff dominated watershed on P speciation in water column and sediment P pools in the headwater region and compare to that of the wetland region of East Creek, a tidal tributary of the Chesapeake Bay.

4.3 Materials and methods

4.3.1 Sampling sites

East Creek, a tidal tributary of the Chesapeake Bay, is located in Somerset County, Maryland (Figure 4.1). The creek stretches about 10 km and drains runoff derived primarily from agricultural fields to the bay. The sediment sampling sites span from a ditch draining agricultural fields to the mouth of the creek at the bay. The long-term presence of concentrated poultry production and historical application of P (both inorganic fertilizer and poultry manure) on agricultural fields beyond crop removal rates have caused buildup of legacy P [Cabreria and Sims, 2000; Sims *et al.*, 2000] at this site to some of the highest concentrations in the region [Coale and Layton, 1999]. Being located in a critical source area (Eastern Shore of the Chesapeake bay) for nutrient release that is hydrologically connected to the Chesapeake Bay, this watershed provides a unique opportunity to explore the role of P load on sediment P speciation, including retention and remobilization from sediments.

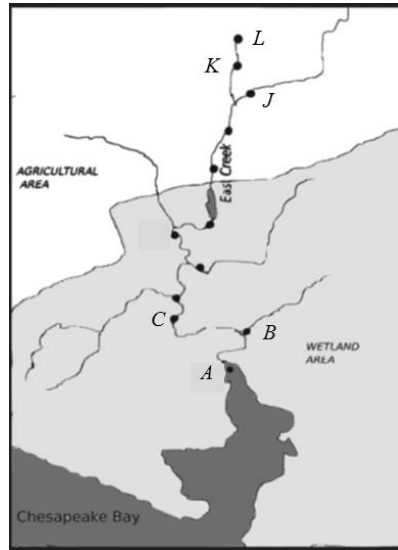


Figure 4.1 Map of East Creek and locations of water and sediment core sampling sites (adapted from Stout et al., 2016).

4.3.2 Collection and characterization of sediment and water samples

Sediment cores were collected from twelve sites along the creek using a vacuum core sampler by retracting a piston inside a 7.6 cm liner as described in Upreti et al. (2015). This method was found to recover loose, unconsolidated sediments, and pore water with a >95 % success rate. Once retrieved, sediment cores were stored in sealed liners on ice during transport to the laboratory. On returned to the laboratory, cores were immediately sliced into 2 cm depth intervals and pore water was extracted by centrifugation ($12000 \times g$; 50 min). About 1 mL of pore water sample from selected depth intervals was collected in separate air tight vials and kept frozen for measurement of pore water oxygen isotope ratios ($\delta^{18}O_W$). Remaining pore water was saved for measurement of $\delta^{18}O_P$. All collected sediment samples were immediately freeze dried, thoroughly mixed and homogenized, ground, and size separated. The samples were size separated to $< 212 \mu m$ as to be consistent with smaller size fractions

recommended in literature [e.g., *Hedley et al., 1982; Psenner et al., 1988; Ruttenberg, 1992*] and to avoid incomplete extraction of targeted P pools. All further processing, measurements and analyses were performed on this size fraction of the sediments.

Surface water immediately above the sediment core locations was also collected from all sites. Volume of sample varied by site based on our preliminary analyses and was within 8 to 64 L. Suspended particles in the surface water were separated by centrifugation ($12000 \times g$; 50 min) and then freeze dried before sequential extraction of P pools (see below). Concentrations of P_i in pore water and surface water samples were measured by using the phosphomolybdate blue method [*Murphy and Riley, 1962*]. Total P (TP) in the pore water samples was measured by inductively coupled plasma optical emission spectrometer (ICP-OES) in the Soil Testing Laboratory at the University of Delaware. However, TP in surface water samples was measured after persulfate digestion [*Rowland and Haygarth, 1997*] followed by measurement using the colorimetric method [*Murphy and Riley, 1962*].

4.3.3 Extraction of phosphorus pools in suspended particulate matter and sediments

Sequential extraction was performed on sediment and suspended particulate matter to differentiate and quantify P pools. Four sediment P pools (H_2O-P_i , $NaHCO_3-P_i$, $NaOH-P_i$, and HNO_3-P_i) and three particulate P pools ($NaHCO_3-P_i$, $NaOH-P_i$, and HNO_3-P_i) were sequentially extracted using the Hedley et al. (1982) method slightly modified by Tiessen et al. (1984). We included additional rinsing steps (with $0.5 \text{ mol L}^{-1} NaHCO_3$ and H_2O after a particular reagent) following the modification adopted in Joshi et al. (2016) in order to limit the redistribution of extracted P [*Ruttenberg, 1992*]. Concentration of P_i in each pool was quantified by using the phosphomolybdate blue

method [Murphy and Riley, 1962] and further processed for purification before isotope analysis.

4.3.4 Sample purification and silver phosphate precipitation

Surface water, pore water, and extracted solutions from sediment and suspended particulate matter were purified before silver phosphate precipitation. All samples were first treated with non-ionic, macro-porous DAX 8 Superlite™ resin to remove dissolved organic matter (DOM). The surface water and extracted solutions from the sediment were processed to reduce volume and to concentrate P_i by the magnesium induced co-precipitation (MagIC) method [Karl and Tien, 1992]. MagIC pellets were dissolved in $0.5 \text{ mol L}^{-1} \text{ HNO}_3$ and the samples were once again passed through DAX resin to remove any organic matter remaining in the solution. Before purification, pore water samples collected from different depths were combined into four depth intervals (0–10, 12–20, 22–30 and 32–40 cm) to achieve enough P_i content for silver phosphate precipitation. All samples were evaporated in a water bath $<70 \text{ }^\circ\text{C}$ to concentrate P_i and were processed through sequential precipitation steps following methods based on Jaisi and Blake (2010, 2014) but slightly revised and elaborated (for this work see Chapter 2). In brief, phosphate was precipitated as ammonium phosphomolybdate (APM) at low pH, rinsed to remove ions soluble at low pH, and APM precipitates were then dissolved using ammonium citrate. This dissolved phosphate aliquot was then precipitated as magnesium ammonium phosphate (MAP) at high pH, rinsed to remove ions soluble at high pH, and dissolved in HNO_3 . After dissolution of MAP precipitates, the solution was adjusted to neutral pH and treated with cation resin (AG50W-X8, BioRad) to remove cations, primarily Mg^{+2} and NH_4^+ .

The purified P_i was finally precipitated as silver phosphate, the ultimate analyte for O-isotope measurement.

4.3.5 Measurement of phosphate and water oxygen isotope ratios

Phosphate and water oxygen isotope ratios were measured in the laboratory at the University of Delaware. All phosphate oxygen isotope ratios in silver phosphate were measured by using a Thermo-Chemolysis Elemental Analyzer (TC/EA) coupled to a Delta V continuous flow isotope ratio mass spectrometer (IRMS, Thermo-Finnigan, Germany; precision of 0.3‰). Measured isotopic values were calibrated against YR1-1aR2 and YR3-2 standards that were originally calibrated using a conventional fluorination method [Vennemann *et al.*, 2002].

Water oxygen isotope ratios ($\delta^{18}O_w$) were measured by using a GasBench (Thermo Scientific) coupled to the IRMS. First, 0.3 mL water samples were injected into a 12 mL round-bottom borosilicate Exetainer (prefilled with 0.3 mL L^{-1} CO_2 in He) and isotopic equilibration of CO_2 - H_2O was performed in a GasBench for 24 h at 26.2 °C. Then $\delta^{18}O_{CO_2}$ in the headspace was measured using an IRMS. The $\delta^{18}O_w$ values were calculated based on the fractionation factor between CO_2 and H_2O (Cohn and Urey, 1938). Two USGS water standards ($\delta^{18}O_w$ values of -9.25 and -1.25‰) were used to calibrate the measured $\delta^{18}O_w$ values.

4.4 Results

4.4.1 Dissolved phosphorus in the surface water

Concentrations (P_i and P_o) and isotopic compositions of P_i in the surface water from sites near the agriculture-dominated region headwater (J, K, and L) and wetland region near the bay (A, B, and C) are shown in Figure 4.2 (a, b). Concentrations of

both P_i and P_o were highest in the sites in the agricultural ditch and nearby sites of the agricultural fields but decreased sharply in the sites towards the bay. For example, P_i concentration at Site L (located in a drainage ditch by the agricultural fields) was $\sim 18 \mu\text{mol L}^{-1}$, almost one log order higher than the P concentration at site A (at the mouth of creek) ($\sim 2 \mu\text{mol L}^{-1}$). The P_i concentrations in the ditch varied from 23 to $55 \mu\text{mol L}^{-1}$ depending on tide season, pH and phytoplankton blooms [Upreti et al., 2015; Bear, 2016]. All sites in the ditch next to the agricultural field were dominated by dissolved P with this pool comprising 61 to 83% of total P. Dissolved P_o concentration in the main channel of East Creek varied from 0.7 to $3.6 \mu\text{mol L}^{-1}$.

The isotopic compositions of dissolved P_i in the surface water from the sites near the agriculture-dominated region (J, K, and L) varied from 19.2 to 22.7‰ (Figure 4.2 b). Near the bay due to low concentration of P_i , isotopic composition could not be determined. Interestingly, $\delta^{18}\text{O}_P$ values of dissolved P_i in the agriculture-dominated headwater region are within the range of equilibrium isotopic compositions, calculated following Chang and Blake, (2015), based on measured surface water oxygen isotopes and temperature at the time sampling as well as temperature variation within a month (15 days before and after sampling). The exception to this is the site L, where $\delta^{18}\text{O}_P$ values are about $\sim 1.5\%$ heavier than the equilibrium values.

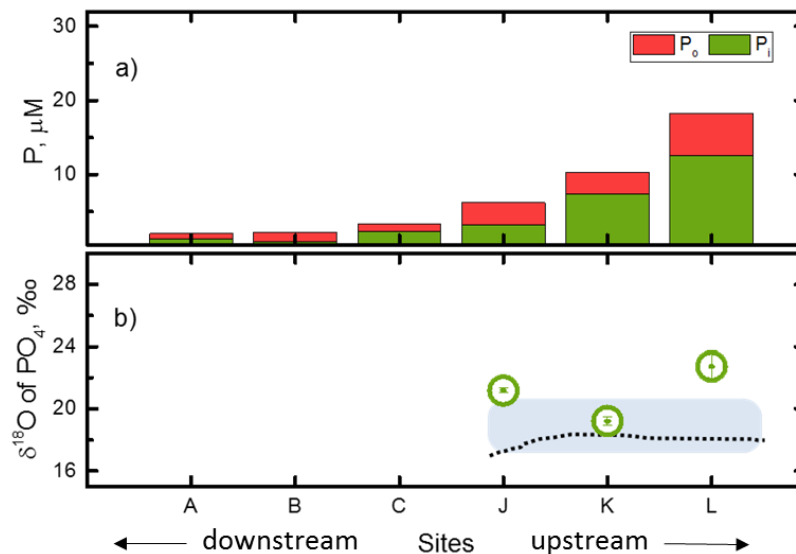


Figure 4.2 Concentrations of P_i and P_o in water samples collected from sites in the wetland region near the bay (A, B, and C) and the agriculture-dominated region in the headwater (J, K, and L) (a) and isotope values of dissolved P_i in water samples from the sites near the agricultural fields (b). The dark dotted line indicates equilibrium $\delta^{18}\text{O}_P$ composition calculated from measured water $\delta^{18}\text{O}_W$ values and temperature at the time of sampling and the shaded region corresponds to that of monthly temperature average of the sampling month.

4.4.2 Concentration and isotopic composition of P pools in suspended particulate matter

The concentrations and isotopic compositions of P_i pools ($\text{NaHCO}_3\text{-}P_i$, $\text{NaOH-}P_i$, and $\text{HNO}_3\text{-}P_i$) in suspended particulate matter collected from sites near the agriculture dominated region in the headwater (J, K, and L) and the wetland region near the bay (A, B, and C) are shown in Figure 4.3 (a, b). The $\text{NaHCO}_3\text{-}P_i$ and $\text{NaOH-}P_i$ are two major P_i pools in suspended particulate matter in the sites near the fields. In general, the trend of total P_i in these pools decreased towards the bay, similar to that of dissolved P. The suspended particulate matter at Site K was the highest in both $\text{NaHCO}_3\text{-}P_i$ ($\sim 45 \mu\text{mol g}^{-1}$) and $\text{NaOH-}P_i$ ($\sim 60 \mu\text{mol g}^{-1}$). Although these P_i pools

decreased significantly towards the bay, the relative decrease in NaOH-P_i was proportionally higher than that of the NaHCO₃-P_i pool. For example, NaHCO₃-P_i and NaOH-P_i pools in site A decreased by ~68 and 92%, respectively, compared to those at site K. However, the amount of P in the HNO₃-P_i pool was relatively similar in all studied sites.

Separation, purification, precipitation of silver phosphate and analysis of the isotopic compositions of NaHCO₃-P_i and NaOH-P_i pools from suspended particulate matter was challenging due to high concentration of contaminants and low P_i concentration. For example, low P_i in both NaHCO₃ and NaOH extracted solutions limited the measurement of isotopic compositions in these P_i pools from wetland sites near the bay. The $\delta^{18}\text{O}_p$ values of NaHCO₃-P_i from headwater sites ranged from 18.1 to 18.8‰ and were within the range of equilibrium isotopic compositions calculated according to Chang and Blake, (2015) as explained in section 4.4.1. However, the $\delta^{18}\text{O}_p$ values of NaOH-P_i pool are slightly heavier (~1.5–2‰) than equilibrium isotopic compositions.

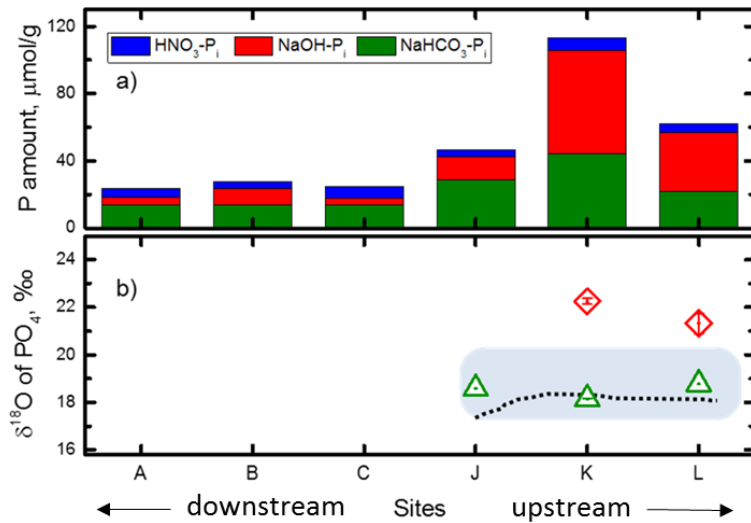


Figure 4.3 Phosphate (P_i) pools in the suspended particulate matter in creek water at sites in the wetland region near the bay (A, B, and C) and the agriculture-dominated region in the headwater (J, K, and L) (a) and their corresponding isotopic compositions (b). The equilibrium isotope values and range are the same as in Figure 4.2.

4.4.3 Isotopic composition of oxygen in the pore water

Isotopic compositions of oxygen ($\delta^{18}\text{O}_w$) in surface water and sediment pore water measured from the sites near the agriculture-dominated region in the headwater (J, K, and L) and wetland region near the bay (A, B, and C) are shown in Figure 4.4. The surface water $\delta^{18}\text{O}_w$ values range between -2.7 to -3.1‰ with heavier isotopic values in the sites near the bay compared to the headwater region. The overall trend of pore water $\delta^{18}\text{O}_w$ values was similar for all sites i.e., heavier $\delta^{18}\text{O}_w$ values in the shallow depth samples (< 20 cm) and became lighter with increasing depths. Similarly to surface water $\delta^{18}\text{O}_w$ values, the $\delta^{18}\text{O}_w$ values of pore water were heavier in the sites near the bay compared to the agriculture-dominated region in the headwater. For example, $\delta^{18}\text{O}_w$ values of pore water at site A range between -2.2 to -3.2‰ at four different depth intervals (0–12, 12–22, 22–32, and 32–42 cm). On the other hand,

$\delta^{18}\text{O}_w$ values of pore water samples at site L were -3.7 and -4.6‰ at 0 to 12 and 12 to 18 cm depth intervals, respectively.

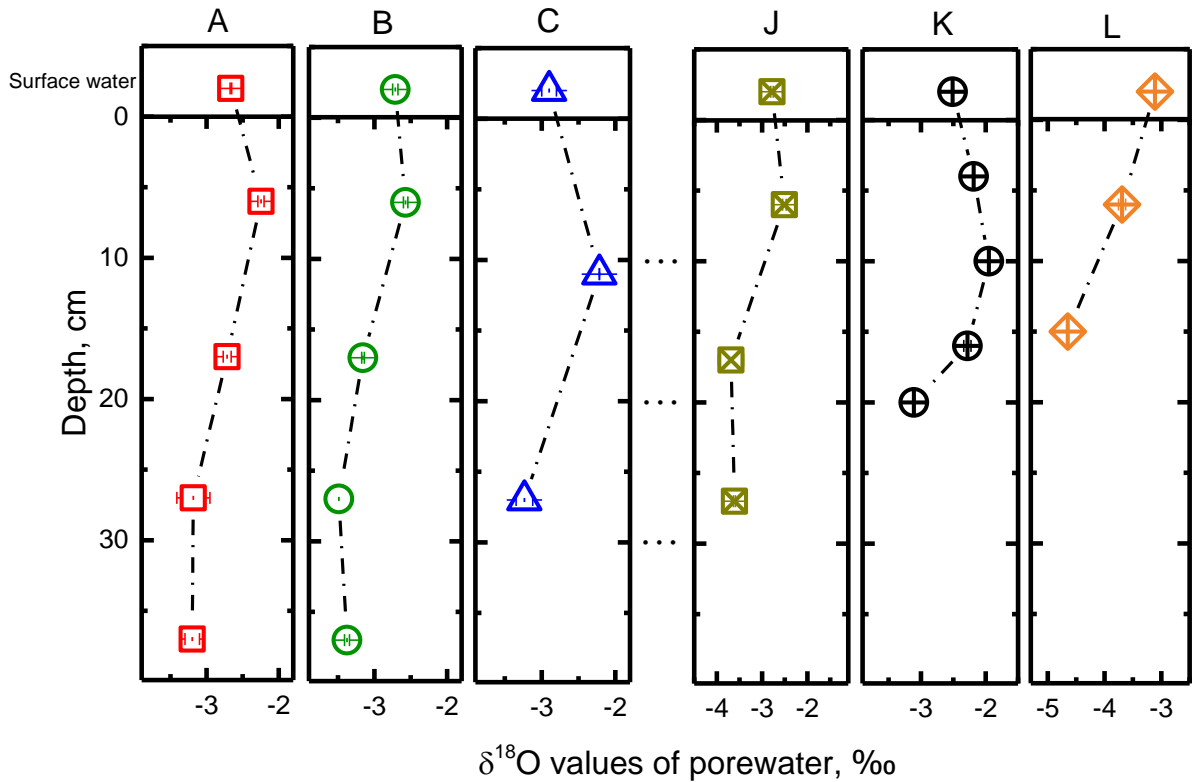


Figure 4.4 Water oxygen isotope ratios in the pore water at selected depths from sites in the wetland region near the bay (A, B, and C) and the agriculture-dominated region in the headwater (J, K, and L). Depth < 0 cm means the surface water in the creek. The line traces are showing the trends and not actual fitting results.

4.4.4 Concentration and isotopic composition of dissolved phosphate in the pore water

Concentrations of dissolved P_i in the pore water and isotopic compositions from sites in the headwater region (J, K, and L) and wetland region near the bay (A, B, and C) are shown in Figure 4.5. The pore water P_i concentration profiles show

distinctly different trends in sites near the bay compared to sites near the agriculture-dominated region. In general, sites near the bay show low P_i concentration in the shallow depths and steadily increasing P_i concentrations with depth. In contrast, sites near the agriculture-dominated region show very high P_i concentrations (50–200 $\mu\text{mol L}^{-1}$) in the shallow depths (up to 15 cm) and then rapidly decrease as the depth increases.

The $\delta^{18}\text{O}_P$ values in sediment pore water P_i varied widely (from 15.1–23.5‰) but with distinctly different trends in the sites in the wetland and headwater regions, and when compared with the calculated equilibrium isotopic composition, show interesting trends, calculated from measured pore water $\delta^{18}\text{O}_W$ values of -2.25 to -3.69‰ (Figure 4.4) and a temperature of 17 °C at 0 to 12 cm depth according to Chang and Blake (2015). The $\delta^{18}\text{O}_P$ values of pore water P_i in sites near the bay were mostly within equilibrium isotopic composition suggesting complete microbial cycling of pore water P_i . On the other hand, the $\delta^{18}\text{O}_P$ values of pore water P_i from sites L and K were distinctly lighter (~ 2 –4.5‰) than the calculated equilibrium isotopic values, potentially indicating isotopic signatures of manure applied in the agricultural fields and/or remineralization of organic matter (see below for detail).

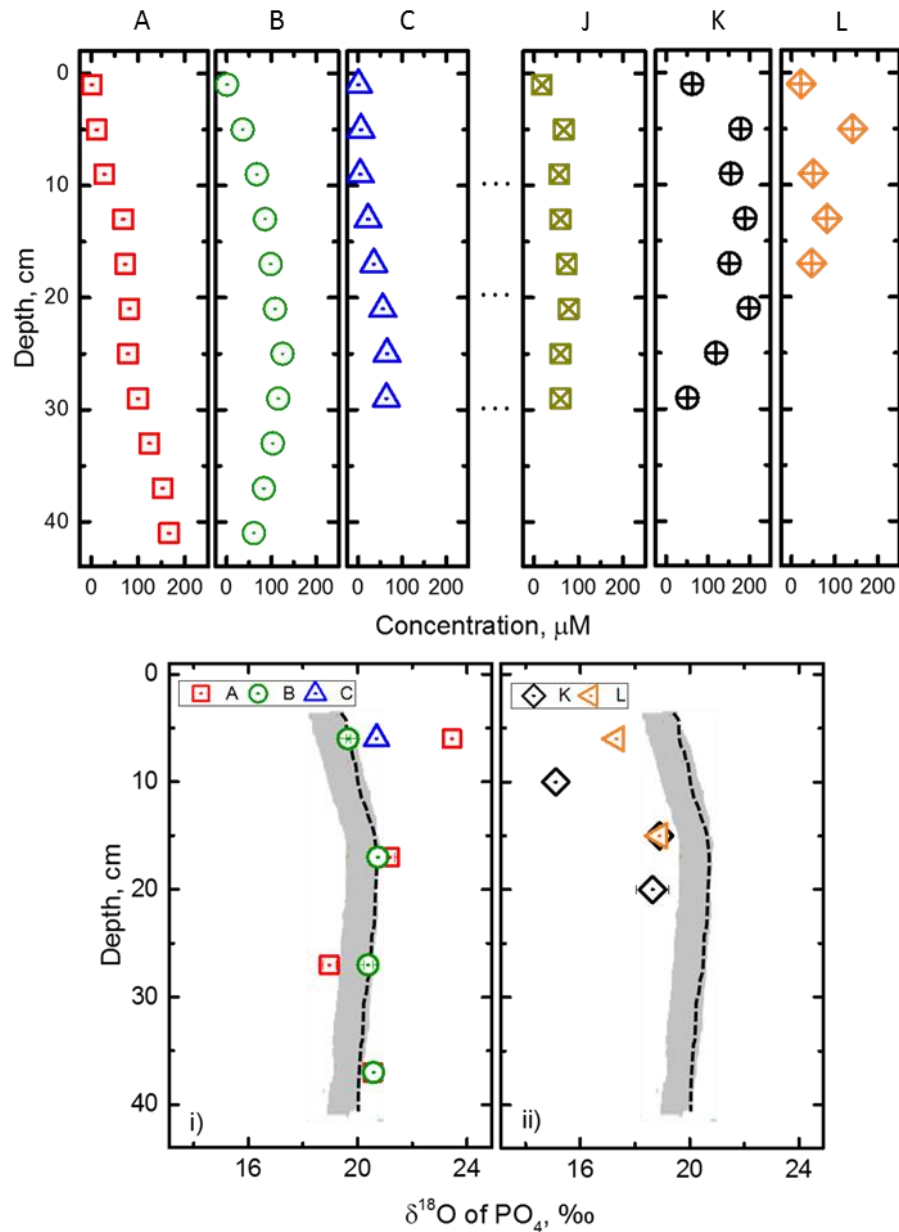


Figure 4.5 Concentrations and isotopic compositions (sites in the wetland region near the bay (A, B, and C) (i) and the agriculture-dominated region in the headwater (J, K, and L) (ii) of pore water phosphate. The dark dotted line indicates equilibrium $\delta^{18}\text{O}_P$ composition calculated from measured pore water $\delta^{18}\text{O}_W$ values and temperature at the time of sampling and the shaded region corresponds to that of monthly temperature average of the sampling month.

4.4.5 Phosphorus pools in the sediments

Concentrations of P_i (H_2O - P_i , $NaHCO_3$ - P_i , $NaOH$ - P_i , and HNO_3 - P_i) pools in the surficial sediment (0–2 cm) on the bottom of the creek in the sites near the agricultural fields (J, K, and L) and the bay (A, and C) are shown in Figure 4.6. The results show that the ditch sediments (sites K and L) had very high concentrations of P_i pools as expected from high pore water P as well dissolved P in the water column (see above). In contrast, the main channel sediments (Sites A, C, and J) had low concentrations of each P_i pool. Interestingly, distribution of P_i pools in the sediment varied among sites and did not follow a particular trend. For example, $NaHCO_3$ - P_i and $NaOH$ - P_i were dominant P_i pools in the ditch sites K and L. But HNO_3 - P_i pool was dominant at site A. H_2O - P_i made up a very small percentage of P_i at each site. This variable distribution could suggest the role of localized creek channel morphology, hydrology, and biogeochemical processes that have larger impacts on deposition and resuspension of suspended particulate matter, and remineralization and remobilization of sedimentary P (see discussion below).

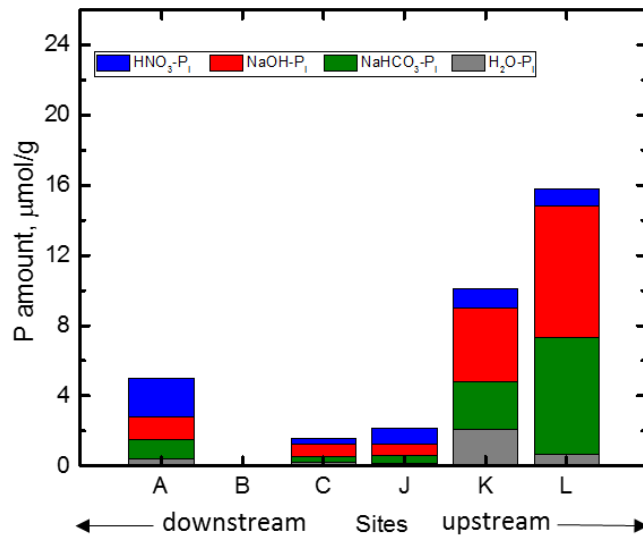


Figure 4.6 Concentrations of sediment P_i pools (H₂O-P_i, NaHCO₃-P_i, NaOH-P_i, and HNO₃-P_i) in the river bed sediment (0–2 cm) in the wetland region near the bay (A, and C) and the agriculture-dominated region in the headwater (J, K, and L).

4.5 Discussion

4.5.1 Phosphorus loss from land and transport and cycling in the water column

Pore water oxygen isotope ratios provide additional insights into the direction of groundwater flow as well as the contribution of coastal waters into the groundwater. Based on the trend of the pore water $\delta^{18}\text{O}_w$ values (Figure 4.4), subsurface flow of the groundwater appears to be dominated mainly by the agricultural region towards the wetland region. The heavier isotope values of the pore water in the deeper sediment column (>15 cm) at sites A and B suggest the mixing of incoming bay water with the subsurface ground water from highlands compared to sites J and L. Our result of the surface water $\delta^{18}\text{O}_w$ values at site A, in the wetland region, lies within the trend the

$\delta^{18}\text{O}_\text{W}$ values of the surface water along the salinity gradient in the Chesapeake bay [Li *et al.*, 2016b].

Higher concentrations of dissolved P (both P_i and P_o) in surface water and P_i pools ($\text{NaHCO}_3\text{-P}_\text{i}$, NaOH-P_i , and $\text{HNO}_3\text{-P}_\text{i}$) in suspended particulate matter in the headwater region compared to the wetland region near the bay suggests agricultural fields as a potential source of P (both dissolved and PP). High dissolved P concentration in the ditch (site L) near the fields is most likely due to shallow subsurface input of groundwater with high P concentration which is also supported by pore water $\delta^{18}\text{O}_\text{W}$ values. The lighter $\delta^{18}\text{O}_\text{W}$ values of pore water at site L compared to other sites (see Figure 4.4) and $\delta^{18}\text{O}_\text{W}$ values of pore water becoming even lighter with depth in all sites most likely resulted from subsurface input of shallow groundwater in the deeper sediment section. The surface water including ditch water undergoes evaporation and Rayleigh type fractionation results in isotope enrichment in the residual water. On the other hand, rainwater that percolates to groundwater is not impacted from evaporation and is expected to be lighter than the surface water. In fact, subsurface transport in the flat land surfaces of heavily manure applied fields in the Delmarva Peninsula has been increasingly realized as a major transport pathway of P [Mozaffari and Sims, 1994] and the highest potential of vertical leaching was identified in fine textured soils [Kleinman *et al.*, 2015]. Similarly, shallow subsurface lateral flow from the fields to ditches has also been identified as a key pathway of P transport [Kleinman *et al.*, 2007]. Agricultural fields in this region are extensively drained with open ditches which serve as direct channels of nutrient transport from fields to streams [Needelman *et al.*, 2007]. However, since P is largely fixed by clay minerals and oxides of Fe, Al and Mn in soils and sediments, dissolved P

concentrations in groundwater is often insignificant (Denver, 1986). If reactive sites in these minerals are saturated, which is the common case in the Eastern shore region of the Delmarva Peninsula dissolved P concentrations can be higher [*Cabrera and Sims, 2000; Sims et al., 2000*].

Sediment could be a source of P to the water column if the upward P flux at the sediment-water interface is higher than the downward flux. Particularly, upward flux of P_i could originate from remineralization of organic matter in the sediment (see section 4.5.2 for details). A constant positive gradient of pore water P_i concentration in the sediment (Figure 4.5) suggests dissolved P_i flux into the overlying water column at the sediment-water interface. This interpretation is consistent with the results from controlled laboratory incubations of East Creek sediments which show sediments releasing P under natural (site-specific) conditions [*Upreti et al., 2015*]. The amount of P release from sediment could be variable along the creek. On the other hand, low P concentration in the sites near the bay (~1 log order less than near the fields) is most likely due to dilution of the creek water by the incoming tides.

The isotopic compositions of dissolved P_i in the surface water and sediment P_i pools provide additional insights into the sources of dissolved P. For example, $\delta^{18}O_p$ values of dissolved P_i from sites J and K are within the equilibrium isotopic compositions (Figure 4.2) suggesting near-complete isotope exchange between dissolved P_i and water suggesting any P flux is in balance with active microbial uptake and recycling in this region [*Longinelli and Nuti, 1973; Blake et al., 1997; Paytan et al., 2002; Jaisi and Blake, 2010; Jaisi et al., 2010; Joshi et al., 2015*]. While there are limited number of data points, restricting reasonable interpretation of the trend, $\delta^{18}O_p$ values of dissolved P_i at site L are ~1.5‰ heavier than calculated equilibrium isotopic

compositions, suggesting that the flux of P is higher than microbial cycling of P, and thus P_i retains its partial inheritance source signatures. Interestingly, $\delta^{18}O_P$ values of the NaOH- P_i pool in the suspended particulate matter are similar to this value as well (see Figure 4.3). One plausible explanation for the source of P_i could be that both particulate P and dissolved P derived from the same or similar land sources and measured P_i could have originated largely from reductive dissolution of Fe(III) oxyhydroxide minerals, the most common mineral in the suspended particulate matter. Although the NaOH- P_i pool is considered as moderately or conditionally available for microorganisms [Tiessen *et al.*, 1983], the out-of-equilibrium isotopic composition of the NaOH- P_i pool suggests that this P pool is not available for microorganisms and thus carries its original source signature and therefore is useful for tracing sources [Bear, 2016]. On the other hand, $\delta^{18}O_P$ values of NaHCO₃- P_i are within equilibrium isotopic compositions, suggesting complete microbial cycling, as expected because this P pool is considered bioavailable [Olsen *et al.*, 1954; Bowman *et al.*, 1978; Tiessen *et al.*, 1983].

4.5.2 Contrasting pathways of phosphorus cycling in sediments in agriculture-dominated headwater sites and wetland sites near the bay

Concentrations and $\delta^{18}O_P$ values of dissolved P_i in pore water and P_i pools in the sediment suggest an overall difference in the pathways and biogeochemical cycling of P in the sites near the agricultural runoff-dominated region and the wetland region near the bay. Changes in physiochemical properties such as reductive dissolution of Fe-oxide minerals, pH promoted dissolution, ionic exchange and/or microbial activity such as degradation of organic matter are potential mechanisms or pathways of P cycling that may contribute to high pore water P_i concentrations.

Higher concentrations (50–200 $\mu\text{mol L}^{-1}$) of pore water P_i in the shallow depths (up to 15 cm) and lighter than equilibrium isotopic compositions in the headwater sites (Figure 4.5) suggest that pore water P_i has different sources than P_i in surface waters. The surface waters in the ditch have slightly heavier than equilibrium isotope values and thus indicate a source signature. Isotopic compositions of freshly regenerated P_i from organic matter degradation is lighter for all organic P compounds, irrespective of whether they are monoesters or diesters, due to incorporation of water oxygen (which is much lighter than phosphate oxygen) and its largely negative fractionation factors of incorporated water during degradation [*Liang and Blake, 2006, 2009*]. Since the isotopic compositions of both agricultural soil and manure applied in the agricultural fields were heavier than equilibrium isotopic compositions (e.g., ~22–26‰, Bear, 2016), the only mechanism that generates lighter than equilibrium isotope values of the pore water P_i is organic matter remineralization. Furthermore, the rate of organic matter degradation should outcompete the recycling of regenerated P_i so that the isotope signatures are still retained.

Flux of more labile organic P as well as the activities of microbial communities play an important role in assimilation and release into both the water column and pore water as part of the remineralization process of dissolved and particulate organic matter from autochthonous and allochthonous sources [*Pusch et al., 1998; Withers and Jarvie, 2008*]. Microbial degradation of organic matter largely depends on quality and retention of organic matter, inorganic nutrient supply, and temperature [*Lock, 1993; Pusch et al., 1998; Upreti et al., 2015*]. Near the agricultural fields (e.g., ditches), physiochemical and hydrological conditions are relatively more conducive for organic matter degradation than near the bay. Agricultural runoff with high $\text{PP}/\text{P}_o/\text{P}_i$ content

promotes high microbial activity in the ditches, where phytoplankton blooms are visible and this increases the pH. The role of pH was found to be the most significant among other physicochemical and biological factors that cause P release/retention in the sediment in East Creek [Upreti *et al.*, 2015]. For example, microbial processes have been found to account for 10–40% of P uptake in the ditch draining the agricultural fields in the Delmarva region [Sharpley *et al.*, 2007]. An increase in microbial P pools also promotes P release after the death or lysis of microorganisms. Microbial biomass detached from ditch banks is attributed to be the dominant particulate P in the Delmarva ditches [Kleinman *et al.*, 2007].

Wetland regions near the bay, on the other hand, show distinctly different pore water P_i concentration profiles (i.e., lower in the shallow and increase in deeper depths) and $\delta^{18}O_P$ values from those in the headwater region. Periodic redox fluctuations in the wetland during flooding and draining cycles promote reductive dissolution of Fe-oxide minerals and release of P_i associated with these minerals into the pore water. The redox fluctuation is more common in wetland sediments receiving tidal pulsing. The near-equilibrium $\delta^{18}O_P$ values of pore water P_i suggest near-complete microbial cycling of pore water P_i [Blake *et al.*, 1997, 2005] in the wetland region.

There are different variables that may cause release and retention of P in the sediment. Redox potential has been regarded as a central variable of interest in aquatic and wetland ecosystems (e.g., [Baas Becking *et al.*, 1960]). Changes in other physiochemical properties and microbial activity also contribute to high pore water P_i concentrations. A previous controlled laboratory study on surface water and sediment cores collected along the entire stretch of the creek showed that increase in microbial

activity correlated with higher P release, with upstream sediments releasing more P than downstream sediments in East Creek [Upreti *et al.*, 2015]. In addition, pH was found to be an important parameter in P release, with an increase in pH beyond 7.0, resulting in higher P release from the sediments. Agricultural ditches where pH could increase to as high as 10.0 are attributed as the major factor of P release [Bear, 2016]. Because the redox variability is expected to be high in the wetland while pH is expected to be high in the agricultural ditches, these two factors are expected to play major roles in release and retention of P from riverbed sediments in East Creek.

4.6 Conclusions and implications

Agricultural fields are considered an important non-point P source to hydrologically connected water bodies, causing water quality problems such as eutrophication. In the region with high intensity livestock production such as the Delmarva Peninsula, continued input of manure in excess of crop requirements leads to soil P saturation and P loss via dissolved and particulate forms from agricultural regions. These processes impact P speciation and cycling in surface water, pore water and sediment. As expected, the effect of P load was more prominent in the sites near the agricultural fields and gradually decreased towards the bay. A distinctly different P cycling pathway was identified in the surface water and pore water in the agricultural ditch sites: in surface water dissolved P still was incompletely cycled by microorganisms, suggesting the flux of from agricultural lands was high, but in pore water P_i released from the degradation of organic matter dominated. On the other hand, in the wetland region near the bay, P release most likely from reductive dissolution during redox fluctuation was fully cycled by microorganisms. Understanding sediment P pools and the mechanisms by which sediment P could be

released have important implications for understanding of different sources that are contributing to P exported from the watershed. Thus it is expected that findings and new insights gained on P sources and cycling from the current study in the East Creek watershed could be extended to other comparable watersheds in the region.

4.7 Acknowledgements

We thank Michael Scharf, Ashely Deny, Kiran Upreti, Jing Yan, and Lisa Stout for sampling assistance and total P measurement. Funding for this research was supported by USDA NIFA grants (2013-67019- 21373 and 2015-67020-23603). Funding for Ashely Deny, an undergraduate summer intern, was provided by NSF EPSCoR.

REFERENCES

- Angert, A., T. Weiner, S. Mazeh, F. Tamburini, E. Frossard, S. M. Bernasconi, and M. Sternberg (2011), Seasonal variability of soil phosphate stable oxygen isotopes in rainfall manipulation experiments, *Geochim. Cosmochim. Acta*, 75(15), 4216–4227.
- Angert, A., T. Weiner, S. Mazeh, and M. Sternberg (2012), Soil phosphate stable oxygen isotopes across rainfall and bedrock gradients., *Environ. Sci. Technol.*, 46(4), 2156–62.
- Anschutz, P., S. Zhong, B. Sundby, A. Mucci, and C. Gobeil (1998), Burial efficiency of phosphorus and the geochemistry of iron in continental margin sediments, *Limnol. Oceanogr.*, 43(1), 53–64.
- Ballantine, D. J., D. E. Walling, A. L. Collins, and G. J. L. Leeks (2009), The content and storage of phosphorus in fine-grained channel bed sediment in contrasting lowland agricultural catchments in the UK, *Geoderma*, 151, 141–149.
- Bear, K. (2016), Tracking sources of particulate phosphorus in river waters: A case study in East Creek, a Chesapeake Bay watershed, University of Delaware.
- Baas Becking, L. G. M., I. R. Kaplan, and D. Moore (1960), Limits of the natural environment in terms of pH and oxidation-reduction potentials, *J. Geol.*, 68(3), 243–284.
- Benitez-Nelson, C. R. (2000), The biogeochemical cycling of phosphorus in marine systems, *Earth Sci. Rev.*, 51, 109–135.
- Blake, R. E., J. R. O’Neil, and G. A. Garcia (1997), Oxygen isotope systematics of biologically mediated reactions of phosphate: I. Microbial degradation of organophosphorus compounds, *Geochim. Cosmochim. Acta*, 61(20), 4411–4422.
- Blake, R. E., J. R. O’Neil, and A. V. Surkov (2005), Biogeochemical cycling of phosphorus: Insights from oxygen isotope effects of phosphoenzymes, *Am. J. Sci.*, 305, 596–620.

- Bowman, R. A., S. R. Olsen, and F. S. Watanabe (1978), Greenhouse evaluation of residual phosphate by four phosphorus methods in neutral and calcareous soils, *Soil Sci. Soc. Am. J.*, 42(3), 451–454.
- Cabrera, M. L., and J. T. Sims (2000), Beneficial uses of agricultural, municipal, and industrial by-products, in *Beneficial uses of poultry by-products: Challenges and opportunities*, edited by J. . Power and W. Dick, pp. 425–450, Soil Science Society of America, Madison, Wisconsin, USA.
- Callender, E. (1982), Benthic phosphorus regeneration in the Potomac River Estuary YR - 1982, *Hydrobiologia*, 91-92.
- Caraco, N., J. Cole, and G. Likens (1990), A comparison of phosphorus immobilization in sediments of freshwater and coastal marine systems, *Biogeochemistry*, 9(3), 277–290.
- Chambers, R., and W. Odum (1990), Porewater oxidation, dissolved phosphate and the iron curtain, *Biogeochemistry*, 10(1), 37–52.
- Chang, S.J., and R.E. Blake (2015), Precise calibration of equilibrium oxygen isotope fractionations between dissolved phosphate and water from 3 to 37 °C. *Geochim. Cosmochim. Acta*, 150, 314–329.
- Coale, F., and S. Layton (1999), *Phosphorus site index for Maryland. Report to the Northeast Phosphorus Index Work Group*, College Park, MD.
- Cohn, M., and H.C. Urey (1938), Oxygen exchange reactions of organic compounds and water. *J. Am. Chem. Soc.*, 60, 679–687.
- Davies, C. L., B. W. J. Surridge, and D. C. Gooddy (2014), Phosphate oxygen isotopes within aquatic ecosystems: Global data synthesis and future research priorities, *Sci. Total Environ.*, 496(0), 563–575.
- Denver, J. M (1986), Hydrological and geochemistry of the unconfined aquifer, west-central and southwestern Delaware. Newark, DE: Delaware Geological Survey, University of Delaware.
- Föllmi, K. B. (1996), The phosphorus cycle, phosphogenesis and marine phosphate-rich deposits, *Earth-Science Rev.*, 40(1–2), 55–124.
- Fox, L. E. (1989), A model for inorganic control of phosphate concentrations in river waters, *Geochim. Cosmochim. Acta*, 53(2), 417–428.

- Froelich, P. N. et al. (1988), Early diagenesis of organic matter in Peru continental margin sediments: Phosphorite precipitation, *Mar. Geol.*, 80(3–4), 309–343.
- Hedley, M. J., W. B. Stewart, and B. S. Chauwan (1982), Changes in inorganic and organic soil phosphorus fractions induced by cultivation practices and by laboratory incubations. *Soil Sci. Soc. Am. J.*, 46, 970–976.
- House, W. A., and F. H. Denison (2002), Exchange of inorganic phosphate between river waters and bed-sediments, *Environ. Sci. Technol.*, 36(20), 4295–4301.
- Jaisi, D. P., and R. E. Blake (2010), Tracing sources and cycling of phosphorus in Peru Margin sediments using oxygen isotopes in authigenic and detrital phosphates, *Geochim. Cosmochim. Acta*, 74(11), 3199–3212.
- Jaisi, D. P., and R. E. Blake (2014), Advances in using oxygen isotope ratios of phosphate to understand phosphorus cycling in the environment, in *Advances in Agronomy*, vol. 125, pp. 1–53, Academic Press.
- Jaisi, D. P., R. K. Kukkadapu, and R. E. Blake (2010), Fractionation of oxygen isotopes in phosphate during its interactions with iron oxides, *Geochim. Cosmochim. Acta*, 74(4), 1309–1319.
- Jensen, H. S., P. B. Mortensen, F. O. Andersen, E. Rasmussen, and A. Jensen (1995), Phosphorus cycling in a coastal marine sediment, Aarhus Bay, Denmark, *Limnol. Oceanogr.*, 40(5), 908–917.
- Jordan, T. E., J. C. Cornwell, W. R. Boynton, and J. T. Anderson (2008), Changes in phosphorus biogeochemistry along an estuarine salinity gradient: The iron conveyor belt, *Limnol. Oceanogr.*, 53(1), 172–184.
- Joshi, S. R., R. K. Kukkadapu, D. J. Burdige, M. E. Bowden, D. L. Sparks, and D. P. Jaisi (2015), Organic matter remineralization predominates phosphorus cycling in the Mid-bay sediments in the Chesapeake Bay, *Environ. Sci. Technol.*, 49(10), 5887–5896.
- Joshi, S. R., X. Li, and D. P. Jaisi (2016), Transformation of phosphorus pools in an agricultural soil: An application of oxygen-18 labeling in phosphate, *Soil Sci. Soc. Am. J.*, 80, 69–78.
- Karl, D. M. (2000), Aquatic ecology: phosphorus, the staff of life, *Nature*, 406(6791), 31–33.

- Karl, D. M., and G. Tien (1992), MagIC: A sensitive and precise method for measuring dissolved phosphorus in aquatic environments, *Limnol. Oceanogr.*, 37(1), 105–11.
- Kleinman, P. et al. (2012), Managing manure for sustainable livestock production in the Chesapeake Bay Watershed, *J. Soil Water Conserv.*, 67(2), 54A–61A.
- Kleinman, P. J. A., A. L. Allen, B. A. Needelman, A. N. Sharpley, P. A. Vadas, L. S. Saporito, G. J. Folmar, and R. B. Bryant (2007), Dynamics of phosphorus transfers from heavily manured Coastal Plain soils to drainage ditches, *J. Soil Water Conserv.*, 62(4), 225–235.
- Kleinman, P. J. A., C. Church, L. S. Saporito, J. M. McGrath, M. S. Reiter, A. L. Allen, S. Tingle, G. D. Binford, K. Han, and B. C. Joern (2015), Phosphorus leaching from agricultural soils of the Delmarva Peninsula, USA, *J. Environ. Qual.*, 44, 524–534.
- Li, J., P. Reardon, M. P. James, S. R. Joshi, Y. Bai, K. Bear, and D. P. Jaisi (2016a), *Phosphorus cycling in the water column of the Chesapeake Bay: Roles of sinking particulates in phosphorus regeneration and sequestration.*
- Li, J., Y. Bai, K. Bear, S. Joshi, and D. Jaisi (2016b), *The limiting nutrients in the Chesapeake Bay: insights from particulate nutrient stoichiometry and phosphate oxygen isotope compositions.*
- Liang, Y., and R. E. Blake (2006), Oxygen isotope signature of Pi regeneration from organic compounds by phosphomonoesterases and photooxidation, *Geochim. Cosmochim. Acta*, 70(15), 3957–3969.
- Liang, Y., and R. E. Blake (2009), Compound and enzyme-specific phosphodiester hydrolysis mechanisms revealed by $\delta^{18}\text{O}$ of dissolved inorganic phosphate: Implications for marine P cycling, *Geochim. Cosmochim. Acta*, 73(13), 3782–3794.
- Lock, M. A. (1993), Attached microbial communities in rivers, in *Aquatic microbiology*, edited by T. E. Ford, pp. 113–138, Oxford: Blackwells.
- Longinelli, A., and S. Nuti (1973), Revised phosphate-water isotopic temperature scale, *Earth Planet. Sci. Lett.*, 19(3), 373–376.
- Mozaffari, M., and J. T. Sims (1994), Phosphorus availability and sorption in an Atlantic Coastal plain watershed dominated by animal-based agriculture, *Soil Sci.*, 157(2).

- Murphy, J., and J. P. Riley (1962), A modified single solution method for the determination of phosphate in natural waters, *Anal. Chim. Acta*, 27(0), 31–36.
- Needelman, B. ., D. . Ruppert, and R. E. Vaughan (2007), The role of ditch soil formation and redox biogeochemistry in mitigating nutrient and pollutant losses from agriculture., *J. Soil Water Conserv.*, 62, 207–215.
- Olsen, S. R., C. V Cole, F. S. Watanabe, and L. A. Dean (1954), Estimation of available phosphorus by extraction with sodium bicarbonate, *USDA Circ. 939, U.S. Govt. Print. Off. Washington, D.C.*
- Paytan, A., Y. Kolodny, A. Neori, and B. Luz (2002), Rapid biologically mediated oxygen isotope exchange between water and phosphate, *Global Biogeochem. Cycles*, 16(1), 13–18.
- Psenner, R., B. Bostrom, M. Dinka, K. Petterson, R. Pucsko, A. Sager, and F. T. Mackenzie (1988), No Title. *Arch. Hydrobiol, Beih Ergebn Limnol.* 30, 98–103.
- Pusch, M., D. Fiebig, I. Brettar, H. Eisenmann, B. K. Ellis, L. A. Kaplan, M. A. Lock, M. W. Naegeli, and W. Traunspurger (1998), The role of micro-organisms in the ecological connectivity of running waters, *Freshw. Biol.*, 40(3), 453–495.
- Rowland, A. P., and P. M. Haygarth (1997), Determination of total dissolved phosphorus in soil solutions, *J. Environ. Qual.*, 26, 410–415.
- Ruttenberg, C. (1992), Development of a sequential extraction method for different forms of phosphorus in marine sediments, *Limnol. Ocean.*, 37(7), 1460–1482.
- Sharpley, A., H. P. Jarvie, A. Buda, L. May, B. Spears, and P. Kleinman (2013), Phosphorus legacy: Overcoming the effects of past management practices to mitigate future water quality impairment, *J. Environ. Qual.*, 42(5), 1308–1326.
- Sharpley, A. N., T. Krogstad, P. Kleinman, and B. Haggard (2007), Managing natural processes in drainage ditches for nonpoint source phosphorus control, *J. soil water Conserv.*, 62(4), 197–206.
- Sims, J. T., A. C. Edwards, O. F. Schoumans, and R. R. Simard (2000), Integrating soil phosphorus testing into environmentally based agricultural management practices., *J. Environ. Qual.*, 29(1), 60–71.
- Stout, L. M., S. R. Joshi, T. M. Kana, and D. P. Jaisi (2014), Microbial activities and phosphorus cycling: An application of oxygen isotope ratios in phosphate, *Geochim. Cosmochim. Acta.*, 138, 101–116.

- Svendsen, L. M., B. Kronvang, P. Kristensen, and P. Græsbøl (1995), Dynamics of phosphorus compounds in a lowland river system: Importance of retention and non-point sources, *Hydrol. Process.*, 9(2), 119–142.
- Tiessen, H., J. W. B. Stewart, and J. O. Moir (1983), Changes in organic and inorganic composition of two grassland soils and their particle size fractions during 60–90 years of cultivation, *J. Soil Sci.*, 34, 815–823.
- Tiessen, H., J. W. B. Stewart, and C. V. Cole (1984), Pathways of phosphorus transformations in soils of differing pedogenesis. *Soil Sci. Soc. Am. J.*, 48, 853–858.
- Upreti, K., S. R. Joshi, J. McGrath, and D. P. Jaisi (2015), Factors Controlling Phosphorus Mobilization in a Coastal Plain Tributary to the Chesapeake Bay, *Soil Sci. Soc. Am. J.*, 79, 826–837.
- Vennemann, T. W., H. C. Fricke, R. E. Blake, J. R. O. Neil, and A. Colman (2002), Oxygen isotope analysis of phosphates : A comparison of techniques for analysis of Ag_3PO_4 , *Chem. Geol.*, 185, 321–336.
- Withers, P. J. A., and H. P. Jarvie (2008), Delivery and cycling of phosphorus in rivers: A review, *Sci. Total Environ.*, 400, 379–395.
- Zohar, I., A. Shaviv, M. Young, C. Kendall, S. Silva, and A. Paytan (2010), Phosphorus dynamics in soils irrigated with reclaimed waste water or fresh water - A study using oxygen isotopic composition of phosphate, *Geoderma*, 159, 109–121.

Chapter 5

ORGANIC MATTER REMINERALIZATION PREDOMINATES PHOSPHORUS CYCLING IN THE MID-BAY SEDIMENTS IN THE CHESAPEAKE BAY

5.1 Abstract

Chesapeake Bay, the largest and most productive estuary in the U.S., suffers from varying degrees of water quality issues fueled by both point and non-point source nutrient sources. Restoration of the Bay is complicated by the multitude of nutrient sources, their variable inputs, and complex interaction between imported and regenerated nutrients. These complexities not only restrict formulation of effective restoration plans but also open up debates on accountability issues with nutrient loading. A detailed understanding of sediment phosphorus (P) dynamics provides information useful in identifying the exchange of dissolved constituents across the sediment-water interface and helps to better constrain the mechanisms and processes controlling the coupling between sediments and the overlying waters. Here we used phosphate oxygen isotope ratios ($\delta^{18}\text{O}_\text{P}$) in concert with sediment chemistry, XRD, and Mössbauer spectroscopy on sediments retrieved from an organic rich, sulfidic site in the mesohaline portion of the mid-Bay to identify sources and pathway of sedimentary P cycling and to infer potential feedbacks on bottom water hypoxia and surface water eutrophication. Authigenic phosphate isotope data suggest that the regeneration of inorganic P from organic matter degradation (remineralization) is the predominant, if not sole, pathway for authigenic P precipitation in the mid-Bay

sediments. This indicates that the excess inorganic P generated by remineralization should have overwhelmed any pore-water and/ or bottom-water before a fraction of this could be precipitated as authigenic P. This is the first research that identifies the predominance of remineralization pathway and recycling of P within the Chesapeake Bay. Therefore, these results have significant implications for the current understanding of sediment P cycling and P exchange across the sediment-water interface in the Bay, particularly in terms of the sources and pathways of P that sustain hypoxia and may potentially support phytoplankton growth in the surface water.

5.2 Introduction

5.2.1 Chesapeake Bay and coastal hypoxia

Chesapeake Bay, the largest and most productive estuary in the U.S., suffers from varying degrees of summertime bottom water hypoxia and surface water eutrophication, fueled by both point and non–point source nutrient loadings. Restoration of the Bay has been difficult¹ because of the multitudes of nutrient sources and hydrological conditions and complex interacting factors including climate forcing.² From 1985 to 2008, the average monthly mean ratio of dissolved inorganic nitrogen to phosphorus (DIN : DIP) was higher than the Redfield ratio (i.e., 16 for N/P) in all seasons except midsummer.³ This suggests that phosphorus (P) could be a limiting nutrient in these seasons and also at the start of phytoplankton bloom if absolute nutrient concentrations are not in excess of biological demand. The manner in which a particular P source is introduced, recycled, and removed from the Bay is an important question not only of scientific importance but also for effective nutrient

management strategies as well as testing the efficacy of specific nutrient management plans.

Coastal hypoxia has spread exponentially worldwide since the 1960s⁴ as have oxygen minimum zones in the ocean.⁵ While hypoxia can have natural causes, it can also be induced by human activities, or occurs as a result of the interactions of or feedback from natural and anthropogenic processes. Proliferation of hypoxia due to enhanced anthropogenic nutrient loading is quite common in many coastal environments where water column chemistry is easily influenced by sediment processes. Changes in bottom water dissolved oxygen exert an influence on early diagenetic pathways in sediments (more anaerobic at the expense of aerobic pathways), as well as on the stability of Fe oxides and organic debris that settle in the sediments, the reoxidation of reduced metabolites in the sediment, the direction of nutrient flux at the sediment-water interface, and the extent of benthic-pelagic coupling (e.g., see refs 6–8). These intimately connected processes and feedbacks occur in response to hypoxia and require a better understanding of how sedimentary P dynamics are affected by temporally-varying bottom water redox conditions.

5.2.2 Organic matter remineralization vs. Fe-P coupled (remobilization) pathway of P cycling

Sedimentary P dynamics are controlled primarily by depositional fluxes of organic matter and ferric Fe-bound P, and P cycling depends on the bottom water redox conditions. Remineralization of organic matter containing P generates local gradients of inorganic P (PO_4^{3-}) in marine and lacustrine sediments (e.g., see refs 9–11) and has been invoked as the key process involved in the precipitation of authigenic P minerals (authigenic P), primarily carbonate fluoroapatite but also possibly

vivianite, and represent as a major sink in the global P cycle.¹² Furthermore, redox-driven sequestration of P and release of polyphosphate by some sulfide oxidizing bacteria such as *Thiomargarita* and *Beggiatoa* has also been linked to the precipitation of authigenic P (e.g., see refs 13 and 14). On the other hand, reductive dissolution of Fe (oxyhydro)oxides and subsequent release of adsorbed and/or co-precipitated P associated with Fe oxides also generates a local flux of P, which may precipitate as authigenic P.^{15–17} The Fe and P biogeochemical cycles are highly sensitive to redox conditions, particularly because Fe solubility depends on its oxidation state, and therefore Fe redox transformations induce precipitation or dissolution of Fe-minerals (e.g., see refs 18–21). The strong coupling of Fe and P cycling at redox interfaces has been documented worldwide (e.g., see refs 6, 9, 17, 22, and 23) and is often considered to be the major pathway of P cycling in hypoxic and anoxic bottom water and sediment columns including those that resulted in the formation of Precambrian phosphorites (e.g., see refs 24). A quantitative understanding of organic matter mineralization vs coupled Fe–P pathways of P cycling, however, is limited and is either based on model results (e.g., see refs 7 and 8) or approximated using pore water chemistry or depth profiles of sediment P pools (e.g., see refs 16, 25, and 26). This is because authigenic P, the mineral product (sink) of both pathways, cannot easily be linked to its source or precipitation pathway. These issues cannot be fully addressed using these approaches because of their inability to distinguish among contributions from sources or from specific biogeochemical processes that produce inorganic P.

Published results for Chesapeake Bay sediments indicate that the remobilized P from sediments represents a large nutrient source to the water column as compared to external input such as from terrestrial and atmospheric sources. For example, the P

released from sediments was calculated to exceed total annual terrestrial and atmospheric P input by 44–214%,²⁷ and to support 6–74% of phytoplankton P demand.²⁸ A large sediment organic matter depositional flux (equivalent to 40–60% of total primary productivity²⁹) as well as a large efflux of DOC and other nutrients from sediment^{28,30} suggests that the regeneration of inorganic P from organic matter remineralization should contribute to high levels of dissolved P in pore water near the sediment-water interface. Previous studies of sediment and pore water profiles of sulfate, dissolved and solid-phase inorganic sulfur compounds and CO₂, along with measured sulfate reduction rates in the mid-Bay have confirmed the dominance of sulfate reduction (as compared to methanogenesis) coupled to organic matter remineralization^{30,31} similar to that seen in other environments such as Cape Lookout Bight.⁶ Similarly organic matter remineralization has been suggested as the major source of authigenic P precipitation in more rapidly accumulating sediments^{6,25,32} comparable to our site in the Chesapeake Bay. The most significant organic matter remineralization (and subsequent pore water super-saturation with respect to authigenic P pool) occurs at shallow depths where the concentration of labile organic matter is high and constantly replenished from settling organic debris. Other examples of authigenic P formation in shallow sediment depths include Santa Barbara basin,³³ Long Island Sound, the Mississippi Delta,^{25,34} and Baja California.²⁶ Contrary to this, authigenic P being deposited in sediment column after precipitation in the water column as opposed to being precipitated *in situ* (i.e., in the sediment column) has been recently argued in Arkona basin of the Baltic Sea.⁷

It is yet unclear how remineralization (referred hereafter to indicate degradation of organic matter) vs remobilization (referred hereafter to indicate

reductive dissolution primarily of iron oxides) varies in the sediment column and how the predominance of one pathway impacts P flux across the sediment-water interface as well as helps sustain hypoxia in bottom water and potentially refuels eutrophication on surface water. Given that ~90% of terrestrial input of P to the Bay is either in the form of dissolved organic or some form of particulate material, they are not considered directly available to phytoplankton.²⁷ On the other hand, dissolved P derived from remobilization or remineralization is virtually fully bioavailable and thus plays more effective role on supporting phytoplankton bloom. However, identification of the sources and pathways of regenerated P is largely unresolved in the Chesapeake Bay. In this research, we aimed to identify the relative importance of remineralization vs remobilization pathways of authigenic P precipitation in the mid-Bay where bottom-water becomes seasonally anoxic (e.g., see refs 35 and 36). To achieve this goal, we sequentially extracted P pools from sediment cores and determined the phosphate oxygen isotope ratios ($\delta^{18}\text{O}_\text{P}$) of ferric Fe-bound and authigenic P, two major sinks of P in the sediments. Our results suggest that remineralization is the predominant, if not sole, pathway for authigenic P precipitation in mid-Bay sediments.

5.3 Experimental section

5.3.1 Sampling sites and sediment characterization

The sediment cores were collected from the western slope of the central channel in the mesohaline portion of the mid-Chesapeake Bay (bottomwater salinity =10–20 psu) at 38° 34.1', 76° 26.6'. Sediment deposited at this site are primarily delivered by the Susquehanna River but also includes some bank materials.³⁷ This site undergoes seasonal hypoxia/anoxia in bottom water during summer months with

underlying anoxic sediments that are often euxinic with substantial production of hydrogen sulfide (e.g., see refs 35, 36, and 38). Details of the biogeochemical characteristics of sediment and nutrient dynamics at this site are described in a number of previous publications.^{28,30,39–43}

All sediments were collected in the month of July by using box core and multicore devices. Sediment cores were chilled right after retrieval in ice as well as during transportation and then stored at $-80\text{ }^{\circ}\text{C}$ before processing. All cores were sliced into 1 or 3 cm intervals down to 32 cm under a N_2 atmosphere. The pore water was extracted by centrifugation, and then the sediment slices were freeze-dried and size separated ($<200\text{ }\mu\text{m}$). All analyses were performed using this size fraction of the sediments.

5.3.2 Extraction of sediment P pools

Sediments from all depths were sequentially extracted by using the SEDEX method originally developed by Ruttenberg⁴⁴ to determine concentrations of P in different operationally-defined sedimentary pools: (i) exchangeable P; (ii) ferric Fe-bound P; (iii) authigenic P (authigenic carbonate fluoroapatite, biogenic apatite and CaCO_3 -bound P); and (iv) detrital apatite P (residual inorganic P). ^{31}P NMR analysis of sediment did not detect any Al oxide-bound P in these sediments;⁴³ therefore this extraction method was not revised to account for Al oxide-bound P. Concentration of inorganic P in each pool was measured by the phosphomolybdate blue method.⁴⁵ To account matrix interference in colorimetric and inductively coupled plasma (ICP) measurements of the citrate-dithionite-bicarbonate (CDB) extracted solution, we concentrated P by using MagIC (magnesium-induced co-precipitation;⁴⁶) method, and

inorganic P was quantified after dissolving MagIC pellets. Please note that this additional step resulted in an underestimation of P pools.⁴³

The total P and concentration of other ions (Fe, Mn, Ca, Mg, and Al) in selected sediments were measured after complete digestion of sediment by using Katanax K1 Fluxer (Katanax, Quebec, Canada) at 1000 °C for 10 min. To confirm the identity of readily dissolving Fe minerals (by comparing ⁵⁷Fe- Mössbauer spectra of pristine and partially extracted sediments, see following text), sediment was dissolved in 0.5 N HCl for 1 hr in room temperature.⁴⁷ The concentrations of total P and other elements in all extraction methods were measured by using inductively coupled plasma optical emission spectrometer (ICP-OES) in the Soil Testing Laboratory at the University of Delaware.

5.3.3 Sample purification and measurement of phosphate $\delta^{18}\text{O}_p$ values

All extracted inorganic P pools were converted to silver phosphate for isotopic analyses as described below. We first used the MagIC method^{46,48} to reduce sample volume and concentrate P. It was followed by Superlite™ DAX-8 resin treatment to selectively trap organic matter (e.g., see ref 49). The partially processed samples were further purified by using sequential precipitation and recrystallization methods.^{50,51} Cations in the samples were removed by cation resin exchange before phosphate was converted into silver phosphate, the ultimate analyte for O isotope measurement. A separate P standard and a sample for which ¹⁸O labeled water (with final $\delta^{18}\text{O}_w$ values = 50.0‰) was spiked in all reagents were processed in parallel to test the validity of sample processing and to identify any hydrolysis of organic P during sample treatment. The test result was negative because we did not find any significant difference in $\delta^{18}\text{O}_p$ values in sample processed in ¹⁸O labeled water.

All phosphate oxygen isotope ratios were measured at the stable isotope facility at the University of Delaware. Silver phosphate was analyzed by online high-temperature thermal decomposition using a Thermo Chemolysis/Elemental Analyzer (TC/EA) coupled to a Delta V continuous flow isotope ratio monitoring mass spectrometer (IRMS; Thermo-Finnigan, Darmstadt, Germany) with precision of $\pm 0.3\%$. As a precaution, the presence of any impurity (possible culprits could be residual organic matter from samples or nitrate from reagent used in silver phosphate precipitation) was tested as total carbon and nitrogen with a CHN analyzer interfaced with existing IRMS. $\delta^{18}\text{O}_\text{P}$ values of samples were calibrated against conventionally fluorinated silver phosphate standards.⁵²

5.3.4 X-Ray diffraction and ^{57}Fe Mössbauer spectroscopy

X-ray diffraction (XRD) data on sediments from three different depths (0–1, 12–15, and 30–32 cm) were collected using a Panalytical MPD instrument with Cu K-alpha radiation ($\lambda = 1.54056 \text{ \AA}$). Diffraction data were analyzed by using JADE 9.5 (Materials Data Inc.) and the PDF4+ database (ICDD).

Sediments from different depths as well as residual sediments after the 0.5 N HCl extraction were analyzed by ^{57}Fe Mössbauer spectroscopy to identify the composition of Fe bearing minerals.^{53,54} In brief, Mössbauer spectra were collected using a 50 mCi (initial strength) $^{57}\text{Co/Rh}$ source. The velocity transducer MVT-1000 (WissEL) was operated in a constant acceleration mode (23 Hz, $\pm 12 \text{ mm/s}$ or 5 mm/s). An Ar–Kr proportional counter was used to analyze transmitted radiation, and the signal was stored in a multichannel scalar (MCS) as a function of energy (transducer velocity) using a 1024 channel analyzer. We collected spectra at room temperature (RT), 77 K, 35 K, 10 K, and 6 K to better resolve the identity of Fe minerals. A

closed-cycle cryostat (ARS, Allentown, PA) was employed to collect below-RT spectra. The Mössbauer spectral data were modeled with the Recoil software using a Voigt-based structural fitting.⁵⁵

5.4 Results and discussion

5.4.1 Sediment composition: XRD and Mössbauer results

XRD data show that the sediments are composed predominantly of quartz, pyrite, chlorite, and muscovite (Figure 5.1). While the presence of vermiculite and smectite (Fe containing clay minerals) and vivianite and apatite (P containing minerals) were suspected in XRD results, extended X-ray absorption fine structure (EXAFS) and solid-state ³¹P NMR identified the presence of these minerals in the sediment.⁴³ Please note that presence of vivianite in this site has been reported before^{56,57} and our recent results.⁴³ Furthermore, a significant increase in Fe(II) concentration (attaining ~300 μM) at 1–2 cm depth and rapid decline by more than a log order for >3 cm depth also indicates the removal of Fe(II) precipitate as vivianite besides pyrite.⁵⁸ XRD results did not show any particular difference in crystalline mineral compositions among sediments from three different sediment depths (0–1, 12–15, and 30–32 cm).

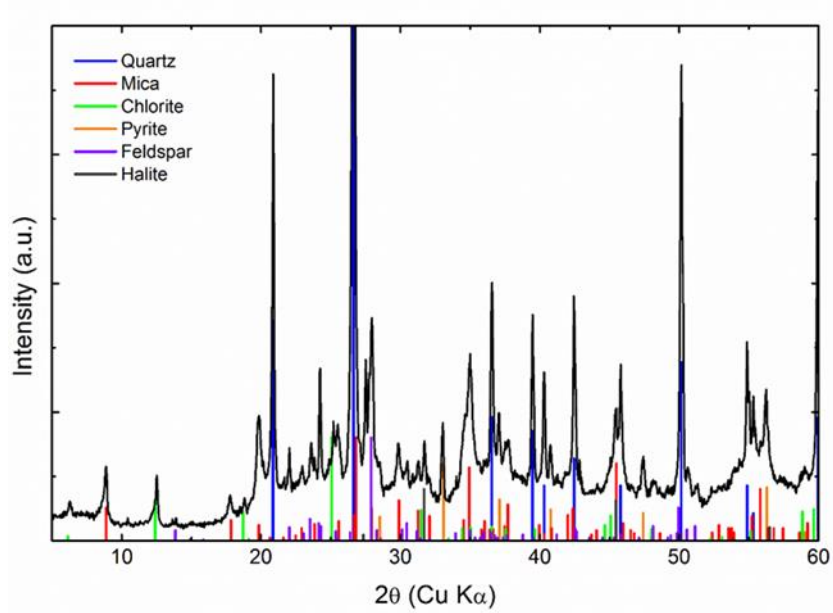


Figure 5.1 Major mineral phases in the pristine sediments from 0–1, 12–15 and 30–32 cm depth. Please note that except pyrite, Fe and P bearing minerals were below detection limit of XRD diffraction.

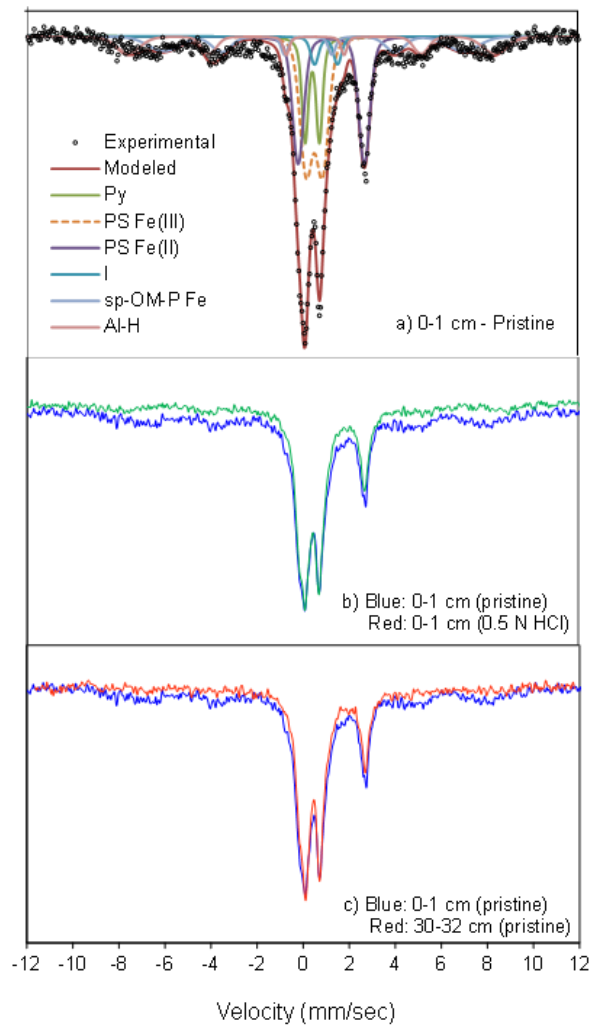


Figure 5.2 Mössbauer spectra at 10 K: (a) Modeled spectrum of 0–1 cm with various Fe-minerals (Py = pyrite; I = Ilmenite, PS = phyllosilicate, Al-H = aluminum hematite, sp-OM-P = small-particle Fe-oxide with OM and P coatings), (b) comparison showing the absence of sp-OM-P sextet in the 0.5 N HCl-treated 0–1 cm sample (green trace), and (c) comparison of 0–1 and 30–32 cm showing little or no sp-OM-P sextet in the 30–32 cm sediment.

Mössbauer spectra of pristine and 0.5 N HCl treated sediments obtained at 10 K are shown in Figure 5.2. Major Fe mineralogy of the 0–1 cm sediment includes

pyrite (Py), phyllosilicate/clay (PS), ilmenite (I), and a suite of iron oxides. Spectra obtained at various temperatures (Figure 5.3) and the conspicuous differences between Mössbauer spectra of pristine and 0.5 N HCl treated samples (Figure 5.2b) further suggest the outer and inner sextets of the 10 K modeled spectrum are likely to be Al-substituted hematite (Al-H) and small-particle poorly crystalline iron oxide with P and/or organic matter (OM) coatings (*sp*-OM-P), respectively. The assignment of the inner sextet to *sp*-OM-P is based on the following lines of evidences: (a) sextet features due to goethite, lepidocrocite, and ferrihydrite are absent in >35 K spectra⁵⁹ (Figure 5.3); b) the transformation of doublet to sextet occurs at relatively lower temperatures in OM-ferrihydrite than in pure ferrihydrite;⁶⁰ c) P- and OM-ferrihydrite are relatively more stable and less bio-reducible than pure ferrihydrite^{61,62} supported by the persistence of Fe-oxide sextet (inner) in the anoxic sediment; d) the absence of *sp*-OM-P Fe sextet in 0.5 N HCl-treated sediment (Figure 5.2b) as poorly crystalline Fe-oxides are readily soluble in HCl;⁶³ and e) concentration of ions in the 0.5 N HCl extraction (Table 5.1).

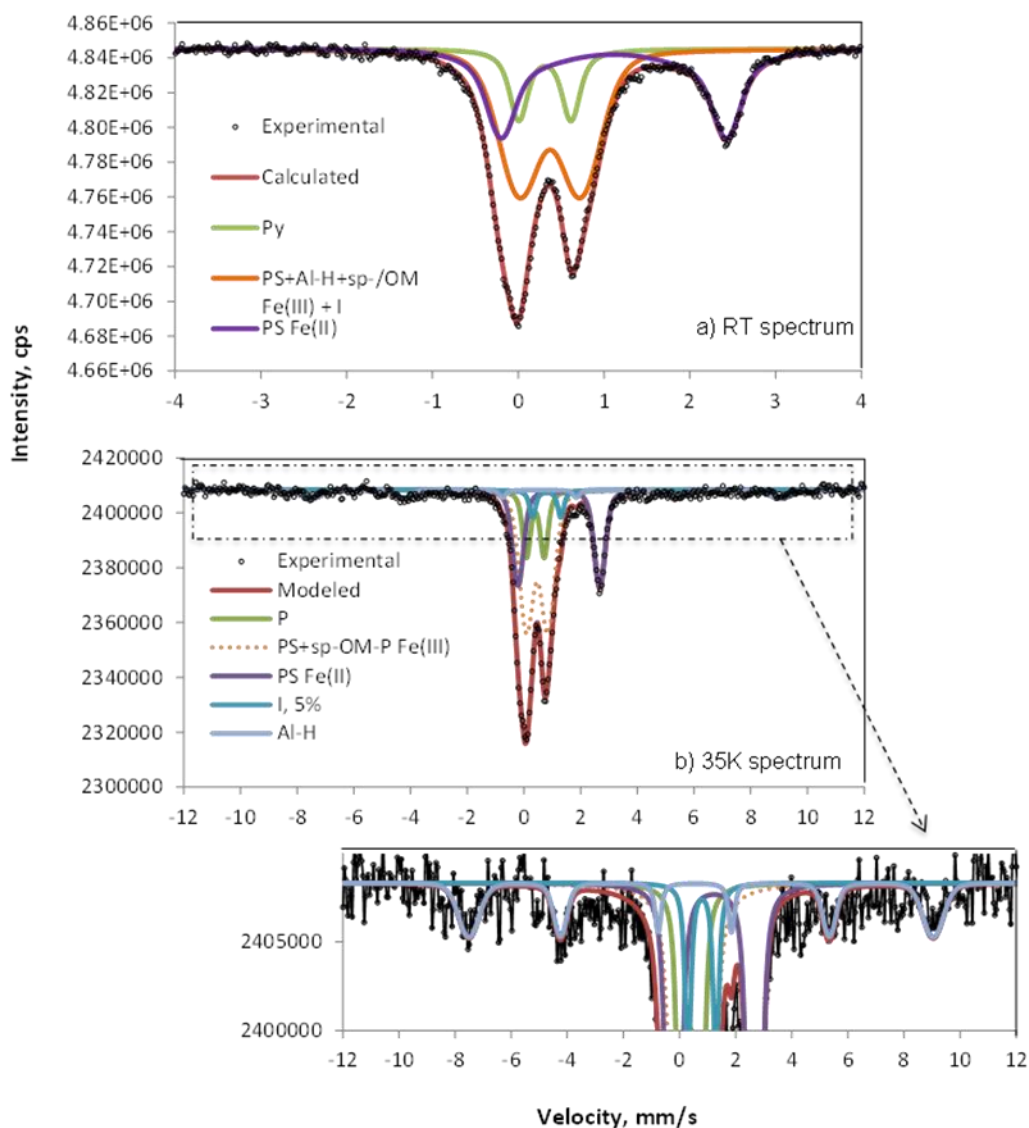


Figure 5.3 Variable temperature spectra of pristine sediment from 0-1 cm. Spectra at various temperatures were obtained to gain insights into semi-quantitative Fe mineral distribution. Inset in (b) shows the sextet that was apparent at 35 K spectra. P = Pyrite ((low-spin (LS) Fe(II)) content is fixed based on chemical composition and XRD derived pyrite content. PS Fe(II) is mostly clay because vivianite is less than a % of the total Fe (based on 0.5 N HCl extractable P). PS = phyllosilicate; I = Ilmenite; Al-H = Aluminum substituted hematite; sp = small-particle; OM = organic matter.

Table 5.1 Concentration of dissolved ions in 0.5 N HCl extracted solution from pristine sediments for 24 hrs (expressed as wt %) from three different depths in the Chesapeake Bay

Sample ID	Al	Fe	Mg	Mn	P
CB M3 0–1 cm	0.27	1.15	0.27	0.025	0.050
CB M3 12–15 cm	0.24	0.57	0.24	0.010	0.037
CB M3 30–32 cm	0.25	0.68	0.29	0.010	0.041
Sample ID	Fe (total)	Fe (II)	Fe (III)		
	%	%	%		
CB M3 0–1 cm	1.14	0.23	0.91		
CB M3 12–15 cm	0.57	0.23	0.34		
CB M3 30–32 cm	0.67	0.24	0.44		

The relative amount of pyrite, ilmenite, Al-hematite, and phyllosilicate minerals (including Fe(II)/Fe(III) ratio in PS) in the 30–32 cm sediment is more or less similar to that of the 0–1 cm sediment (Figure 5.2c). The significant difference between sediments from these two depths, however, is the near complete absence of *sp*-OM-P Fe-oxide in the 30–32 cm sediment, which is evident from qualitative comparison of their 10 K spectra (Figure 5.2c). Lower extractable Fe(III) in the deeper sediments but with more or less similar acid-extractable Fe(II), Al, Mg, and Si (Table 5.1) indicates relatively strong anoxic conditions in the deeper sediments, as expected. The additional amount of Fe(III) in the 0–1 cm sediment, ~15% of the total Fe, is similar to its Mössbauer spectroscopy-derived *sp*-OM-P Fe-oxide content. Similarly the Fe(II)/Fe(III) ratio of ~1 in phyllosilicates (PS) from the three sediment depths suggests that the clay Fe is highly reduced⁶⁴ but in relatively similar extents among the depths. Mössbauer spectra at 6 K suggest that the phyllosilicates are relatively Fe-rich (e.g., chlorite) and the sediments contain little or no siderite, magnetite, and green rust. The presence of vivianite approximated from dissolution results was low (Table 5.1)

compared to that obtained from Fe EXAFS results⁴³ which indicate 8–18% Fe as vivianite. The reason for this difference is unclear. Overall, our data suggest the *sp*-OM-P complex is more stable than pure Fe oxides, consistent with high concentration of ferric Fe-bound P.

5.4.2 Sediment P composition and P pools

Sequential extraction data indicate that the ferric Fe-bound P is the most predominant P pool (depth-averaged concentration of $5.29 \pm 0.29 \mu\text{mol/g}$) followed by authigenic P (depth-averaged concentration of $3.70 \pm 0.44 \mu\text{mol/g}$) (Figure 5.4a). Loosely sorbed and detrital P pools are very small and contribute only 8.9 and 0.5% of the extracted P, respectively. Therefore, the roles of these two pools in overall P cycling are expected to be insignificant. Sediments from this site in the Bay are dominated by phyllosilicate minerals (Figures 5.1 and 5.2), and dissolution, at least partially, of ferruginous phyllosilicates during CDB treatment¹⁹ releases P associated with these minerals. Increased layer charge of residual clay minerals after CDB treatment also promotes P release. While Fe oxides may still not be fully dissolved during hypoxic/anoxic conditions in sediments^{16,65,66} particularly due to the presence of *sp*-OM-P Fe oxides (see preceding discussion), reductive dissolution of iron phyllosilicates is expected to be quite low.^{19,20} It is likely that the majority of Fe oxides in the study site are of “detrital” origin (i.e., imported as opposed to precipitated in the water/sediment column) because detrital iron oxides are less reactive towards reductive dissolution than that of amorphous iron oxides precipitated in the water column or at the sediment-water interface.

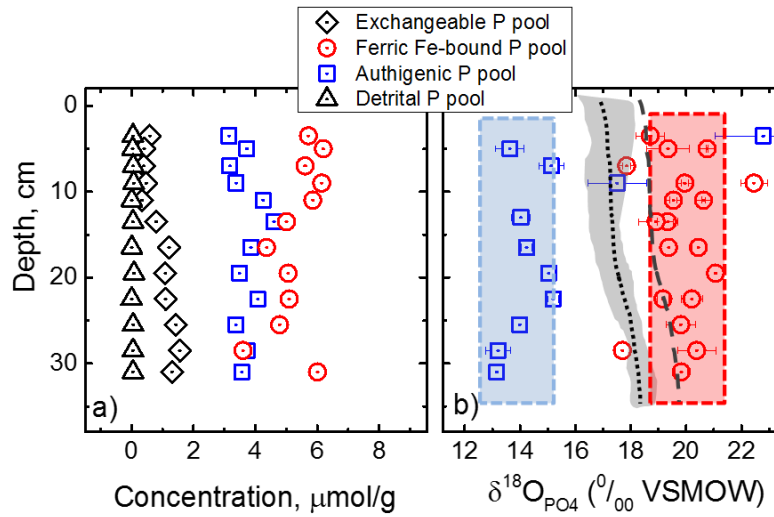


Figure 5.4 Concentration and corresponding $\delta^{18}\text{O}_p$ values of P pools in the sediment: (a) Ferric Fe-bound P dominates sediment P pools and (b) $\delta^{18}\text{O}_p$ values of ferric Fe-bound and authigenic P. The dotted line represents the equilibrium $\delta^{18}\text{O}_p$ values (per ref 70) at the site using August temperature (per ref 69) and pore water $\delta^{18}\text{O}_w$ values and the shaded region for the entire year. The dashed line is equilibrium $\delta^{18}\text{O}_p$ values per ref 71. All isotope values in this paper are reported to Vienna Standard Mean Ocean Water (VSMOW).

Authigenic P is the second most abundant P pool in the sediment column. The concentration of P in this pool steadily increases with depth until ~15 cm and becomes similar to that of ferric Fe-bound P in deeper sections (Figure 5.4a). In general, the concentrations of authigenic and ferric Fe-bound P form mirror-images across sediment depth. Such profiles, along with the stoichiometry of inorganic constituents in the porewater, e.g., dissolved sulfate, ammonia, and reactive P, are used as evidence of sink switching as P from one pool (e.g., organic matter or ferric Fe) is transformed into the other (e.g., authigenic P precipitation).^{16,25,26,34} While it is generally assumed that P released from the reductive dissolution of iron oxides could precipitate as

authigenic P, this assumption may not necessarily be true because similar profiles may be generated if original ferric Fe-bound P varies with depths and authigenic P is formed from other sources (see later discussion).

Concentrations of total sediment P along with that of extractable inorganic and organic P provide information about P speciation and relative availability of P for biological cycling or remineralization. In general, the total inorganic P extracted by the SEDEX method varied from 40.4–57.8% of the total P [i.e., 18.0–22.1 $\mu\text{mol/g}$; Table 5.2] obtained from complete dissolution. This low amount of extractable P could, in part, be due to the underestimation of ferric Fe-bound and authigenic P pools that were measured after MagIC extraction as opposed to ICP measurement.⁴³ Sediment organic P characterization using solution ³¹P NMR spectroscopy indicates that the organic P accounts for 20–26% of the total P at 0–1 cm depth (the rest being inorganic P) and is composed primarily of monoester-P, diester-P (mainly DNA-P), and pyrophosphate.⁴³ This means that the 0–1 cm sediments contain ~50% P as SEDEX extractable inorganic P with the remainder being equally split between organic and residual P (i.e., the fraction not extracted by the SEDEX method). Previous studies have noted that there has been no increase in P deposition commensurate with increased P loading in the Bay, while both nitrogen and carbon steadily increased in past ~100 yrs.⁶⁷ While this inconsistency is often used as an evidence for remobilization of P from sediments consistent with higher Redfield ratio [total organic C (TOC) in the sediment varies from 28 to 77 mg/g^{28,30,42}], the nonlinear response of deposition to overall system loading in the Chesapeake Bay⁶⁷ has raised several questions regarding the role of different sources and biogeochemical processes to release P from sediments.

Table 5.2 Elemental concentration of Fe, Ca, Fe, Mn, P and S in sediment from different depths. Inorganic P% is calculated from solution $^{31}\text{P}^{43}$ extracted from the sediment.

Depth, cm	Element concentration ($\mu\text{mol/g}$)					Inorganic P %
	Ca	Fe	Mn	P	S	
0–1	256.5	746.7	10.9	19.2	290.8	78.1
2–3	127.2	689.9	9.3	21.0	216.2	67.6
8–10	150.3	660.7	11.3	20.0	278.0	72.5
12–15	158.0	716.0	13.0	22.1	312.0	75.2
18–21	251.9	647.9	10.1	19.5	349.1	77.5
24–27	139.5	685.4	12.7	19.2	287.9	78.7
30–32	209.2	656.6	11.6	18.9	323.7	78.7

5.4.3 Isotopic composition of sediment P pools

The isotopic composition of ferric Fe-bound P varies within a narrow range (from 18.7 to 20.8‰) except for a few outliers at ~17.8 and 22.4‰ (Figure 5.4b). Overall, the isotope data are consistently similar over the entire sediment depth (32 cm) that covers about 40 years of sedimentation history.⁶⁸ Based on the measured pore water $\delta^{18}\text{O}_\text{w}$ values of -3.57 to -4.38‰ and a temperature of 12–20 °C at 0–35 cm depth⁶⁹, the equilibrium phosphate isotopic composition, according to Longinelli and Nuti,⁷⁰ is $18.23 \pm 1.07\text{‰}$. Under summertime conditions when intense degradation of organic matter occurs, equilibrium isotopic composition becomes $17.55 \pm 0.32\text{‰}$. Interestingly, measured $\delta^{18}\text{O}_\text{P}$ values of the majority of the ferric Fe-bound P are heavier than the equilibrium isotopic composition, meaning that the original isotopic compositions are largely unaltered and therefore likely indicate their origin to specific P sources. Please note that this range of isotopic composition is not expected if dissolved P is trapped with authigenic Fe oxides that are formed in the redoxcline during transient oxic-anoxic oscillations and settled into the sediment columns, or during reoxidation of Fe(II) at the sediment-water interface after the water column

becomes oxic such as in winter months. In both cases, the isotopic compositions of ferric Fe-bound P should oscillate between that of authigenic P and equilibrium P isotopic composition. Clearly this is not the case. It means ferric Fe-bound P pool in these sediments is largely composed of iron phyllosilicates (and Fe oxides as *sp*-OM-P complex) that are mostly resistant to dissolution in the anoxic sediment column (see earlier text). Limited dissolution of iron oxides likely indicates detrital nature of these minerals such as those derived from terrestrial P sources. For example, detrital ferric Fe-bound P could be associated with Fe rich-clays and iron oxide colloids that are conservatively transported and buried in the sediments without significant remobilization in postdepositional environments.

If the equilibrium isotopic composition is calculated as per Chang and Blake (2014),⁷¹ it becomes heavier by 0.9 to 2.3‰ to that of Longinelli and Nuti.⁷⁰ In this case, the majority of the ferric Fe-bound P isotopic compositions lie near equilibrium values. In either case, our results open up a new opportunity to explore more on this P pool particularly the identity of terrestrial P sources and to differentiate variable inputs of these sources in the past. Further research, however, is needed to identify these P sources as well as determine the fidelity of iron phyllosilicate and iron oxide colloids as conservative carriers of terrestrial P sources.

The isotopic compositions of authigenic P in the sediments are most interesting and intriguing for two reasons: a) their $\delta^{18}\text{O}_\text{P}$ values are the lightest among any isotope data obtained so far from marine sediments, and b) they are starkly different than those of ferric Fe-bound P. Such light $\delta^{18}\text{O}_\text{P}$ values are at the lower range that could possibly be produced immediately after the phosphohydrolase catalyzed hydrolysis of organic P compounds. Assuming the bulk of organic P is formed in Spring-early summer

months with surface and shallow depth temperature of 18–24 °C⁷² and in equilibrium with measured surface water $\delta^{18}\text{O}_\text{W}$ values of -3.89 to -4.01‰ as per Longinelli and Nuti,⁷⁰ the $\delta^{18}\text{O}_\text{P}$ values of organic P vary in the range of 17.2–19.1‰. The $\delta^{18}\text{O}_\text{P}$ values of freshly regenerated inorganic P from monoesters and diesters, accounting of water oxygen fractionation factors,^{50,73} is $\leq 12\%$. While this calculation is overly generalized from limited organic P compounds and enzymes studied so far and hence the caution is warranted, it is true that incorporation of one or two O atoms from water into inorganic P results in light $\delta^{18}\text{O}_\text{P}$ values of the freshly produced inorganic P.^{50,73–77} Any subsequent biological uptake and recycling of the fresh inorganic P changes its $\delta^{18}\text{O}_\text{P}$ values towards equilibrium isotopic composition ($18.23 \pm 1.07\%$) over time (see pore water $\delta^{18}\text{O}_\text{P}$ results). The time taken to approach isotopic equilibrium depends upon the rate of isotope exchange with water which varies with biological activity. For example, laboratory experiments have shown that the complete equilibrium is attained in ~50–100 h.^{78,79} Super saturation of pore water P should initiate the precipitation of authigenic P minerals through numerous phosphate intermediates or precursors⁴³. The precipitation and growth kinetics of apatite are rapid, for example 2–4 h in simulated laboratory experiments.⁸⁰ These lines of evidences suggest that authigenic P should have precipitated immediately after remineralization and its isotopic composition is then locked up.^{81,82} Please note that the isotope fractionation between apatite and dissolved phosphate is low ($<1.0\%$,⁸¹). This interpretation is consistent with a past study of Peru Margin sediments⁵¹ where $\delta^{18}\text{O}_\text{P}$ values enabled in distinguishing the coexistence of three different generations of authigenic P pools: (a) that precipitated at/near the sediment-water interface with the isotope values preserved during subsequent burial and diagenesis for more than five

million years, (b) that derived from remineralization of organic matter with subsequent incomplete re-equilibration (similar to this study), and (c) that recently precipitated in the sediment column. Furthermore, organic C:total P ratios in our study site was found to be much higher than Redfield ratio, reflecting preferential decomposition of organic P relative to C.⁶⁷ Similarly, N:total P ratio was found to be increased in younger sediments. These results independently support the selective remineralization and release of P from organic matter. In fact, the role of organic matter remineralization on pore water P has been found to be bigger than expected before in several other environments (e.g., Baltic Sea^{7,8,79}).

There are, however, two outliers of authigenic P $\delta^{18}\text{O}_\text{P}$ values that require additional comments. Even though it is an overstretch to interpret two isolated data points, they at least show an interesting coincidence. One point lies intermediately between isotopic compositions of authigenic and ferric Fe bound P. This could be due to the physical mixing of two P sources (one released from remineralization and other from remobilization) in the sample analyzed. The other point lies within the range of isotopic composition of dissolved P in marine environments.^{48,82} Given that the Chesapeake Bay imports significant amount of P (37% total P budget in the Bay) from marine sources,²⁷ it is likely that imported dissolved P from ocean could concentrate and undergo surface-catalyzed precipitation. While the presence of this coincidence cannot be independently verified, alternative explanation or other potential sources or processes that produce heavy $\delta^{18}\text{O}_\text{P}$ values are currently unknown.

5.4.4 Concentration and isotopic composition of pore water P

Concentration of pore water P generally increases with depth and reaches ~ 500 μM at ~20 cm depth (Figure 5.5). However, concentrations at 8–26 cm depth

show wide fluctuations. Low pore water P concentration at the shallow depth is consistent with corresponding high concentration of authigenic P (Figure 5.4a). Interestingly, $\delta^{18}\text{O}_\text{P}$ values of pore water P are either near equilibrium or heavier than equilibrium as per Longinelli and Nuti.⁷⁰ Because pore water P is the residual P left from authigenic P precipitation or any P released from reductive dissolution of Fe oxides, it can undergoes active biological cycling which alters its $\delta^{18}\text{O}_\text{P}$ values towards equilibrium. However, heavier than equilibrium $\delta^{18}\text{O}_\text{P}$ values are intriguing and the reason for it is yet unclear. Recent fractionation factors calculated by Chang and Blake⁷¹ in Ag_3PO_4 measured in TC/EA are offset by +0.9 to +2.3‰ from that of the Longinelli and Nuti⁷⁰ in which the fractionation factors were determined using fluorination of BiPO_4 . Therefore equilibrium calculation based on Chang and Blake⁷¹ appears to be more relevant to this study. It is, however, important to note that the pore water P profile reflects the snapshot at the time of sediment sampling and does not record a series of events. Therefore, temporal dimension of the sediment biogeochemical processes cannot be extracted from pore water data.

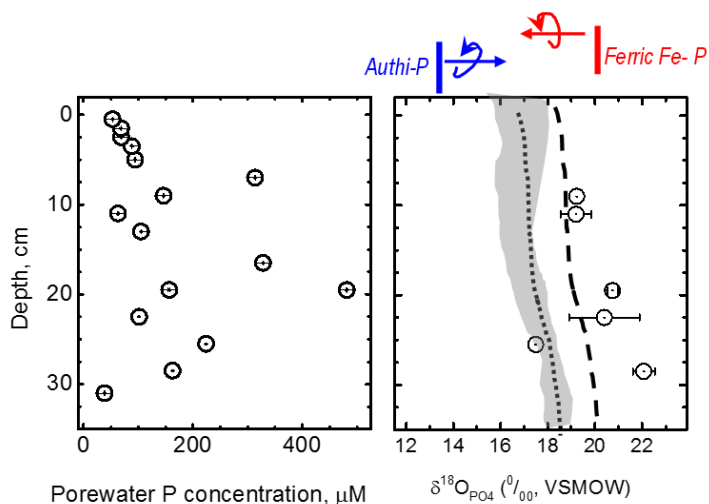


Figure 5.5 Concentration and corresponding $\delta^{18}\text{O}_p$ values of porewater P. Dotted and dashed lines represent the equilibrium $\delta^{18}\text{O}_p$ values calculated using measured water $\delta^{18}\text{O}_w$ values and temperature, following refs 70 and 71, respectively. The arrows from mean $\delta^{18}\text{O}_p$ values of authigenic and ferric Fe-bound P indicate direction of isotope excursion due to biological cycling.

5.4.5 Insignificant coupled Fe:P cycling (remobilization) pathway

The bottom water in the study site becomes seasonally hypoxic and sediment becomes almost entirely anoxic.^{36,38} In this condition, the Fe–P cycling (remobilization) pathway might be expected to be the dominant pathway because the coupled Fe–P cycling is enhanced by low bottom-water oxygen condition and results in higher benthic flux of P (e.g., see 13 and 84). During hypoxia, sediments act as a net source of P as Fe oxides in the sediment are reductively dissolved. Conversely, the opposite is true when the slow oxygenation of bottom water eliminates hypoxia so that the sediments become a net sink for P. In hypoxic/anoxic sediments Fe^{2+} produced in the sediment column diffuses up and oxidizes near the redoxcline and traps dissolved P. In our study, $\delta^{18}\text{O}_p$ values of ferric Fe-bound P can be used to test the presence of coupled Fe-P pathway and identify sink switching relationship. If the P derived from

remobilization pathway supersaturates the pore water with respect to authigenic P precipitation, the $\delta^{18}\text{O}_\text{P}$ values of the authigenic P thus evolved should vary between its parental (i.e., ferric Fe-bound P, $20.05 \pm 1.2\text{‰}$) and the equilibrium isotopic composition ($18.23 \pm 1.07\text{‰}$). While labile Fe oxides should dissolve in reducing environments (in hypoxic/anoxic water and sediment columns) as well as new Fe oxides form near the redoxcline, isotope data suggests that the reductively dissolved P is not sufficient enough to precipitate as authigenic P and any new Fe oxide formed in redoxcline is either dissolved during sedimentation or does not contribute any significant fraction to ferric Fe-bound P pool. This interpretation and the fact that ferric Fe-bound P is the largest P pool in this site require some unconventional interpretation on the fate of ferric Fe-bound P besides being detrital source. This calls for further exploration on the identity of minerals dissolved by CDB reagent and fate of iron oxides in anoxic sediment columns.

Decoupling of Fe–P cycling could also be due to the removal of Fe^{2+} from solution into iron sulfides in sulfidic bottom water environments.⁸⁵ Similarly, simultaneous precipitation of Fe and P as vivianite^{56,57} decreases the amount of Fe^{2+} that could diffuse up to the redoxcline. Fe:P molar ratios in freshwater and brackish sediments have been often used to identify the extent of Fe-P coupling. For example, Fe is consumed into sulfides in brackish sediments and the ratio becomes $\ll 1.0$.⁸⁶ This ratio in porewater in our study site varied from 0.2 to 0.5 and was consistent with past results in the mid-Bay sediments (i.e., 0.1 to 0.2).⁵⁸ This means that the removal of Fe as sulfide might have limited coupled Fe-P pathway in the sulfidic environments in the mid-Bay. While there could be considerable mixing of P originated from different sources and those derived from different biogeochemical processes (such as

incoming from ocean, transported by rivers, remineralized and remobilized during different episodes of hypoxic and anoxic condition in sediment and water columns), and could be trapped with freshly precipitated iron oxides, our isotope results suggest that the role of Fe–P pathway should be insignificant in the mid-Bay.

5.4.6 Predominance of organic matter remineralization pathway of P cycling

Geochemical reactions involving sorption and desorption of P with Fe oxides as well as release of P due to reductive dissolution do not impart significant isotope change.⁸⁷ Therefore isotope fractionation between dissolved (pore water) and sorbed P to iron oxides on prolonged reaction time scales is negligible.⁸⁷ Furthermore, changes in $\delta^{18}\text{O}_\text{P}$ values due to precipitation and dissolution of apatite is $<1.0\%$.^{74,81} As a result dynamic processes occurring in the sediment column involving precipitation and re-dissolution of authigenic P as well as sorption, desorption, and reductive dissolution of minerals and release of P do not impart any significant isotope effect. It means there are not any known mechanisms that generate dissolve P from ferric Fe-minerals with $\delta^{18}\text{O}_\text{P}$ values $\sim 6\%$ lighter than its source. On the other hand, authigenic P precipitated from remineralization pathway can have isotope compositions that vary from freshly produced inorganic P to complete isotopic equilibrium. Once precipitated, $\delta^{18}\text{O}_\text{P}$ values of authigenic P are faithfully preserved and not altered even on geological time scales.^{51,81,82} These lines of evidences strongly point out that there are no other known mechanisms which can produce an unusually light isotopic composition of authigenic P besides organic matter remineralization.

Based on our isotope results and other ancillary geochemical data from this site^{30,43,58,88}, we developed a schematic model of P cycling across the sediment-water interface (Figure 5.6). We explain the remineralization pathway as follows: Rain of

organic debris from dead phytoplankton to hypoxic bottom water and to the sediment column is followed by its hydrolysis. Previous calculation suggests that about the half of the organic carbon from primary production is deposited in the sediment column⁸⁹ which means the other half is mineralized in the water column. Because an unusually high concentration of inorganic P is produced from the remineralization of organic matter and the dissolved P generated from this pathway far exceeds any existing bottom water and/or pore water P derived from other sources or biogeochemical processes, the diffusion of this P pool should overwhelm the bottom water and potentially the surface water. Rather sharp gradient in pore water P concentration in the upper 10–20 cm depth (which reaches ~500 μM , Figure 5.5) clearly indicates upward diffusive flux of dissolved P into the overlying water. This interpretation is consistent with that of Bray et al.⁵⁶ in which the pore water P was interpreted to be a potential nutrient source for the overlying water and that of Cowan and Boynton²⁸ in which 6–74% of remobilized P was calculated to reach to surface water to support eutrophication. A high dissolved P results in immediate precipitation of authigenic P without any appreciable changes in isotopic composition (i.e., without significant biological cycling). While relatively light and heavier isotopic compositions of authigenic P could be further differentiated to identify the time gap between remineralization and precipitation i.e., the rate and extent of remineralization, the narrow ranges of $\delta^{18}\text{O}_p$ values indicate comparable rates of authigenic P precipitation in the past ~40 years.

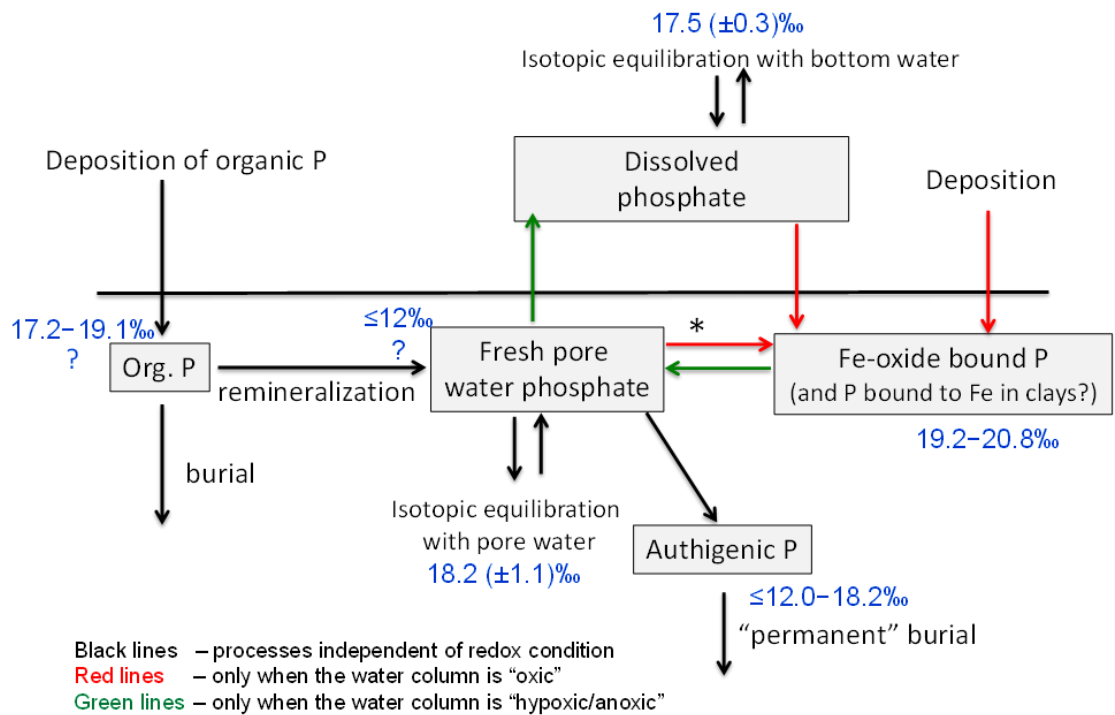


Figure 5.6 P cycling near sediment-water interface interpreted from isotope data. Please note ? symbol indicates uncertainty of data and * indicates that both reactions may not necessarily be highly redox-sensitive if some of this ferric Fe-bound P is associated with ferric iron in clays (otherwise there would be no ferric Fe-bound P found at depth in these sediments).

5.5 Conclusions and implications

This research, for the first time, identifies the predominance of organic matter remineralization as the predominant pathway of P cycling in the Chesapeake Bay. It is noteworthy to mention that neither the predominant source of authigenic P derived from organic matter has been previously reported from the Chesapeake Bay nor has the preservation of the isotopic signature immediately after remineralization of organic matter been found anywhere else in the world. It also highlights the usefulness of P isotopic composition as a vital tracer to detect the specific pathways of P cycling in different coastal and marine environments.

The extent to which benthic processes release or retain phosphorus can exert a major control on pelagic primary production by supplying a key nutrient, and this in turn can control the extent of hypoxia and eutrophication. Given that a portion of inorganic P produced from organic matter degradation precipitates as authigenic P, the bulk of the dissolved P should diffuse up to the bottom water and sustain the dead zone. Identification of the pathways that ultimately regulate the supply of inorganic P in the bottom water or P exchange across sediment-water interface provides critical information needed to better understand benthic-pelagic coupling and devise appropriate nutrient management plans in the Chesapeake Bay.

5.6 Acknowledgements

This research was supported by grants from MD-DE-PA Soybean Boards, and partly from USDA (2013-67019-21373) and Delaware EPSCoR (1301765).

Mössbauer analyses and XRD measurements were performed at Environmental Molecular Sciences Laboratory (EMSL), a national scientific user facility sponsored by the Department of Energy's Office of Biological and Environmental Research, at Pacific Northwest National Laboratory (PNNL). PNNL is a multiprogram national laboratory operated for the US Department of Energy by the Battelle Memorial Institute under Contract DE-AC06-76RLO 1830.

REFERENCES

- (1) Erickson, B. E. Cleaning the Chesapeake Bay. *Chemical and Engineering News* 89. ACS. 2011, pp. 10–14.
- (2) Boesch, D. F.; Coles, V. J.; Kimmel, D. G.; Miller, W. D. Coastal dead zones & global climate change: Ramifications of climate change for Chesapeake Bay hypoxia; 2007.
- (3) Prasad, M. B. K.; Sapiano, M. R. P.; Anderson, C. R.; Long, W.; Murtugudde, R. Long-term variability of nutrients and chlorophyll in the Chesapeake Bay: A retrospective analysis, 1985–2008. *Estuaries and Coasts* 2010, 33, 1128–1143.
- (4) Diaz, R. J.; Rosenberg, R. Spreading dead zones and consequences for marine ecosystems. *Science* 2008, 321, 926–929.
- (5) Stramma, L.; Johnson, G. C.; Sprintall, J.; Mohrholz, V. Expanding oxygen-minimum zones in the tropical oceans. *Science* 2008, 320, 655–658.
- (6) Klump, J. V.; Martens, C. S. Biogeochemical cycling in an organic-rich coastal marine basin. Sedimentary nitrogen and phosphorus budgets based upon kinetic models, mass balances, and the stoichiometry of nutrient regeneration. *Geochim. Cosmochim. Acta* 1987, 51, 1161–1173.
- (7) Reed, D. C.; Slomp, C. P.; Gustafsson, B. G. Sedimentary phosphorus dynamics and the evolution of bottom-water hypoxia: A coupled benthic-pelagic model of a coastal system. *Limnol. Oceanogr.* 2011, 56, 1075–1092.
- (8) Reed, D. C.; Slomp, C. P.; de Lange, G. J. A quantitative reconstruction of organic matter and nutrient diagenesis in Mediterranean Sea sediments over the Holocene. *Geochim. Cosmochim. Acta* 2011, 75, 5540–5558.
- (9) Klump, J. V.; Martens, C. S. Biogeochemical cycling in an organic rich coastal marine basin—II. Nutrient sediment-water exchange processes. *Geochim. Cosmochim. Acta* 1981, 45, 101–121.
- (10) Froelich, P. N.; Bender, M. L.; Luedtke, N. A.; Heath, G. R.; DeVries, T. The marine phosphorus cycle. *Am. J. Sci* 1982, 282, 474–511.

- (11) Filippelli, G. M.; Delaney, M. L. Phosphorus geochemistry of equatorial Pacific sediments. *Geochim. Cosmochim. Acta* 1996, 60, 1479–1495.
- (12) Föllmi, K. B. The phosphorus cycle, phosphogenesis and marine phosphate-rich deposits. *Earth-Science Rev.* 1996, 40, 55–124.
- (13) Ingall, E.; Jahnke, R. Influence of water-column anoxia on the elemental fractionation of carbon and phosphorus during sediment diagenesis. *Mar. Geol.* 1997, 139, 219–229.
- (14) Schulz, H. N.; Brinkhoff, T.; Ferdelman, T. G.; Mariné, M. H.; Teske, A.; Jørgensen, B. B. Dense populations of a giant sulfur bacterium in Namibian Shelf sediments. *Science* 1999, 284, 493–495.
- (15) Emerson, S.; Widmer, G. Early diagenesis in anaerobic lake sediments—II. Thermodynamic and kinetic factors controlling the formation of iron phosphate. *Geochim. Cosmochim. Acta* 1978, 42, 1307–1316.
- (16) Slomp, C. P.; Epping, E. H. G.; Helder, W.; Raaphorst, W. Van. A key role for iron-bound phosphorus in authigenic apatite formation in North Atlantic continental platform sediments. *J. Mar. Res.* 1996, 54, 1179–1205.
- (17) Jilbert, T.; Slomp, C. P. Iron and manganese shuttles control the formation of authigenic phosphorus minerals in the euxinic basins of the Baltic Sea. *Geochim. Cosmochim. Acta* 2013, 107, 155–169.
- (18) Anschutz, P.; Zhong, S.; Sundby, B.; Mucci, A.; Gobeil, C. Burial efficiency of phosphorus and the geochemistry of iron in continental margin sediments. *Limnol. Oceanogr.* 1998, 43, 53–64.
- (19) Jaisi, D. P.; Dong, H.; Liu, C. Influence of biogenic Fe(II) on the extent of microbial reduction of Fe(III) in clay minerals nontronite, illite, and chlorite. *Geochim. Cosmochim. Acta* 2007, 71, 1145–1158.
- (20) Jaisi, D. P.; Eberl, D. D.; Dong, H.; Kim, J. The formation of illite from nontronite by mesophilic and thermophilic bacterial reaction. *Clays Clay Miner.* 2011, 59, 21–33.
- (21) Konhauser, K. O.; Kappler, A.; Roden, E. E. Iron in microbial metabolisms. *Elements* 2011, 7, 89–93.
- (22) Einsele, W. Über die beziehungen des eisenkreislaufszum phosphatkreislauf im eutrophen see. *Arch. Hydrobiol* 1936, 29, 664–686.

- (23) Poulton, S. W.; Canfield, D. E. Ferruginous conditions: A dominant feature of the ocean through Earth's history. *Elements* 2011, 7, 107–112.
- (24) Nelson, G. J.; Pufahl, P. K.; Hiatt, E. E. Paleooceanographic constraints on Precambrian phosphorite accumulation, Baraga Group, Michigan, USA. *Sediment. Geol.* 2010, 226, 9–21.
- (25) Ruttenger, K. C.; Berner, R. A. Authigenic apatite formation and burial in sediments from non-upwelling, continental margin environments. *Geochim. Cosmochim. Acta* 1993, 57, 991–1007.
- (26) Schuffert, J. D.; Jahnke, R. A.; Kastner, M.; Leather, J.; Sturz, A.; Wing, M. R. Rates of formation of modern phosphorite off western Mexico. *Geochim. Cosmochim. Acta* 1994, 58, 5001–5010.
- (27) Boynton, W. R.; Garber, J. H.; Summers, R.; Kemp, W. M. Inputs, transformations, and transport of nitrogen and phosphorus in Chesapeake Bay and selected tributaries. *Estuaries* 1995, 18, 285–314.
- (28) Cowan, J. W.; Boynton, W. Sediment-water oxygen and nutrient exchanges along the longitudinal axis of Chesapeake Bay: Seasonal patterns, controlling factors and ecological significance. *Estuaries* 1996, 19, 562–580.
- (29) Boynton, W. R.; Kemp, W. M.; Barnes, J. M.; Matteson, L. L.; Rohland, F. M.; Jasinski, D. A.; Kimble, H. L. Chesapeake Bay water quality monitoring program, level one data report #10, Part 1: Interpretive Report; 1993.
- (30) Burdige, D. J.; Homstead, J. Fluxes of dissolved organic carbon from Chesapeake Bay sediments. *Geochim. Cosmochim. Acta* 1994, 58, 3407–3424.
- (31) Tuttle, J.; Jonas, R.; Malone, T. Origin, development and significance of Chesapeake Bay anoxia. In *Contaminant Problems and Management of Living Resources*; Majumdar, S. K.; Hall, L. W. J.; Herbert, M. A., Eds.; Pennsylvania Academy of Sciences: Phillipsburg, Pennsylvania, 1987; pp. 442–472.
- (32) Louchouart, P.; Lucotte, M.; Duchemin, E.; De Vernal, A. Early diagenetic processes in recent sediments of the Gulf of St-Lawrence: phosphorus, carbon and iron burial rates. *Mar. Geol.* 1997, 139, 181–200.
- (33) Reimers, C. E.; Ruttenger, K. C.; Canfield, D. E.; Christiansen, M. B.; Martin, J. B. Porewater pH and authigenic phases formed in the uppermost sediments of the Santa Barbara Basin. *Geochim. Cosmochim. Acta* 1996, 60, 4037–4057.

- (34) Martens, C. S.; Berner, R. A.; Rosenfeld, J. K. Interstitial water chemistry of anoxic Long Island Sound sediments. 2. Nutrient regeneration and phosphate removal. *Limnol. Ocean.* 1978, 23, 605–617.
- (35) Kemp, W. M.; Sampou, P. A.; Garber, J.; Turtle, J.; Boynton, W. Seasonal depletion of oxygen from bottom waters of Chesapeake Bay: roles of benthic and planktonic respiration and physical exchange processes. *Mar. Ecol. Prog. Ser.* 1992, 85, 137–152.
- (36) Hanson, T. E.; Luther, G. W.; Findlay, A.; MacDonald, D.; Hess, D. Phototrophic sulfide oxidation: Environmental insights and a method for kinetic analysis. *Frontiers in Microbiology*, 2013, 4.
- (37) Hobbs Carl H.; Kerhin, R. T.; Carron, M. J.; Halka, J. P. Chesapeake Bay Sediment Budget. *J. Coast. Res.* 1992, 8, 292–300.
- (38) Hagy, J. D.; Boynton, W. R.; Keefe, C. W.; Wood, K. V. Hypoxia in Chesapeake Bay, 1950–2001: Long-term change in relation to nutrient loading and river flow. *Estuaries* 2004, 27, 634–658.
- (39) Bratton, J. F.; Colman, S. M.; Seal, R. R. Eutrophication and carbon sources in Chesapeake Bay over the last 2700 yr: Human impacts in context. *Geochim. Cosmochim. Acta* 2003, 67, 3385–3402.
- (40) Burdige, D. J.; Zheng, S. The biogeochemical cycling of dissolved organic nitrogen in estuarine sediments. *Limnol. Oceanogr.* 1998, 43, 1796–1813.
- (41) Marvin-DiPasquale, M. C.; Capone, D. G. Benthic sulfate reduction along the Chesapeake Bay central channel. I. Spatial trends and controls. *Mar. Ecol. Prog. Ser.* 1998, 168, 213–228.
- (42) Zimmerman, A. R.; Canuel, E. A. A geochemical record of eutrophication and anoxia in Chesapeake Bay sediments: Anthropogenic influence on organic matter composition. *Mar. Chem.* 2000, 69, 117–137.
- (43) Li, W.; Joshi, S. R.; Hou, G.; Burdige, D.; Sparks, D. L.; Jaisi, D. P. Characterizing phosphorus speciation of Chesapeake Bay sediments using chemical extraction, ^{31}P NMR, and X-ray absorption fine structure spectroscopy. *Environ. Sci. Technol.* 2015, 49, 203–211.
- (44) Ruttenberg, C. Development of a sequential extraction method for different forms of phosphorus in marine sediments. *Limnol. Ocean.* 1992, 37, 1460–1482.

- (45) Murphy, J.; Riley, J. P. A modified single solution method for the determination of phosphate in natural waters. *Anal. Chim. Acta* 1962, 27, 31–36.
- (46) Karl, D. M.; Tien, G. MagIC: A sensitive and precise method for measuring dissolved phosphorus in aquatic environments. *Limnol. Oceanogr.* 1992, 37, 105–116.
- (47) Zachara, J. M.; Fredrickson, J. K.; Li, S.-M.; Kennedy, D. W.; Smith, S. C.; Gassman, P. L. Bacterial reduction of crystalline Fe³⁺ oxides in single phase suspensions and subsurface materials. *Am. Mineral.* 1998, 83, 1426–1443.
- (48) Colman, A. S.; Blake, R. E.; Karl, D. M.; Fogel, M. L.; Turekian, K. K. Marine phosphate oxygen isotopes and organic matter remineralization in the oceans. *Proc. Natl. Acad. Sci. U. S. A.* 2005, 102, 13023–13028.
- (49) Tamburini, F.; Bernasconi, S. M.; Angert, A.; Weiner, T.; Frossard, E. A method for the analysis of the $\delta^{18}\text{O}$ of inorganic phosphate extracted from soils with HCl. *Eur. J. Soil Sci.* 2010, 61, 1025–1032.
- (50) Liang, Y.; Blake, R. E. Oxygen isotope signature of Pi regeneration from organic compounds by phosphomonoesterases and photooxidation. *Geochim. Cosmochim. Acta* 2006, 70, 3957–3969.
- (51) Jaisi, D. P.; Blake, R. E. Tracing sources and cycling of phosphorus in Peru Margin sediments using oxygen isotopes in authigenic and detrital phosphates. *Geochim. Cosmochim. Acta* 2010, 74, 3199–3212.
- (52) Vennemann, T. W.; Fricke, H. C.; Blake, R. E.; Neil, J. R. O.; Colman, A. Oxygen isotope analysis of phosphates : A comparison of techniques for analysis of Ag₃ PO₄. *Chem. Geol.* 2002, 185, 321–336.
- (53) Jaisi, D. P.; Kukkadapu, R. K.; Stout, L. M.; Varga, T.; Blake, R. E. Biotic and abiotic pathways of phosphorus cycling in minerals and sediments: Insights from oxygen isotope ratios in phosphate. *Environ. Sci. Technol.* 2011, 45, 6254–6261.
- (54) Kukkadapu, R. K.; Zachara, J. M.; Fredrickson, J. K.; Kennedy, D. W. Biotransformation of two-line silica-ferrihydrite by a dissimilatory Fe(III)-reducing bacterium: Formation of carbonate green rust in the presence of phosphate. *Geochim. Cosmochim. Acta* 2004, 68, 2799–2814.

- (55) Rancourt, D. G.; Ping, J. Y. Voigt-based methods for arbitrary-shape static hyperfine parameter distributions in Mössbauer spectroscopy. *Nucl. Instruments Methods Phys. Res. Sect. B Beam Interact. with Mater. Atoms* 1991, 58, 85–97.
- (56) Bray, J. T.; Bricker, O. P.; Troup, B. N. Phosphate in interstitial waters of anoxic sediments: Oxidation effects during sampling procedure. *Sci.* 1973, 180, 1362–1364.
- (57) Matisoff, G.; Bricker III, O. P.; Holdren Jr, G. R.; Kaerk, P. Spatial and temporal variations in the interstitial water chemistry of Chesapeake Bay sediments; Johns Hopkins Univ., Baltimore, Md.(USA), 1975.
- (58) Cornwell, J. C.; Sampou, P. A. Environmental controls on iron sulfide mineral formation in a coastal plain estuary. In *Geochemical Transformations of Sedimentary Sulfur*; Vairavamurthy, M. A.; Schoonen, M. A. A., Eds.; ACS Symposium Series; American Chemical Society: Washington, DC, 1995; Vol. 612, pp. 12–224.
- (59) Murad, E.; Cashion, J. Mössbauer spectroscopy of environmental materials and their industrial utilization. 2004.
- (60) Eusterhues, K.; Wagner, F. E.; Häusler, W.; Hanzlik, M.; Knicker, H.; Totsche, K. U.; Kögel-Knabner, I.; Schwertmann, U. Characterization of ferrihydrite-soil organic matter coprecipitates by X-ray diffraction and Mössbauer Spectroscopy. *Environ. Sci. Technol.* 2008, 42, 7891–7897.
- (61) Majzlan, J. Thermodynamic stabilization of hydrous ferric oxide by adsorption of phosphate and arsenate. *Environ. Sci. Technol.* 2011, 45, 4726–4732.
- (62) Shimizu, M.; Zhou, J.; Schröder, C.; Obst, M.; Kappler, A.; Borch, T. Dissimilatory reduction and transformation of ferrihydrite-humic acid coprecipitates. *Environ. Sci. Technol.* 2013, 47, 13375–13384.
- (63) Fredrickson, J. K.; Zachara, J. M.; Kennedy, D. W.; Dong, H.; Onstott, T. C.; Hinman, N. W.; Li, S. Biogenic iron mineralization accompanying the dissimilatory reduction of hydrous ferric oxide by a groundwater bacterium. *Geochim. Cosmochim. Acta* 1998, 62, 3239–3257.
- (64) Kukkadapu, R. K.; Zachara, J. M.; Fredrickson, J. K.; McKinley, J. P.; Kennedy, D. W.; Smith, S. C.; Dong, H. Reductive biotransformation of Fe in shale–limestone saprolite containing Fe(III) oxides and Fe(II)/Fe(III) phyllosilicates. *Geochim. Cosmochim. Acta* 2006, 70, 3662–3676.

- (65) Lukkari, K.; Leivuori, M.; Hartikainen, H. Vertical distribution and chemical character of sediment phosphorus in two shallow estuaries in the Baltic Sea. *Biogeochemistry* 2008, 90, 171–191.
- (66) Cosmidis, J.; Benzerara, K.; Morin, G.; Busigny, V.; Lebeau, O.; Jézéquel, D.; Noël, V.; Dublet, G.; Othmane, G. Biomineralization of iron-phosphates in the water column of Lake Pavin (Massif Central, France). *Geochim. Cosmochim. Acta* 2014, 126, 78–96.
- (67) Cornwell, J.; Conley, D.; Owens, M.; Stevenson, J. C. A sediment chronology of the eutrophication of Chesapeake Bay. *Estuaries* 1996, 19, 488–499.
- (68) Zimmerman, A. R.; Canuel, E. A. Sediment geochemical records of eutrophication in the mesohaline Chesapeake Bay. *Limnol. Oceanogr.* 2002, 47, 1084–1093.
- (69) Reeburgh, W. S. Observations of gases in Chesapeake Bay sediments. *Limnol. Ocean.* 1969, 14, 368–375.
- (70) Longinelli, A.; Nuti, S. Revised phosphate-water isotopic temperature scale. *Earth Planet. Sci. Lett.* 1973, 19, 373–376.
- (71) Chang, S. J.; Blake, R. E. Precise calibration of equilibrium oxygen isotope fractionations between dissolved phosphate and water from 3–37 °C. *Geochim. Cosmochim. Acta* 2015, 150, 314–319.
- (72) Zhang, X.; Roman, M.; Kimmel, D.; McGilliard, C.; Boicourt, W. Spatial variability in plankton biomass and hydrographic variables along an axial transect in Chesapeake Bay. *J. Geophys. Res. Ocean.* 2006, 111.
- (73) Liang, Y.; Blake, R. E. Compound and enzyme-specific phosphodiester hydrolysis mechanisms revealed by $\delta^{18}\text{O}$ of dissolved inorganic phosphate: Implications for marine P cycling. *Geochim. Cosmochim. Acta* 2009, 73, 3782–3794.
- (74) Blake, R. E.; O’Neil, J. R.; Garcia, G. A. Enzyme-catalyzed oxygen isotope exchange between inorganic phosphate and water: Reaction rates and temperature dependence at 5.7–30 °C. *Miner. Magaz* 1998, 62A, 163–164.
- (75) Jaisi, D. P.; Blake, R. E.; Liang, Y.; Chan, S. J. Exploration of compound-specific organic-inorganic phosphorus transformation using stable isotope ratios in phosphate. In *Applied manure and nutrient chemistry for sustainable agriculture and environment*; He Z, Z. H., Ed.; Springer Dordrecht Heidelberg New York London, 2014; pp. 267–292.

- (76) Jaisi, D. P.; Blake, R. E. Advances in using oxygen isotope ratios of phosphate to understand phosphorus cycling in the environment. In *Advances in Agronomy*; Academic Press, 2014; Vol. 125, pp. 1–53.
- (77) Von Sperber, C.; Kries, H.; Tamburini, F.; Bernasconi, S. M.; Frossard, E. The effect of phosphomonoesterases on the oxygen isotope composition of phosphate. *Geochim. Cosmochim. Acta* 2014, 125, 519–527.
- (78) Blake, R. E.; O’Neil, J. R.; Surkov, A. V. Biogeochemical cycling of phosphorus: Insights from oxygen isotope effects of phosphoenzymes. *Am. J. Sci.* 2005, 305, 596–620.
- (79) Stout, L. M.; Joshi, S. R.; Kana, T. M.; Jaisi, D. P. Microbial activities and phosphorus cycling: An application of oxygen isotope ratios in phosphate. *Geochim. Cosmochim. Acta* 2014, 138, 101–116.
- (80) Van Cappellen, P.; Berner, R. A. Fluorapatite crystal growth from modified seawater solutions. *Geochim. Cosmochim. Acta* 1991, 55, 1219–1234.
- (81) Liang, Y.; Blake, R. E. Oxygen isotope fractionation between apatite and aqueous-phase phosphate: 20–45 °C. *Chem. Geol.* 2007, 238, 121–133.
- (82) Blake, R. E.; Chang, S. J.; Lepland, A. Phosphate oxygen isotopic evidence for a temperate and biologically active Archaean ocean. *Nature* 2010, 464, 1029–1032.
- (83) Jilbert, T.; Slomp, C. P.; Gustafsson, B. G.; Boer, W. Beyond the Fe-P-redox connection: Preferential regeneration of phosphorus from organic matter as a key control on Baltic Sea nutrient cycles. *Biogeosciences* 2011, 8, 1699–1720.
- (84) Colman, A. S.; Holland, H. D. Global diagenetic flux of phosphorus from marine sediments to the oceans: Redox sensitivity and the control of atmospheric oxygen levels. In *Marine Authigenesis: from Global to Microbial*; Glenn, C. R.; Lucas, J.; Prévôt-Lucas, L., Eds.; SEPM Spec. Pub. No. 66, 2000.
- (85) Rozan, T. F.; Taillefert, M.; Trouwborst, R. E.; Glazer, B. T.; Ma, S.; Herszage, J.; Valdes, L. M.; Price, K. S.; Luther III, G. W. Iron-sulfur-phosphorus cycling in the sediments of a shallow coastal bay: Implications for sediment nutrient release and benthic macroalgal blooms. *Limnol. Oceanogr.* 2002, 47, 1346–1354.

- (86) Gunnars, A.; Blomqvist, S. Phosphate exchange across the sediment-water interface when shifting from anoxic to oxic conditions an experimental comparison of freshwater and brackish-marine systems. *Biogeochemistry* 1997, 37, 203–226.
- (87) Jaisi, D. P.; Blake, R. E.; Kukkadapu, R. K. Fractionation of oxygen isotopes in phosphate during its interactions with iron oxides. *Geochim. Cosmochim. Acta* 2010, 74, 1309–1319.
- (88) Colman, S. M.; Halka, J. P.; Hobbs C. H. III. Patterns and rates of sediment accumulation in the Chesapeake Bay during the Holocene rise in sea level. *Soc. Sedimentry Geol. Spec. Publ.* 1992, 1–30.
- (89) Roden, E. E.; Tuttle, J. H.; Boynton, W. R.; Kemp, W. M. Carbon cycling in mesohaline Chesapeake Bay sediments 1: POC deposition rates and mineralization pathways. *J. Mar. Res.* 1995, 53, 779–819.

Chapter 6

PHOSPHORUS SOURCES AND CYCLING IN SEDIMENTS IMPACTED BY BOTTOM WATER HYPOXIA IN THE CHESAPEAKE BAY

6.1 Abstract

The Chesapeake Bay, one of the most biologically productive estuaries in United States, has severely degraded water quality due to excessive input of phosphorus (P) contributing to surface water eutrophication and bottom water hypoxia. Bottom water hypoxia in the bay may impact sediment P speciation and pathways of P cycling and direction of the flux of P across the sediment-water interface. Sediments from three sites along the salinity gradient of the Bay were analyzed to determine the concentrations and oxygen isotope ratios ($\delta^{18}\text{O}_\text{P}$) of P in various sediment fractions characterized by a sequence of extraction. Our isotope measurements and geochemical results show ferric Fe-bound and authigenic apatite P are two major P sinks in the Chesapeake Bay sediments, regardless of bottom water hypoxia. The regeneration of P_i from organic matter degradation (i.e., coupled C-P (rem mineralization) pathway) is the predominant pathway for authigenic apatite P precipitation in the three sites studied, albeit the extent is slightly different. Consistently similar but slightly heavier than equilibrium isotope values of the ferric Fe-bound P pool for the entire depth indicate potential terrestrial P sources, which could have mixed in different proportions with recycled P and Fe minerals in the bay. These findings highlight the significance of coupled C-P cycling that favors the precipitation of authigenic apatite P. These findings are expected to have significant

implications on the current understanding of sediment P cycling and P exchange across the sediment–water interface in the Bay.

6.2 Introduction

Phosphorus concentrations in sediment and exchange between the sediment and the overlying water are key processes controlling P cycling and budgets in the water column and are related to net primary production and potential for CO₂ sequestration (Karl, 2014). The balance between P deposition to sediment) and long-term P burial in less reactive phases determine the efflux of P across the sediment-water interface. Flux of inorganic P (P_i) at the sediment-water interface is primarily driven by P release from organic matter degradation and reductive dissolution of P-bound Fe oxides. Whereas in sediments underlying oxic bottom waters P efflux is controlled by balance between P released from organic matter remineralization (coupling of P and C cycles) and retention of P by iron oxides that serves as a phosphorus sink (Hupfer and Lewandowski, 2008; Katsev et al., 2006b; McManus et al., 1997), the release of P from reductive dissolution of Fe oxides (coupling of Fe and P cycles) is considered more important in hypoxic/anoxic sediments, serving as a P source to the overlying waters (e.g., Dellwig et al., 2010; Einsele, 1936; Klump and Martens, 1987; Kraal et al., 2012; Mortimer, 1942, 1941; Slomp et al., 1996). Still, quantitative understanding of the difference between coupled C-P vs Fe-P pathways of P cycling is limited and is either based on model results (e.g., Reed et al., 2011a,b) or qualitatively justified from profiles of porewater composition or sediment P pools (e.g., Ruttenberg and Berner, 1993; Schuffert et al., 1994; Slomp et al., 1996).

Chesapeake Bay suffers from varying degrees of summertime bottom water hypoxia and surface water eutrophication, fueled by both point and non–point nutrient

sources. The seasonal hypoxia/anoxia is produced and maintained in the bottom waters of the upper and middle regions of the Chesapeake Bay, the extent of which is controlled primarily by spring freshet and during the development of salinity stratification (Boicourt, 1992; Hagy et al., 2004; Officer et al., 1984), and decomposition of organic matter in the water column and sediments (Jonas and Tuttle, 1990; Kemp et al., 1992; Lewis et al., 2007). The hypoxia gradually subsides over the fall season.

Changes in bottom water dissolved oxygen exert an influence on early diagenetic pathways in sediments (more anaerobic at the expense of aerobic pathways), as well as on the stability of Fe oxides and organic debris that settle in the sediments and the re-oxidation of reduced metabolites deposited in the sediment. For example, previous studies reported large sediment P efflux (estimated to 25–30% up to even >100% of total P input) into the water column (Anschutz et al., 1998; Cornwell et al., 1996), suggesting that sediments are an important source of P to the water column of the bay. The sediments in the Chesapeake Bay store about 94% of total P inputs, which is greater than combined terrestrial and atmospheric input of P (Boynton et al., 1995). As this large amount of P stored in the sediment could potentially be remobilized and become a P source for the water column, characterizing species of sediment P and their differential reactivity in response to variations in biogeochemical conditions is essential to understand the transformations and fate of sediment P in the bay and its potential as an internal P source or long-term P sink. This also has a direct impact on the direction and magnitude of nutrient fluxes at the sediment-water interface, and the extent of benthic-pelagic coupling (Klump and Martens, 1987; Reed et al., 2011a, b). For example, there is a direct relationship of subpynocline

concentration of P_i (sediment P efflux) in response to bottom water O_2 concentration (Testa and Kemp, 2012).

The major objectives of this research is to understand how bottom water hypoxia impacts sediment P pools, particularly in regard to mobilization of P_i (i.e., Fe-P coupled pathway) or remineralization of organic P (P_o) (i.e., C-P coupled pathway) from sediments and the feedback effect of these two pathways of P cycling in P flux across the sediment-water interface. This objective was achieved with a comparative study among sites along the salinity gradient in the Chesapeake Bay that have oxic and hypoxic bottom waters, as well as how the degree and length of hypoxia varies among sites. This work builds on the previous study in the mid-Bay sediments where organic matter remineralization was found to be the most dominant pathway of P cycling in the sediment below the hypoxic water column (Joshi et al., 2015).

6.3 Materials and methods

6.3.1 Sampling sites and sediment characterization

Sediment cores were collected from the North (N), middle (M) and the South (S) sites located on the western slope of the Chesapeake Bay central channel (Figure 6.1). Site N (~10 m depth; Burdige and Gardner, 1998) is located near the mouth of the Susquehanna River in the Northern Bay, where bottom water salinities range from < 0.1 to ~10. This site has the highest sedimentation rate and is influenced strongly by land-derived sediment input from the Susquehanna River, the dominant source of sediment influx to the bay (Langland and Cronin, 2003). Site M (35 m depth) lies in the mesohaline portion of the Bay (bottom water salinities are ~10–20) where seasonal anoxia/hypoxia generally occurs in the bottom waters during the summer months. This

site is an organic rich, sulfidic sedimentary environment with underlying anoxic sediments that are often euxinic with substantial production of hydrogen sulfide (e.g., Hanson et al., 2013; Kemp et al., 1992). It has a lower sedimentation rate (7 mm yr^{-1}) than site N and is composed primarily of fine-grained sediments. Site S (12 m depth) is located in the southern Bay and has the lowest sedimentation rate with dominant sediment inputs from shoreline erosion and influx from the ocean (Hobbs et al., 1992; Langland and Cronin, 2003; Skrabal, 1991). At this site, the water column salinities range from 20 to 30. Site M undergoes seasonal hypoxia/anoxia in the bottom water (summer hypoxia/anoxia), whereas at the sites N and S, the water column is well oxygenated throughout the year with some exceptions of limited hypoxia in certain years.

Sediment collection and processing is described in Joshi et al. (2015). In brief, sediment cores were collected with box core and multicore devices and were chilled on ice during transportation. The cores were stored at $-80 \text{ }^{\circ}\text{C}$ before processing. The cores were sliced into 1 or 3 cm intervals down to 35 cm depth under a N_2 atmosphere. Sediment slices were freeze-dried after removing pore water by centrifugation, and then size separated ($< 200 \text{ }\mu\text{m}$). Unless specified, all analyses were performed using this size fraction of the sediments.



Figure 6.1 Location of the sediment sampling sites in the Chesapeake Bay.

6.3.2 X-Ray Diffraction

Mineralogical compositions in sediment samples across the sediment depths from sites N, M, and S were analyzed using X-ray diffraction (XRD) and data were collected using a Panalytical MPD instrument with Cu K-alpha radiation ($\lambda = 1.54056 \text{ \AA}$). We chose sediments from discrete depths from all three sites (except 0–1 and 1–2 cm for site N and 1–2 cm for site S) for the XRD analyses. Similarly, we chose eight (0–1, 2–3, 3–4, 4–6, 6–8, 12–15, 21–24, and 27–30 cm) sediment depths for site M. Diffraction data were analyzed by using JADE 9.5 (Materials Data Inc.) and the PDF4+ database (ICDD).

6.3.3 Total dissolution of sediments

Elemental analysis was carried out to understand the composition of elements associated with P for a number of selected sediments. The sediment samples were mixed thoroughly with fusion reagents (lithium meta-borate and lithium tetra-borate) and a non-wetting reagent (lithium bromide) in a platinum crucible. The mixture was digested in a Katanax K1 Fluxer (Katanax, Quebec, Canada) at 1000 °C for 10 min

and completed melted sediment solution was poured into a Teflon[®] beaker prefilled with 100 mL of 1 mol L⁻¹ HCl. After digestion, concentrations of total P, Fe, Ca, and S in sediments were measured by using inductively coupled plasma optical emission spectrometer (ICP-OES) in the Soil Testing Laboratory at the University of Delaware.

6.3.4 Extraction of sediment phosphorus pools

Sediments from different depth intervals were sequentially extracted using the SEDEX method (Ruttenberg, 1992) to quantify operationally-defined sedimentary P pools. The extracted P pools were (i) exchangeable P; (ii) ferric Fe-bound P (Fe-P hereafter); (iii) authigenic apatite P (authigenic Ca-P hereafter); authigenic carbonate fluoroapatite, biogenic apatite and CaCO₃-bound P; and (iv) detrital apatite P.

Concentrations of P_i in P pools were measured by using the phosphomolybdate blue method (Murphy and Riley, 1962). To account for reagent interference in colorimetric measurement for the ferric Fe-bound P pool, P_i was concentrated by using magnesium induced co-precipitation (MagIC) (Karl and Tien, 1992) to remove DCB reagents. The P_i concentration was measured after dissolving MagIC pellets and neutralizing pH.

6.3.5 Purification of extracted solutions

Two P pools (ferric Fe-bound and authigenic apatite P) were selected for further processing, purification, and precipitation of silver phosphate. The volume of extracted solution in these P pools was reduced and P_i was concentrated by using the MagIC method (Colman et al., 2005; Karl and Tien, 1992). The MagIC pellets were dissolved in 0.5 mol L⁻¹ HNO₃ and then passed through Superlite[™] DAX-8 resin to selectively trap organic matter. The samples were further purified using sequential precipitation and re-crystallization method (Jaisi and Blake, 2010; Liang and Blake,

2006). In brief, the samples were first precipitated as ammonium phosphomolybdate (APM) at low pH. The APM precipitates were washed with 5% ammonium nitrate and separated using 0.1 μm polysulfone filters and then dissolved in ammonium citrate. This step was followed by magnesium ammonium phosphate (MAP) precipitation at high pH. The MAP precipitates were washed with 1:20 ammonium hydroxide and then dissolved in HNO_3 . After neutralizing pH, the samples were further treated with cation resin to remove cations before converting into silver phosphate. These methods have been widely used and the robustness of these methods have been demonstrated in several past studies including sediments from the Chesapeake Bay (e.g., (Angert et al., 2011; Blake et al., 1997; Colman et al., 2005; Gross et al., 2013; Joshi et al., 2015; Kolodny et al., 1983; Tamburini et al., 2012, 2010; Tudge, 1960)). The validity of sample processing and potential hydrolysis of P_o during sample purification steps was tested using a separate phosphate standard and a blank sample. Both phosphate standard and dummy sample were processed using reagents spiked with ^{18}O labeled water (with final $\delta^{18}\text{O}_w$ values 50.0‰). We did not find any significant changes in $\delta^{18}\text{O}_p$ values in samples processed in normal and ^{18}O labeled waters.

6.3.6 Measurement of phosphate oxygen isotope ratios

All phosphate oxygen isotope ratios were measured by online high-temperature thermal decomposition using a Thermo Chemolysis/Elemental Analyzer (TC/EA) coupled to a Delta V continuous flow isotope ratio monitoring mass spectrometer (IRMS; Thermo-Finnigan, Bremen, Germany) with precision of $\pm 0.3\text{‰}$ in the laboratory at the University of Delaware. As a precaution, any impurities (possible culprits could be residual organic matter from samples or nitrate from silver phosphate precipitation reagent) were tested as total carbon and nitrogen with a CHN analyzer

(interfaced with existing IRMS). The $\delta^{18}\text{O}_p$ values of samples were calibrated against conventional fluorination using different silver phosphate standards (Vennemann et al., 2002).

6.4 Results

6.4.1 Mineralogical composition of sediments

XRD analyses of mineralogical composition of sediment samples from N, M, and S sites showed that the sediments predominantly consist of quartz, muscovite, feldspar group minerals, chlorite, and pyrite (Figure. 6.2). Although there was not a noticeable difference in mineralogical compositions among the sites, the quantities of the crystalline minerals were slightly different (data not shown). For example, the highest amount of quartz (> 55%) was present in the sediment samples from all depths from site S. On the other hand, sediments from site M contained the highest amount of muscovite. For each site, there was no particular difference in compositions of crystalline minerals among sediments from different depths. The XRD analysis was not able to identify the clay minerals such as vermiculite and montmorillonite from the sediments. Similarly, authigenic P minerals (such as vivianite and apatite) were not detected, presumably due to small quantities (<2%) below the limit of XRD detection.

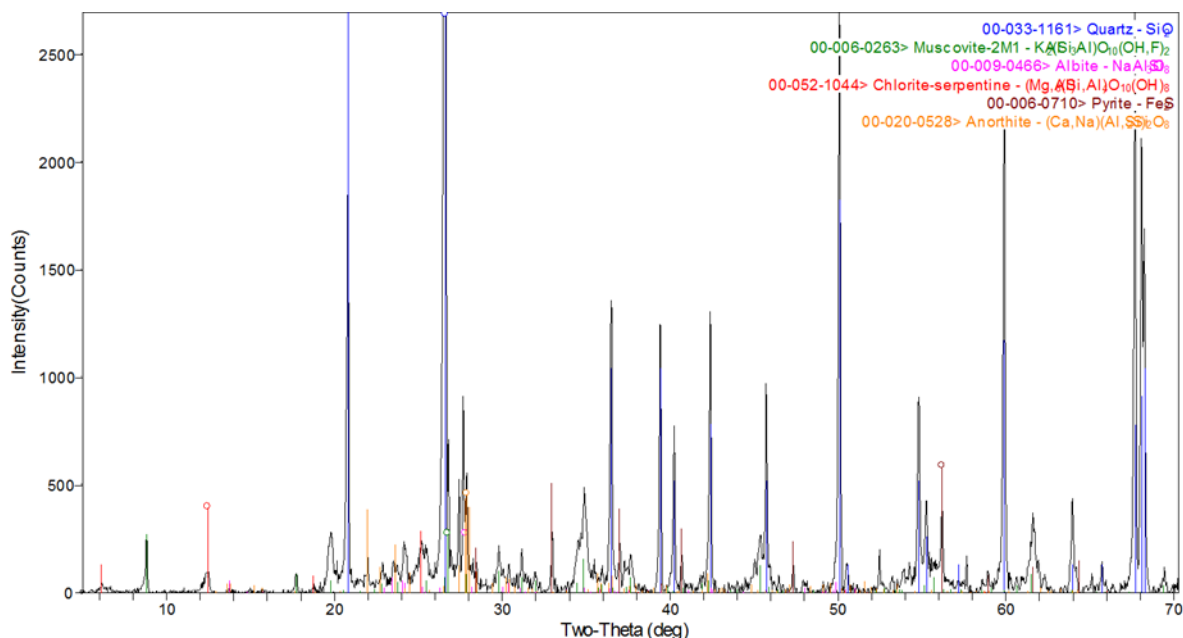


Figure 6.2 Mineralogical composition of sediment at 2 to 3 cm depth from site N. The sediment predominantly consists of quartz, muscovite, feldspar group minerals, chlorite, and pyrite.

6.4.2 Elemental compositions of sediments

Concentrations of total P, Fe, Ca, and S measured after complete dissolution of sediments using Katanax from the N, M, and S sites of the Chesapeake Bay are shown in Figure 6.3. The mid-Bay sediments contained the highest amount of depth-averaged total P ($21.5 \pm 3.3 \mu\text{mol g}^{-1}$) compared to the sediments for sites N and S (14.9 ± 1.9 and $16.9 \pm 1.5 \mu\text{mol g}^{-1}$, respectively). All three sites showed a similar trend of TP content in the sediment: TP decreased with increasing depth. Both sites N and M contained a similar amount of total Fe in the sediments (average 656 ± 40 and $664 \pm 36 \mu\text{mol g}^{-1}$, respectively) and site S contained the least amount of total Fe (average $370 \pm 17 \mu\text{mol g}^{-1}$). However, site S sediments contained the highest amount of total Ca compared to other two sites.

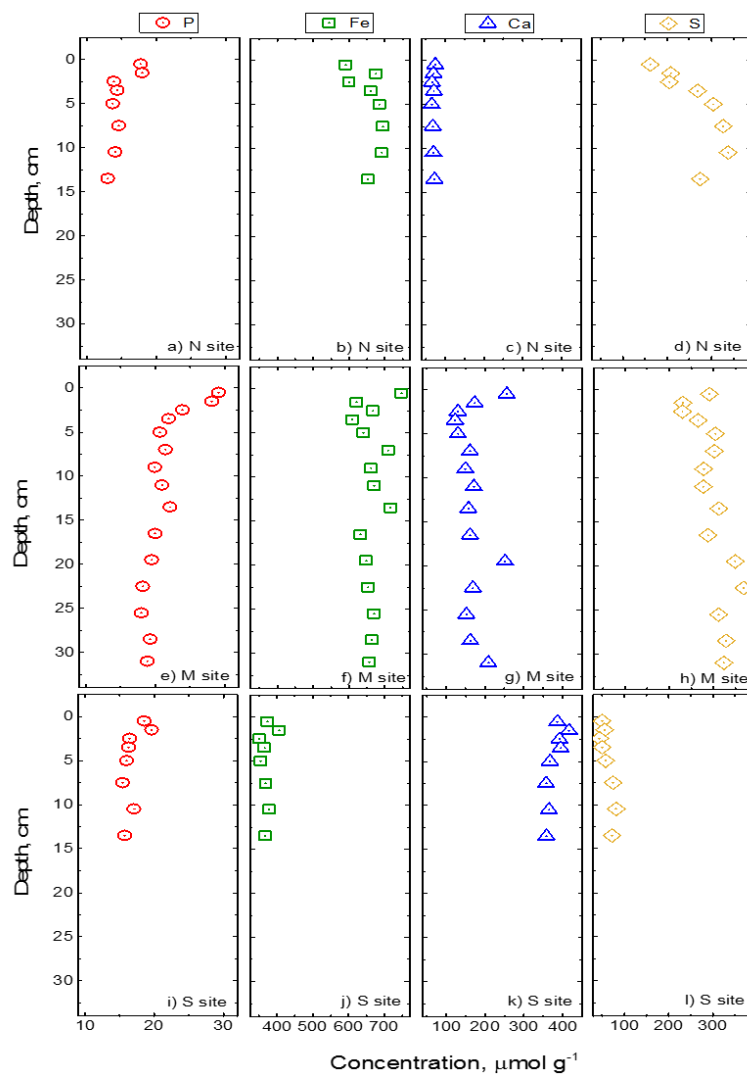


Figure 6.3 Concentrations of P, Fe, Ca, and S in sites N (a, b, c, and d), M (e, f, g, and h), and S (i, j, k, and l) sediments. The sediment samples were digested in a Katanax K1 fluxer and concentrations were measured using inductively coupled plasma optical emission spectrometer (ICP-OES).

6.4.3 Concentration of sediment phosphorus pools

Concentrations of sediment P pools (i.e., exchangeable P, ferric Fe-bound P (Fe-P), authigenic apatite P (Ca-P), and detrital P) from N, M, and S sites of the Chesapeake Bay are shown in Figure 6.4. The results suggest Fe-P and Ca-P pools are

two major sediment P pools in the bay. In comparison to these P pools, loosely sorbed and detrital P pools were relatively small in all three sites.

Fe-P was the predominant P pool followed by Ca-P (Figure 6.4 a and b) in the sediments from N and M sites. Depth-averaged concentrations of P in the Fe-P pool were 4.7 ± 0.7 and $5.3 \pm 0.8 \mu\text{mol g}^{-1}$ for sites N and M, respectively. Similarly, for these sites depth-averaged concentrations of Ca-P were 2.6 ± 0.2 and $3.7 \pm 0.4 \mu\text{mol g}^{-1}$, respectively. However, at site S, the Ca-P pool was the largest P pool followed by Fe-P (Figure 6.4 c). At this site, the depth averaged concentration of Fe-P and Ca-P were 1.9 ± 0.4 and $3.5 \pm 0.3 \mu\text{mol g}^{-1}$, respectively. As mentioned in the method section above, the MagIC step was included before quantifying P pools by the colorimetric method, and thus the concentration of this P pool was smaller than reported in (Li et al., 2015) where P concentration was measured directly on the extracted solution by using ICP-MS.

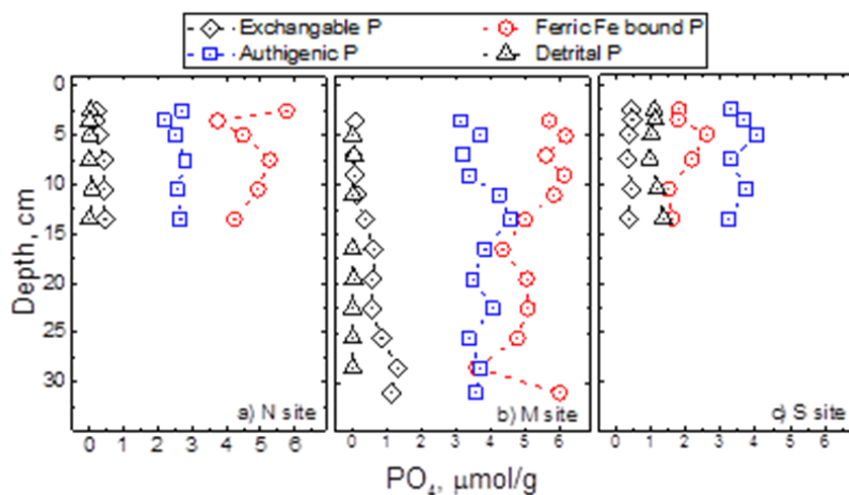


Figure 6.4 Concentration of exchangeable, ferric Fe-bound (Fe-P), authigenic apatite (Ca-P), and detrital P pools in the sediments from a) North (N); b) middle (M); and c) South (S) sites of the Bay.

6.4.4 Isotopic compositions of sediment phosphorus pools

The isotopic compositions of Fe-P and Ca-P pools in the sediments from N, M, and S sites of the Chesapeake Bay are shown in Figure 6.5. The isotopic compositions of loosely sorbed and detrital P pools from all sites, and Fe-P from site S were not determined due to concentrations of P_i lower than that needed for achieving reliable values. The isotope results show that the Fe-P pool in the sediments from site N varied between 18.5 to 20.0‰ and those from site M ranged between 19.2 to 20.8‰, but were similar over the entire depth studied. Based on the measured pore water $\delta^{18}O_w$ values of -5.33 to -6.31‰ and a temperature of 12 to 20 °C at 0 to 15 cm depth (at site N), the equilibrium phosphate isotopic composition, according to Longinelli and Nuti (1973) is 16.37 ± 1.21 ‰. Thus the measured values were mostly heavier than the equilibrium isotopic compositions, except for several data in both sites that were near or within the equilibrium ranges. A stark contrast, on the other hand, was the isotopic compositions of the Ca-P pool for all (N, M, and S) sites, which were much lighter than equilibrium isotopic compositions by 2 to 7‰. Interestingly, ranges of isotope values among all sites did not vary. If the equilibrium isotopic composition is calculated based on Chang and Blake (2015) (dashed lines in Figure 6.5a,b), the ranges of isotope values became heavier only by 0.9 to 2.3‰, compared to those from Longinelli and Nuti (1973). In this case, the majority of the ferric Fe-bound P isotopic compositions still varied but were very close to equilibrium values.

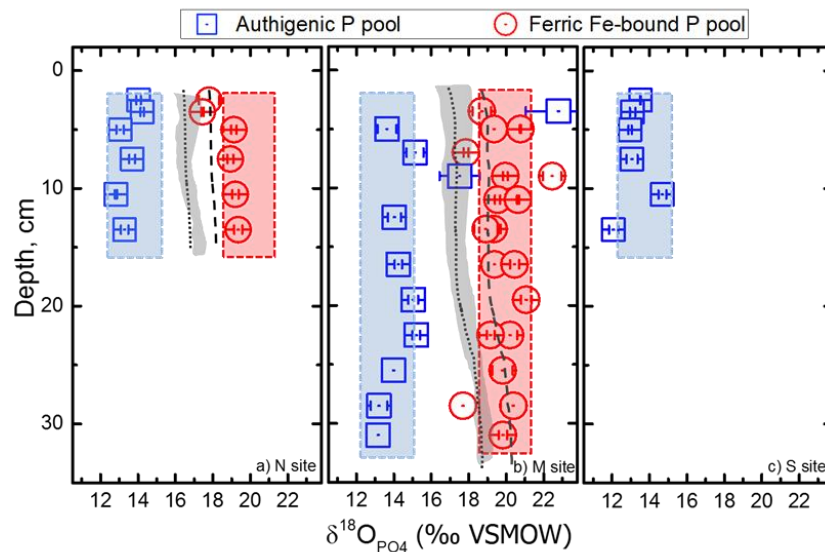


Figure 6.5 Isotopic compositions of Fe-P and Ca-P pools in the sediments from a) North (N); b) middle (M); and c) South (S) sites of the Chesapeake Bay. Thick dotted lines at sites N and M represents the equilibrium isotopic compositions (as per (Longinelli and Nuti, 1973)) calculated using August temperature (Reeburgh, 1969) and porewater oxygen isotope values and the shaded region for the entire year. The dashed line is equilibrium isotopic compositions calculated as per Chang and Blake, 2015 (Chang and Blake, 2015).

6.5 Discussion

6.5.1 Anomalous Fe-P pool and variation of major sediment P sinks along the salinity gradient

Fe-P and Ca-P are two major P sinks in the Chesapeake Bay sediments, regardless of the different bottom water conditions (hypoxic/anoxic versus well oxygenated bottom waters at site M and the other two sites, respectively (Li et al., 2015; Joshi et al., 2015)). However, the contributions of these two sediment P pools as long term P sinks may be different for individual sites depending upon their location

(upper, middle or lower Bay), sediment characteristics, and biogeochemical processes within the water column and sediments.

The ferric Fe-bound P pool is anomalously high and accounts for up to half of all SEDEX P pools in the sediment from sites N and M and its concentration in site S is still high (Figure 6.4), similar to previous studies in freshwater sediments where Fe-P is the major long-term P sink (e.g., Ruban et al., 1999). The Susquehanna River is the most dominant source for sediment influx at site N whereas at site M, the majority of sediment comes from shoreline erosion (Langland and Cronin, 2003). One of the possibilities that is consistent with the high Fe concentrations in the sediments at these two sites (Figure 6.3) and the presence of large amounts of Fe(III) vermiculite, which forms mainly from the weathering of micas (Sparks, 2003), and the major Fe mineral that accounts for 30 to 50% of the total Fe (Li et al., 2015), is the incomplete dissolution Fe-oxide minerals and phyllosilicate minerals during DCB treatment. In fact, incomplete reductive dissolution of Fe phyllosilicate minerals is expected due to the presence of *sp*-OM-P (Jaisi et al., 2011, 2007; Joshi et al., 2015). Similarly high ferric Fe-bound P pools have been reported from permanently stratified lakes with dissolved O₂ <<1 mg L⁻¹ (Cosmidis et al., 2014), and sediments under hypoxic/anoxic bottom waters (e.g., Archipelago Sea and Gulf of Finland in Baltic Sea estuaries (Lukkari et al., 2008) and Goban Spur in the North Atlantic Ocean (Slomp et al., 1996)).

The Fe-P pool is extracted in the step targeting P bound to reactive Fe (oxyhydr)oxides in the SEDEX sequential extraction procedure (Ruttenberg, 1992). Given the anomalous concentration of the Fe-P pool compared to values reported in the literature, it is worth further discussion. In the euxinic environment in the mid-bay

where a substantial amount of hydrogen sulfide is produced (Hagy et al., 2004; Hanson et al., 2013), Fe oxides should have undergone reductive dissolution by H₂S or via microbial respiration. Even though a cautionary statement not to interpret unanalyzed P pools is made in Ruttenberg's original dissertation (Ruttenberg, 1990), this statement is largely ignored and high ferric Fe-P pool is often interpreted as the burial of Fe-bound P in anoxic basins. Therefore, current literature where source-sink switching relationships are developed based on this P pool in the anoxic sediments requires new scrutiny and extensive revision of existing interpretations. Thus, this work will have a major impact on sediment P dynamics including P budget calculations. This embarks on a series of analytical and geochemical questions, the major one being what exactly does the DCB reagent extract? Are Fe oxides really recalcitrant against reductive dissolution in anoxic sediments? Future research in this direction is urgently needed.

The presence of vivianite in the mid-Bay has been reported in the past (Bray et al., 1973; Matisoff et al., 1975) and reconfirmed in our recent studies (Joshi et al., 2015; Li et al., 2015). A phase stability analysis based on summer porewater concentrations of CO₃²⁻ and PO₄³⁻ in the main channel along the axis of the Bay shows the coexistence of siderite and vivianite (Bray et al., 1973). Furthermore, direct characterization Fe bearing minerals using Fe EXAFS showed that a significant amount of vivianite (8–18% of total Fe) is present in the mid-Bay sediments of all depths (Li et al., 2015). Although Fe²⁺ is consumed by H₂S to form iron sulfide and any excess is left for vivianite precipitation (Gächter and Müller, 2003), a copious amount of vivianite is present along with pyrite in the Bay. Thus the quantitative

understanding of vivianite in these sites as well as function of depth is required to address this question.

The second largest sediment P pool (at sites N and M) is authigenic apatite P (Ca-P), which includes authigenic carbonate fluoroapatite, biogenic apatite and CaCO₃-bound P (Ruttenberg, 1992). Concentration of P in this pool was higher in sediments from sites M and S compared to site N (Figure 6.4), suggesting enhanced precipitation of Ca-P minerals in more saline conditions. This might have been facilitated by higher concentration of Ca²⁺ in the more saline part of the Bay. This is consistent with marine sediments where authigenic apatite P is the major long-term P sink (e.g., (Föllmi, 1996; Ruttenberg and Berner, 1993; Slomp et al., 1996)).

Gradual changes in dominance of sediment P sinks within the Chesapeake Bay transect, from Fe-P in the middle – upper bay to Ca-P in the lower bay, suggests spatial variability in P sequestration mechanisms in the bay. In the freshwater and mid-saline regions of the bay, P sequestration is expected to be controlled by Fe-oxide loading from rivers, and other multiple factors that affect precipitation and remobilization of Fe minerals, such as water and sediment column hypoxia/anoxia conditions. In contrast to Fe-P that may be predominantly imported from terrestrial sources (see below for discussion of Fe-P sources), authigenic Ca-P is formed within the sediments. A fraction of Ca-P could also be formed in the water column and then deposited into the sediments in the mesosaline region of the bay (Li et al., 2016). Therefore, in the saline regions, controls of P sequestration (Ca-P formation) may rely largely on other factors that control the thermodynamic favorability of carbonate fluorapatite formation, such as salinity (Ca²⁺ and Mg²⁺ concentrations), P_i concentrations, and alkalinity. Moreover, the different stability of the P sinks (high

stability of Ca-P compared to Fe-P) provides important insights into P remobilization under changing environmental conditions (e.g., pH, redox conditions).

6.5.2 Dominance of coupled Fe-P and C-P pathways: Insights from phosphate oxygen isotope ratios

6.5.2.1 Ferric Fe-bound P and coupled Fe-P pathway:

Isotopic compositions of the ferric Fe-bound P (Fe-P) pool from sites N and M are within narrow ranges but are heavier than equilibrium isotopic compositions, suggesting that the original isotopic compositions of this pool are largely retained. This range of isotope compositions rules out the possibility of specific biogeochemical processes or pathways in the formation of this P pool. For example, this range of isotopic compositions is not expected if dissolved P is trapped with authigenic iron oxides that are formed in the redoxcline during transient oxic–anoxic oscillations and then eventually settled into the sediment columns, or during reoxidation of Fe(II) at the sediment–water interface after the water column becomes gradually oxic after the strength of summer eutrophication wanes. If these conditions do occur in the bay, the isotopic compositions of Fe-P pool should lie in between those of authigenic P and equilibrium P isotopic compositions. There is an intriguing coincidence in similarities in the ranges of Fe-P pool isotope values with the terrestrial P sources: P bound to Fe and Al oxide minerals in soils in the Eastern Shore agricultural fields and suspended particulate matter from East Creek (a tributary to the Chesapeake Bay) have similar isotope values (Bear, 2016; Joshi et al., 2016). A caution, however, is the limited number of isotope results and extremely small coverage of potential Fe-P from the Chesapeake Bay watershed. Furthermore, the method used to extract the Fe-P pool in this study was DCB reagent but for terrestrial Fe-P sources was 0.5 mol L⁻¹ NaOH,

which extract P bound to Fe as well as Al oxides. Nonetheless, isotopic similarity increases the possibilities that Fe-P pools in the bay could be largely from terrestrial origin. This raises additional questions on how isotope values are preserved during the series of biogeochemical reactions that cases dissolution and precipitation of Fe minerals from the source to the sink (sediment). However, variation in oxic/anoxic conditions in the water column impacts the fate of these minerals. For example, stability of Fe-P between sites N and M and thus their fates may be different due to the different water column conditions: at the well oxygenated site N, the majority of Fe-P may deposited into the sediments and become a long-term P sink (although pH changes may cause P release), whereas at the seasonally hypoxic site M, Fe-P may be partially remobilized (reductive dissolution) and serve as an important source of P_i into the water column. This may explain the observed episodic high values of $\delta^{18}O_P$ (higher than equilibrium) in the water column dissolved P pool (Li et al., 2016a). The isotope effect of vivianite precipitation is unclear. Further research to validate the fate of land-driven Fe-P sources and fidelity of isotope values of this P pool is required.

6.5.2.2 Authigenic Ca-P and coupled C-P pathways:

An intriguing observation in this study is the same range of isotopic compositions of the authigenic apatite P (Ca-P) pool in well-oxygenated N and S sites as well as the seasonally hypoxic/anoxic site M. Much lighter isotope values of the Ca-P pool suggest that this P pool has been formed from rapid precipitation of P_i released from the remineralization of organic matter (i.e., coupled C-P pathway) rather than from the reductive dissolution of Fe oxide minerals (i.e., coupled Fe-P pathway) (see Joshi et al., 2015 for additional discussion on pathways). This means that organic matter remineralization is the predominant pathway to generate P_i for Ca-P in the

sediments at all sites, regardless of the water column redox conditions. While the insignificance of bottom water hypoxia on the intensity of the coupled Fe-P or C-P pathway is not expected, there are several possibilities if the remineralization occurs in the sediment column. Sediments typically become anoxic below several millimeters to centimeters regardless of the water column redox conditions (Li et al., 2012), and therefore the impact of water column redox conditions (oxic versus anoxic) on Ca-P precipitation would only be expected if Ca-P were partially formed within the water column. In the Chesapeake Bay mesosaline region, Ca-P was hypothesized to form in the water column and deposit into the sediments (Li et al., 2016b). However, the extent of hypoxia/anoxic in the bottom water and surface sediments has been considered in controlling Fe-P immobilization (Cowan and Boynton, 1996; Katsev et al., 2006a), efficient remineralization of relatively labile particulate P_o in the water column occurs in both oxic and anoxic conditions (Li et al., 2016b). In fact, particulate P_o could be more efficiently remineralized in the oxic water column, although the bottom hypoxic/anoxic waters the seasonally stratified water column allow accumulations of P_i , which increase the thermodynamic favorability of carbonate fluorapatite precipitation (higher Ca-P saturation index due to high P_i concentrations).

While our data suggest coupled C-P cycling as the predominant pathway for authigenic P precipitation, there remain several additional unresolved issues regarding sites of authigenic P precipitation and extent of P efflux under the C-P pathway. Based on the localization of authigenic P, organic matter remineralization is considered to occur at shallow depths below the sediment-water interface such as in the Santa Barbara basin (Reimers et al., 1996), Long Island Sound and Mississippi Delta (Ruttenberg and Berner, 1993), and Baja California (Schuffert et al., 1994). Contrary

to this, authigenic P being ‘deposited’ as opposed to being precipitated *in situ* has been recently argued for the Arkona basin of the Baltic Sea (Reed et al., 2011b). While microbial respiration is coupled to organic matter oxidation, a pathway claimed to be dominant in the Bay (Jonas and Tuttle, 1990; Jonas, 1997, 1992; Kemp et al., 1992), the intensity and predominance of each respiration pathway as well as the amount of P_i produced from remineralization may vary vertically in the water column due to changes in redox conditions, reaction energetics, and the composition and availability of labile organic matter (e.g., (Burdige, 2011)). Therefore, a direct correlation of these diverse reactions with the generation of P_i cannot be established. Furthermore, the relative importance of an indirect versus direct microbial role for P_i flux in response to changes in redox conditions in bottom waters and sediments is often disagreed upon (e.g., (Carlton and Wetzel, 1988; Gächter and Meyer, 1993; Gunnars and Blomqvist, 1997; Ruttenberg, 2003)). It is possible that considerable remineralization of organic matter occurs in the water column and some amount of released P_i precipitates as authigenic P such as on the sinking particulate matter (localized precipitation) and then settles to be ‘deposited’ in the sediment column. Further research on quantitative analyses of authigenic P precipitated in the water column versus sediment column will aid in resolving the role of hypoxia on strengthening or weakening coupled C-P cycling.

Overall, the results suggest that the sources and mechanisms of P sinks (Fe-P and Ca-P) are consistent within the spatially and temporally variable Chesapeake Bay. Given the variability in contributions from different P sinks, i.e., switching from Fe-P to Ca-P with increasing salinity, and the different formation and remobilization mechanisms of these P pools, the efficiency of sediment P sequestration may respond

differently to the changing biogeochemical conditions in the bay. Our constraints on the magnitudes and sources of the sediment P sinks provide important insights into P cycling in the bay and offer a basis for nutrient budget estimations and nutrient cycling models.

6.6 Conclusions and implications

Sedimentary P dynamics are controlled primarily by depositional fluxes of organic matter and ferric Fe-bound P, and their cycling depends on the bottom water redox conditions. The N, M, and S sites in the Chesapeake Bay chosen for this comparative P cycling study have contrasting eutrophication history, sedimentation rate, salinity, and redox conditions among other physiochemical properties. The sediment P pools and particularly their isotopic compositions provide information about the sources and the biogeochemical processes for their formation. By comparative analyses on ferric Fe-P and Ca-P pools of the sites, we identified the omnipresence of organic matter remineralization as the predominant source of the Ca-P pool in the sediments, regardless of the water column redox conditions.

Because the Chesapeake Bay is a national treasure and the nation's first estuary targeted by Congress for restoration, information on sources and processes of nutrient regeneration and cycling will have significant impacts not only for the scientific community but also at public and policy levels. Scientific findings in this study contribute to the decades of collective efforts by Chesapeake Bay Program, state, and local agencies on the bay to identify sources of nutrients, particularly P efflux under C-P and Fe-P pathways in response to bottom water hypoxia, and devise an appropriate restoration plan. Overall, our results will help in reassessment of current nutrient management plans, existing models for total maximum daily load

(TMDL), and possibly widen source-and pathway-based research to identify the dominance of specific reactions and processes and the extent to which different P sources and pathways play roles in impairing water quality. A detailed and integrated understanding, developed from this research, on sediment P speciation and pathways of authigenic apatite P precipitation, provide a framework that could be applied to other comparable coastal and marine environments.

REFERENCES

- Angert, A., Weiner, T., Mazeh, S., Tamburini, F., Frossard, E., Bernasconi, S.M., Sternberg, M., 2011. Seasonal variability of soil phosphate stable oxygen isotopes in rainfall manipulation experiments. *Geochim. Cosmochim. Acta* 75, 4216–4227.
- Anschutz, P., Zhong, S., Sundby, B., Mucci, A., Gobeil, C., 1998. Burial efficiency of phosphorus and the geochemistry of iron in continental margin sediments. *Limnol. Oceanogr.* 43, 53–64.
- Bear, K., 2016. Tracking sources of particulate phosphorus in river waters: A case study in East Creek, a Chesapeake Bay watershed. University of Delaware.
- Blake, R.E., O’Neil, J.R., Garcia, G.A., 1997. Oxygen isotope systematics of biologically mediated reactions of phosphate: I. Microbial degradation of organophosphorus compounds. *Geochim. Cosmochim. Acta* 61, 4411–4422.
- Boicourt, W.G., 1992. Influences of Circulation Processes on Dissolved Oxygen in Chesapeake Bay, in: Smith, D.E., Leffler, M., Mackiernan, G. (Eds.), *Oxygen Dynamics in the Chesapeake Bay: A Synthesis of Recent Research*. Maryland and Virginia Sea Grant Colleges, Publication Nos. UM-SG-TS-92-01 and VSG-92-01, College Park, Maryland, pp. 7–59.
- Boynton, W.R., Garber, J.H., Summers, R., Kemp, W.M., 1995. Inputs, transformations, and transport of nitrogen and phosphorus in Chesapeake Bay and selected tributaries. *Estuaries* 18, 285–314.
- Bray, J.T., Bricker, O.P., Troup, B.N., 1973. Phosphate in interstitial waters of anoxic sediments: Oxidation effects during sampling procedure. *Sci.* 180, 1362–1364.
- Burdige, D.J., 2011. Estuarine and coastal sediments - coupled biogeochemical cycling, in: R., L., Middelburg, J.. (Eds.), *Treatise on Estuarine and Coastal Science*. Elsevier, pp. 279–316.
- Burdige, D.J., Gardner, K.G., 1998. Molecular weight distribution of dissolved organic carbon in marine sediment pore waters. *Mar. Chem.* 62, 45–64.

- Carlton, R.G., Wetzel, R.G., 1988. Phosphorus flux from lake sediments: Effect of epipelagic algal oxygen production. *Limnol. Oceanogr.* 33, 562–570.
- Chang, S.J., Blake, R.E., 2015. Precise Calibration of equilibrium oxygen isotope fractionations between dissolved phosphate and water from 3–37 °C. *Geochim. Cosmochim. Acta.* 150, 314–329.
- Colman, A.S., Blake, R.E., Karl, D.M., Fogel, M.L., Turekian, K.K., 2005. Marine phosphate oxygen isotopes and organic matter remineralization in the oceans. *Proc. Natl. Acad. Sci. U. S. A.* 102, 13023–13028.
- Cornwell, J., Conley, D., Owens, M., Stevenson, J.C., 1996. A sediment chronology of the eutrophication of Chesapeake Bay. *Estuaries* 19, 488–499.
- Cosmidis, J., Benzerara, K., Morin, G., Busigny, V., Lebeau, O., Jézéquel, D., Noël, V., Dublet, G., Othmane, G., 2014. Biomineralization of iron-phosphates in the water column of Lake Pavin (Massif Central, France). *Geochim. Cosmochim. Acta* 126, 78–96.
- Cowan, J.W., Boynton, W., 1996. Sediment-water oxygen and nutrient exchanges along the longitudinal axis of Chesapeake Bay: Seasonal patterns, controlling factors and ecological significance. *Estuaries* 19, 562–580.
- Dellwig, O., Leipe, T., März, C., Glockzin, M., Pollehne, F., Schnetger, B., Yakushev, E. V., Böttcher, M.E., Brumsack, H.-J., 2010. A new particulate Mn–Fe–P-shuttle at the redoxcline of anoxic basins. *Geochim. Cosmochim. Acta* 74, 7100–7115.
- Einsele, W., 1936. Über die Beziehungen des Eisenkreislaufs zum Phosphatkreislauf im eutrophen See. *Arch. Hydrobiol.* 29, 664–686.
- Föllmi, K.B., 1996. The phosphorus cycle, phosphogenesis and marine phosphate-rich deposits. *Earth-Science Rev.* 40, 55–124.
- Gächter, R., Meyer, J.S., 1993. The role of microorganisms in mobilization and fixation of phosphorus in sediments BT - Proceedings of the Third International Workshop on Phosphorus in Sediments, in: Boers, P.C.M., Cappenberg, T.E., van Raaphorst, W. (Eds.), Springer Netherlands, Dordrecht, pp. 103–121.
- Gächter, R., Müller, B., 2003. Why the phosphorus retention of lakes does not necessarily depend on the oxygen supply to their sediment surface. *Limnol. Oceanogr.* 48, 929–933.

- Gross, A., Nishri, A., Angert, A., 2013. Use of phosphate oxygen isotopes for identifying atmospheric-P sources: a case study at Lake Kinneret. *Environ. Sci. Technol.* 47, 2721–7.
- Gunnars, A., Blomqvist, S., 1997. Phosphate exchange across the sediment-water interface when shifting from anoxic to oxic conditions an experimental comparison of freshwater and brackish-marine systems. *Biogeochemistry* 37, 203–226.
- Hagy, J.D., Boynton, W.R., Keefe, C.W., Wood, K. V, 2004. Hypoxia in Chesapeake Bay, 1950–2001: Long-term change in relation to nutrient loading and river flow. *Estuaries* 27, 634–658.
- Hanson, T.E., Luther, G.W., Findlay, A., MacDonald, D., Hess, D., 2013. Phototrophic sulfide oxidation: environmental insights and a method for kinetic analysis. *Front. Microbiol.*
- Hobbs, C.H., Halka, J.P., Kerhin, R.T., Carron, M.J., 1992. Chesapeake Bay sediment budget. *J. Coast. Res.* 8, 292–300.
- Holland, H.D., 1984. *The chemical evolution of the atmosphere and oceans.* Princeton University Press, Princeton, N.J.
- Hupfer, M., Lewandowski, J., 2008. Oxygen controls the phosphorus release from lake sediments – a long-lasting paradigm in limnology. *Int. Rev. Hydrobiol.* 93, 415–432.
- Jaisi, D.P., Blake, R.E., 2010. Tracing sources and cycling of phosphorus in Peru Margin sediments using oxygen isotopes in authigenic and detrital phosphates. *Geochim. Cosmochim. Acta* 74, 3199–3212.
- Jaisi, D.P., Dong, H., Liu, C., 2007. Influence of biogenic Fe(II) on the extent of microbial reduction of Fe(III) in clay minerals nontronite, illite, and chlorite. *Geochim. Cosmochim. Acta* 71, 1145–1158.
- Jaisi, D.P., Eberl, D.D., Dong, H., Kim, J., 2011. The formation of illite from nontronite by mesophilic and thermophilic bacterial reaction. *Clays Clay Miner.* 59, 21–33.
- Jonas, R.B., 1997. Bacteria, dissolved Organics and oxygen consumption in salinity stratified Chesapeake Bay, an anoxia paradigm. *Am. Zool.* 37, 612–620.

- Jonas, R.B., 1992. Microbial processes, organic matter and oxygen demand in the water column., in: Smith, D.E., Leffler, M., Mackiernan, G. (Eds.), *Oxygen Dynamics in the Chesapeake Bay: A Synthesis of Recent Research*. Maryland and Virginia Sea Grant Colleges, College Park, Maryland, pp. 113–148.
- Jonas, R.B., Tuttle, J.H., 1990. Bacterioplankton and organic carbon dynamics in the lower mesohaline Chesapeake Bay. *Appl. Environ. Microbiol.* 56, 747–757.
- Joshi, S.R., Kukkadapu, R.K., Burdige, D.J., Bowden, M.E., Sparks, D.L., Jaisi, D.P., 2015. Organic matter remineralization predominates phosphorus cycling in the Mid-bay sediments in the Chesapeake Bay. *Environ. Sci. Technol.* 49, 5887–5896.
- Joshi, S.R., Li, X., Jaisi, D.P., 2016. Transformation of phosphorus pools in an agricultural soil: An application of oxygen-18 labeling in phosphate. *Soil Sci. Soc. Am. J.* 80, 69–78.
- Karl, D.M., 2014. Microbially mediated transformations of phosphorus in the sea: New views of an old cycle. *Ann. Rev. Mar. Sci.* 6, 279–337.
- Karl, D.M., Tien, G., 1992. MagIC: A sensitive and precise method for measuring dissolved phosphorus in aquatic environments. *Limnol. Oceanogr.* 37, 105–116.
- Katsev, S., Sundby, B., Mucci, A., 2006a. Modeling vertical excursions of the redox boundary in sediments: Application to deep basins of the Arctic Ocean. *Limnol. Oceanogr.* 51, 1581–1593.
- Katsev, S., Tsandev, I., L'Heureux, I., Rancourt, D.G., 2006b. Factors controlling long-term phosphorus efflux from lake sediments: Exploratory reactive-transport modeling. *Chem. Geol.* 234, 127–147.
- Kemp, W.M., Sampou, P.A., Garber, J., Turtle, J., Boynton, W., 1992. Seasonal depletion of oxygen from bottom waters of Chesapeake Bay: roles of benthic and planktonic respiration and physical exchange processes. *Mar. Ecol. Prog. Ser.* 85, 137–152.
- Klump, J.V., Martens, C.S., 1987. Biogeochemical cycling in an organic-rich coastal marine basin. Sedimentary nitrogen and phosphorus budgets based upon kinetic models, mass balances, and the stoichiometry of nutrient regeneration. *Geochim. Cosmochim. Acta* 51, 1161–1173.

- Kolodny, Y., Luz, B., Navon, O., 1983. Oxygen isotope variations in phosphate of biogenic apatites, I. Fish bone apatite—rechecking the rules of the game. *Earth Planet. Sci. Lett.* 64, 398–404.
- Kraal, P., Slomp, C.P., Reed, D.C., Reichart, G.J., Poulton, S., Boer, W., 2012. Sedimentary phosphorus and iron cycling in and below the oxygen minimum zone in the northern Arabian Sea. *Biogeosciences* 9, 2603–2624.
- Langland, M., Cronin, T., 2003. A summary report of sediment processes in Chesapeake Bay and watershed. No. 2003-4123.
- Lewis, B.L., Glazer, B.T., Montbriand, P.J., Luther III, G.W., Nuzzio, D.B., Deering, T., Ma, S., Theberge, S., 2007. Short-term and interannual variability of redox-sensitive chemical parameters in hypoxic/anoxic bottom waters of the Chesapeake Bay. *Mar. Chem.* 105, 296–308.
- Li, J., Bai, Y., Bear, K., Joshi, S., Jaisi, D., 2016a. The limiting nutrients in the Chesapeake Bay: insights from particulate nutrient stoichiometry and phosphate oxygen isotope compositions.
- Li, J., Crowe, S.A., Miklesh, D., Kistner, M., Canfield, D.E., Katsev, S., 2012. Carbon mineralization and oxygen dynamics in sediments with deep oxygen penetration, Lake Superior. *Limnol. Oceanogr.* 57, 1634–1650.
- Li, J., Reardon, P., James, M.P., Joshi, S.R., Bai, Y., Bear, K., Jaisi, D.P., 2016b. Phosphorus cycling in the water column of the Chesapeake Bay: Roles of sinking particulates in phosphorus regeneration and sequestration.
- Li, W., Joshi, S.R., Hou, G., Burdige, D.J., Sparks, D.L., Jaisi, D.P., 2015. Characterizing phosphorus speciation of Chesapeake Bay sediments using Chemical extraction, ³¹P NMR, and X-ray absorption fine structure spectroscopy. *Environ. Sci. Technol.* 49, 203–211.
- Liang, Y., Blake, R.E., 2006. Oxygen isotope signature of Pi regeneration from organic compounds by phosphomonoesterases and photooxidation. *Geochim. Cosmochim. Acta* 70, 3957–3969.
- Longinelli, A., Nuti, S., 1973. Revised phosphate-water isotopic temperature scale. *Earth Planet. Sci. Lett.* 19, 373–376.
- Lukkari, K., Leivuori, M., Hartikainen, H., 2008. Vertical distribution and chemical character of sediment phosphorus in two shallow estuaries in the Baltic Sea. *Biogeochemistry* 90, 171–191.

- Matisoff, G., Bricker III, O.P., Holdren Jr, G.R., Kaerk, P., 1975. Spatial and temporal variations in the interstitial water chemistry of Chesapeake Bay sediments. Johns Hopkins Univ., Baltimore, Md.(USA).
- McManus, J., Berelson, W.M., Coale, K.H., Johnson, K.S., Kilgore, T.E., 1997. Phosphorus regeneration in continental margin sediments. *Geochim. Cosmochim. Acta* 61, 2891–2907.
- Mortimer, C., 1942. The exchange of dissolved substances between mud and water in lakes: III and IV. *J. Ecol* 30, 147–201.
- Mortimer, C., 1941. The exchange of dissolved substances between mud and water in lakes: I and II. *J. Ecol* 29, 280–329.
- Murphy, J., Riley, J.P., 1962. A modified single solution method for the determination of phosphate in natural waters. *Anal. Chim. Acta* 27, 31–36.
- Officer, C.B., Biggs, R.B., Taft, J.L., Cronin, L.E., Tyler, M.A., Boynton, W.R., 1984. Chesapeake Bay anoxia: Origin, development, and significance. *Science* 223, 22–27.
- Poulton, S.W., Canfield, D.E., 2011. Ferruginous conditions: A dominant feature of the ocean through Earth's history. *Elements* 7, 107–112.
- Reeburgh, W.S., 1969. Observations of gases in Chesapeake Bay sediments. *Limnol. Ocean.* 14, 368–375.
- Reed, D.C., Slomp, C.P., de Lange, G.J., 2011a. A quantitative reconstruction of organic matter and nutrient diagenesis in Mediterranean Sea sediments over the Holocene. *Geochim. Cosmochim. Acta* 75, 5540–5558.
- Reed, D.C., Slomp, C.P., Gustafsson, B.G., 2011b. Sedimentary phosphorus dynamics and the evolution of bottom-water hypoxia: A coupled benthic-pelagic model of a coastal system. *Limnol. Oceanogr.* 56, 1075–1092.
- Reimers, C.E., Ruttenger, K.C., Canfield, D.E., Christiansen, M.B., Martin, J.B., 1996. Porewater pH and authigenic phases formed in the uppermost sediments of the Santa Barbara Basin. *Geochim. Cosmochim. Acta* 60, 4037–4057.
- Ruban, V., Brigault, S., Demare, D., Philippe, A.-M., 1999. An investigation of the origin and mobility of phosphorus in freshwater sediments from Bort-Les-Orgues Reservoir, France. *J. Environ. Monit.* 1, 403–407.

- Ruttenberg, C., 1992. Development of a sequential extraction method for different forms of phosphorus in marine sediments. *Limnol. Ocean.* 37, 1460–1482.
- Ruttenberg, K.C., 2003. The global phosphorus cycle, in: Schlesinger, W.. (Ed.), *Treatise on Geochemistry*. Elsevier, pp. 585–643.
- Ruttenberg, K.C., 1990. Diagenesis and burial of phosphorus in marine sediments: Implications for the marine phosphorus budget.
- Ruttenberg, K.C., Berner, R.A., 1993. Authigenic apatite formation and burial in sediments from non-upwelling, continental margin environments. *Geochim. Cosmochim. Acta* 57, 991–1007.
- Schuffert, J.D., Jahnke, R.A., Kastner, M., Leather, J., Sturz, A., Wing, M.R., 1994. Rates of formation of modern phosphorite off western Mexico. *Geochim. Cosmochim. Acta* 58, 5001–5010.
- Skrabal, S.A., 1991. Clay mineral distributions and source discrimination of Upper Quaternary sediments, lower Chesapeake Bay, Virginia. *Estuaries* 14, 29–37.
- Slomp, C.P., Epping, E.H.G., Helder, W., Raaphorst, W. Van., 1996. A key role for iron-bound phosphorus in authigenic apatite formation in North Atlantic continental platform sediments. *J. Mar. Res.* 54, 1179–1205.
- Slomp, C.P., Van der Gaast, S.J., Van Raaphorst, W., 1996. Phosphorus binding by poorly crystalline iron oxides in North Sea sediments. *Mar. Chem.* 52, 55–73.
- Sparks, D.L., 2003. *Environmental soil chemistry*, Second. ed. Elsevier Science.
- Tamburini, F., Bernasconi, S.M., Angert, A., Weiner, T., Frossard, E., 2010. A method for the analysis of the $\delta^{18}\text{O}$ of inorganic phosphate extracted from soils with HCl. *Eur. J. Soil Sci.* 61, 1025–1032.
- Tamburini, F., Pfahler, V., Bünemann, E.K., Guelland, K., Bernasconi, S.M., Frossard, E., 2012. Oxygen isotopes unravel the role of microorganisms in phosphate cycling in soils. *Environ. Sci. Technol.* 46, 5956–62.
- Testa, J.M., Kemp, W.M., 2012. Hypoxia-induced shifts in nitrogen and phosphorus cycling in Chesapeake Bay. *Limnol. Oceanogr.* 57, 835–850.
- Tudge, A.P., 1960. A method of analysis of oxygen isotopes in orthophosphate—its use in the measurement of paleotemperatures. *Geochim. Cosmochim. Acta* 18, 81–93.

Vennemann, T.W., Fricke, H.C., Blake, R.E., Neil, J.R.O., Colman, A., 2002. Oxygen isotope analysis of phosphates : A comparison of techniques for analysis of Ag_3PO_4 . *Chem. Geol.* 185, 321–336.

Chapter 7

CONCLUSIONS AND IMPLICATIONS

This dissertation research aimed to identify pathways and mechanisms of transformation of P pools that could be driven by loading of P, imposed redox and changing biogeochemical conditions and could provide fundamental insights on P cycling in soil and sediments in the Chesapeake Bay and its watershed.

In an agricultural soil, a rapid but step-wise transformation of originally bioavailable P was found to be converted into unavailable P and eventually precipitated as Ca-P minerals. However, formation of residual P ($\text{HNO}_3\text{-P}_i$) was found to be mostly short-circuited from NaOH-P_i . Given that both the pathway and mechanism of P transformation was not identified before, these results provide new insights into the fate of externally applied P in a soil and soil P dynamics which can be utilized to minimize this transformation and improve existing P management practices or development of new P management plans in agricultural soils.

Continuous application of fertilizer and manure in excess of crop requirements leads to soil P saturation and P loss from agricultural fields to hydrologically connected water bodies. In an agricultural-runoff dominated ditch, runoff flux was found to dominate in surface water while remineralization dominated sediment porewater. In the downstream section in the wetland region, P derived most likely from reductive dissolution during redox fluctuation was found to be fully cycled by microorganisms. These results have important implications for understanding of

different sources that contribute to recycling of P exported from the agricultural-runoff dominated creek.

Understanding the coupled Fe-P cycling and C-P cycling pathways in sediments in response to bottom water hypoxia in the Chesapeake Bay provides insights into P effluxes from the sediment-water interface and P burial. Interestingly, the omnipresent C-P pathway was found to be the predominant pathway of authigenic P formation regardless of the water column redox conditions. This is the first study that identified P released from organic matter remineralization as the predominant source of authigenic apatite P in the Chesapeake Bay. The understanding developed on sources and processes of nutrient regeneration and cycling in the bay will have significant impacts not only for the scientific community but also at public and policy levels. Scientific findings in this research contribute to the decades of collective efforts by Chesapeake Bay Program, USDA-NRCS, USGS, USEPA, state, and local agencies to identify sources of nutrients, particularly P efflux under coupled C-P and Fe-P cycling in response to bottom water hypoxia. Overall, these results will help re-assess current nutrient management plans in the bay, existing models for total maximum daily load (TMDL), and possibly widen source-and pathway-based research to identify the dominance of specific reactions and processes and the extent to which different P sources and pathways play a role in impairing water quality. A detailed and integrated understanding developed from this research on sediment P speciation and pathway of authigenic apatite P precipitation provide a framework that could be applied to other comparable coastal and marine environments such as the Northern Gulf of Mexico, Danish Straits, and Changjiang estuary in China; suboxic zones in sedimentary porewater of lakes, estuaries, bays, and oceans; permanently anoxic basins (the Black

Sea, the Arabian Sea, equatorial Pacific, and fjords and even in early Earth environments.

Chapter 8

LIMITATIONS AND FUTURE DIRECTIONS

This research characterized P pools and investigated the mechanisms of P transformation in soils and sediments using several research techniques, which may be subject to uncertainties and limitations. Quantification of P pools in soils and sediments largely relied on sequential extraction techniques (Hedley et al., 1982; Tiessen and Moir, 1993; Ruttenberg, 1992) which are operationally defined. Challenges exist, however, due to heterogeneity and complex nature of soils and sediments. The extraction techniques may bring uncertainties in estimating different P pools, due to multiple reasons, for example: (i) incomplete extraction of a certain pool that causes overestimation of P pools being subsequently extracted, (ii) extraction of P_o and its hydrolysis that causes overestimation of P_i , (iii) complexation of P_i in extract solutions interfering with colorimetric method. Although the extraction methods used in the work have been modified to minimize the error associated with P extraction (e.g., the residual after each extraction was washed using NaHCO_3 and H_2O to minimize the carryover of P_i with residual (Condrón and Nerman, 2011; Ruttenberg, 1992), there could still be unknown errors.

This research identified important pathways and mechanisms of transformation of P pools under different biogeochemical conditions and provided fundamental insights on P cycling. In addition to these findings, this research brought forward several questions, which deserve future investigation:

- Tracking of ^{18}O labeled phosphate identified a rapid but step-wise transformation of originally bioavailable P into unavailable P and precipitation of Ca-P minerals in an agricultural soil. Further research is warranted to better understand the kinetics of Ca-P minerals precipitation in both laboratory and field conditions, and better identify the composition of Ca-P minerals and P speciation using more direct tools, such as synchrotron based X-ray adsorption near edge structure spectroscopy (XANES).
- Organic matter remineralization (coupled C-P cycling) was found to be the predominant pathway for authigenic P precipitation in the Chesapeake Bay sediments regardless of the water column redox conditions. However, the location of the mineral precipitation (in the water column or in sediment column) is largely unknown. Future research on quantitative analyses of location of authigenic P precipitation is desired.
- Ferric Fe bound P pool in the Chesapeake Bay remains largely uncharacterized due to nonspecificity of DCB reagents to series of ferric and ferrous Fe minerals. Additional research is needed in terms of the Fe-P minerals in anoxic sediments, in particular formation of vivianite or burial of allochthonous ferric Fe bound P as a long term P sink.

REFERENCES


- Condon, L.M., and S. Newman. 2011. Revisiting the fundamentals of phosphorus fractionation of sediments and soils. *Journal of Soils and Sediments* 11: 830–840.
- Hedley, M.J., W.B. Stewart, and B.S. Chauwan. 1982. Changes in inorganic and organic soil phosphorus fractions induced by cultivation practices and by laboratory incubations. *Soil Sci. Soc. Am. J.* 46: 970–976.
- Ruttenberg, C. 1992. Development of a sequential extraction for different forms of phosphorus in marine sediments. *Limnol. Oceanogr.* 37: 1460–1482.
- Tiessen, H., J.W.B. Stewart, and J.O. Moir. 1983. Changes in organic and inorganic phosphorus composition of two grassland soils and their particle size fractions during 60–90 years of cultivation. *J. Soil Sci.* 34(4): 815–823.


Appendix A

PERMISSION FOR JOSHI ET AL. 2015

Reprinted with permission from (Joshi, S.R., Kukkadapu, R.K., Burdige, D.J., Bowden, M.E., Sparks, D.L., and Jaisi, D.P., 2015. Organic matter remineralization predominates phosphorus cycling in the Mid-bay sediments in the Chesapeake Bay. Environ. Sci. Technol. 49, 5887–5896). Copyright (2015) American Chemical Society.

7/12/2016 Rightslink® by Copyright Clearance Center

 **RightsLink®** [Home](#) [Create Account](#) [Help](#) [Live Chat](#)

 **ACS Publications** Most Trusted. Most Cited. Most Read. **Title:** Organic Matter Remineralization Predominates Phosphorus Cycling in the Mid-Bay Sediments in the Chesapeake Bay

Author: Sunendra R. Joshi, Ravi K. Kukkadapu, David J. Burdige, et al

Publication: Environmental Science & Technology

Publisher: American Chemical Society

Date: May 1, 2015

Copyright © 2015, American Chemical Society

LOGIN

If you're a copyright.com user, you can login to Rightslink using your copyright.com credentials. Already a Rightslink user or want to learn more?

PERMISSION/LICENSE IS GRANTED FOR YOUR ORDER AT NO CHARGE

This type of permission/license, instead of the standard Terms & Conditions, is sent to you because no fee is being charged for your order. Please note the following:

- Permission is granted for your request in both print and electronic formats, and translations.
- If figures and/or tables were requested, they may be adapted or used in part.
- Please print this page for your records and send a copy of it to your publisher/graduate school.
- Appropriate credit for the requested material should be given as follows: "Reprinted (adapted) with permission from (COMPLETE REFERENCE CITATION). Copyright (YEAR) American Chemical Society." Insert appropriate information in place of the capitalized words.
- One-time permission is granted only for the use specified in your request. No additional uses are granted (such as derivative works or other editions). For any other uses, please submit a new request.

[BACK](#) [CLOSE WINDOW](#)

Copyright © 2016 Copyright Clearance Center, Inc. All Rights Reserved. [Privacy statement](#), [Terms and Conditions](#), [Comments?](#) We would like to hear from you. E-mail us at customercare@copyright.com

Appendix B

PERMISSION FOR JOSHI ET AL. 2016

ACSESS-Alliance of Crop, Soil, and Environmental Science Societies and the original publisher Soil Science Society of America Journal, 80:69–78, 2016, Transformation of Phosphorus Pools in an Agricultural Soil: An Application of Oxygen-18 Labeling in Phosphate, Sunendra R. Joshi, Xiaona Li, and Deb P. Jaisi, **Lisence Number 3906661370780** is given to the publication in which the material was originally published, with kind permission from ACSESS.

7/12/2016	RightClick Printable License
ACCESS-ALLIANCE OF CROP, SOIL, AND ENVIRONMENTAL SCIENCE SOCIETIES LICENSE TERMS AND CONDITIONS	
Jul 12, 2016	
<p>This Agreement between Sunendra R. Joshi ("You") and ACSESS-Alliance of Crop, Soil, and Environmental Science Societies ("ACSESS-Alliance of Crop, Soil, and Environmental Science Societies") consists of your license details and the terms and conditions provided by ACSESS-Alliance of Crop, Soil, and Environmental Science Societies and Copyright Clearance Center.</p>	
License Number	3906661370780
License date	Jul 12, 2016
Licensed Content Publisher	ACSESS-Alliance of Crop, Soil, and Environmental Science Societies
Licensed Content Publication	Soil Science Society of America Journal
Licensed Content Title	Transformation of Phosphorus Pools in an Agricultural Soil: An Application of Oxygen-18 Labeling in Phosphate
Licensed Content Author	Sunendra R. Joshi, Xiaona Li, and Deb P. Jaisi
Licensed Content Date	Jan 2, 2016
Licensed Content Volume Number	80
Licensed Content Issue Number	1
Type of Use	Thesis/Dissertation
Requestor type	Author of requested content
Format	Electronic
Portion	chapter/article
Rights for	Main product
Creation of copies for the disabled	no
With minor editing privileges	no
For distribution to	Worldwide
In the following language(s)	Original language of publication
With incidental promotional use	no
The lifetime unit quantity of new product	0 to 499
The requesting person/organization is:	Sunendra R. Joshi
Order reference number	
Title of your thesis / dissertation	Biogeochemical cycling of phosphorus in the Chesapeake Bay and its watershed: Insights from phosphate oxygen isotope ratios
Expected completion date	Jul 2016
Estimated size (number of pages)	215
https://s100.copyright.com/AppDispatchServlet	